Chemical variability
Chemical variability of phenolic compounds in *Phyllanthus niruri*

Cooperative learning
The potency of cooperative integrated reading and composition in building chemistry students' scientific literacy and self-regulated learnings

Nanoparticles
Novel organophosphorus Schiff base ligands: Synthesis, characterization, ligational aspects, XRD and biological activity studies

Phytochemistry
Potential inhibiting activities of phytochemicals in *Scilla natalensis* bulbs against schistosomiasis

Kinetic evaluation
Oil extraction from seeds of *Carica papaya L.*: Obtaining the lipid profile and thermal evaluation

Editorial Team

Editor-in-Chief

Prof. Assis Vicente Benedetti, São Paulo State University, Institute of Chemistry, Araraquara, Brazil. https://orcid.org/0000-0002-0243-6639

Editors

Prof. Angélica María Baena Moncada, National University of Engineering, Faculty of Sciences, Lima, Peru. https://orcid.org/0000-0002-2896-4392

Prof. Boutros Sarrouh, Federal University of São João Del-Rei, Department of Chemistry, Biotechnology and Bioprocess Engineering, São João Del-Rei, Brazil. https://orcid.org/0000-0003-4476-2309

Prof. Celly Mieko Shinohara Izumi, Federal University of Juiz de Fora, Exact Science Institute, Juiz de Fora, Brazil. https://orcid.org/0000-0001-6489-9201

Prof. Irlon Maciel Ferreira, Federal University of Amapá, Course of Chemistry, Macapá, Brazil. https://orcid.org/0000-0002-4517-0105

Prof. Manuel Ignacio Azocar Guzmán, University of Santiago de Chile, Facultad of Chemistry and Biology Areas, Santiago, Chile. https://orcid.org/0000-0002-3698-4772

Prof. Marcos Carlos de Mattos, Federal University of Ceará, Center of Sciences, Fortaleza, Brazil. https://orcid.org/0000-0003-4291-5199

Prof. Mário Antônio Alves da Cunha, Federal Technological University of Paraná, Department of Chemistry, Pato Branco, Brazil. https://orcid.org/0000-0002-1589-7311

Prof. Michelle Jakeline Cunha Rezende, Federal University of Rio de Janeiro, Institute of Chemistry, Rio de Janeiro, Brazil. https://orcid.org/0000-0002-8282-6636

Prof. Natany Dayani de Souza Assai, Fluminense Federal University, Institute of Exact Sciences, Volta Redonda, Brazil. https://orcid.org/0000-0002-0851-9187

Prof. Natanael de Carvalho Costa, Federal University of Rio de Janeiro, Institute of Physics, Rio de Janeiro, Brazil. https://orcid.org/0000-0003-4285-4672

Prof. Nuria Cinca, Polytechnic University of Catalunya, Hyperion Materials & Technologies, Martorelles, Barcelona, Spain. https://orcid.org/0000-0002-1622-8734

Prof. Omayra Beatriz Ferreiro Balbuena, National University of Asunción, Faculty of Chemical Sciences, Asunción, Paraguay. https://orcid.org/0000-0001-8449-1297

Prof. Patrícia Hatsue Suegama, Federal University of Grande Dourados, Faculty of Exact and Technological Sciences, Dourados, Brazil. http://orcid.org/0000-0001-9421-8454

Prof. Paulo Clairmont Feitosa Lima Gomes, São Paulo State University, Institute of Chemistry, Araraquara, Brazil. http://orcid.org/0000-0002-4837-6352

Prof. Rogéria Rocha Gonçalves, University of São Paulo, Faculty of Philosophy, Sciences and Literature, Ribeirão Preto, Brazil. https://orcid.org/0000-0001-5540-7690

Editorial

The current issue of Eclética Química, the third of 2023, contains original articles focusing on natural products, metal complexes and one dealing with the efficiency of two approaches on scientific literacy and students' regulated learning. The first article is dedicated to the evaluation of the chemical differences among organs and seasonal chemical variability of the aerial parts of *Phyllanthus niruri* L. It was used ultra-high performance liquid chromatography with photodiode array ultraviolet to determine the chromatographic profile and gallic acid, corilagin, and ellagic acid contents. The components contents in different parts of the plant and the seasonal effect are discussed. *P. niruri* L. is largely used in folk medicine for several diseases as hepatitis, diabetes, urinary tract disorders, and kidney stone treatment. Follows an article discussing the effect of the Cooperative Integrated Reading and Composition (CIRC) approach on scientific literacy and students' regulated learning in colligative properties of solution whose efficiency was compared with Direct Instructional Teaching Method (DITM). Increased scientific literacy and self-regulated learning was found for students with CIRC and that the CIRC approach can be applied to other chemistry topics. In the third article, the synthesis of six complexes of copper, nickel, and cobalt with a new bidentate N_2 donor Schiff base was described. Depending on the ligand L, ML_2 and ML_1 complexes were formed which were characterized by metal analysis, XRD, IR, UV-Vis, NMR spectra, magnetic susceptibility and molar conductance. The antioxidant, antibacterial and antifungal activity of the ligands and compounds were investigated. Afterwards, the readers find a theoretical study via *in silico* approach of phytochemicals from *Scilla natalensis* used for treating schistosomiasis. Countries with low sanitation awareness have a strong social and economic impact due to this neglected tropical disease, caused by blood fluke with such rate that the death is alarming. The results may open a door for the design of novel better efficient drug-like molecules. Closes this issue the study of extracted seed oil from *Carica papaya* L. that has chemical and physical properties comparable to other commercially available vegetable oils. The lipid profile was obtained, and thermal characterization performed allowed to conclude that *in natura* oil oleic and palmitic fatty acids are predominant. The dependence on the sample mass and purge gases resulted in several kinetic patterns and the isoconversional methods were used to determine the activation energy.

The Editor and the Editorial team would like to recognize the dedication and effort of authors and reviewers to successful conclude this issue with very interesting articles. Concomitantly, we invite authors, readers, and reviewers to visit the page of the journal and contribute to the next issue and to the two special issues in honor to the Centenary of Debye–Hückel Theory and the Centenary of the famous studies developed by Johannes Nicolaus Brönsted, Thomas Martins Lowry and Gilbert Newton Lewis on the acid-base concepts, continuing the Svante Arrhenius' work.

Assis Vicente Benedetti
Editor-in-Chief of Eclética Química

Digital Databases

DOAJ DIRECTORY OF OPEN ACCESS JOURNALS

SciFINDER® A CAS SOLUTION

FSTA®

REDIB

latindex

Scopus®

Google Scholar

redalyc LA HEMEROTECA CIENTÍFICA EN LÍNEA

evisa.

EBSCO Discovery Service

biblat Bibliografía Latinoamericana en revistas de investigación científica y social

International Nuclear Information System

IAEA | INIS

Supporters

Instituto de Química

unesp UNIVERSIDADE ESTADUAL PAULISTA "JÚLIO DE MESQUITA FILHO"

ABEC® BRASIL Associação Brasileira de Editores Científicos

CNPq

*Click on the images to follow the links.
EBSCO and FSTA has no link available. The address is for subscribers only.

INSTRUCTIONS FOR AUTHORS

BEFORE YOU SUBMIT

1. Check Eclet. Quim.'s focus and scope

Eclética Química is a peer-reviewed quarterly publication supported by Institute of Chemistry of São Paulo State University (UNESP). It publishes original researches as articles, reviews and short reviews in **all areas of Chemistry**.

2. Types of papers

    a. Original articles
    b. Reviews
    c. Short reviews
    d. Communications
    e. Technical notes
    f. Articles in education in chemistry and chemistry-related areas

Manuscripts submitted for publication as full articles and communications must contain original and unpublished results and should not have been submitted elsewhere either partially or whole. Manuscript originating from scientific initiation, course completion monographs, Dissertations or PhD Thesis already deposited in Universities' repositories is accepted without considering it a violation of the journal's rules. Eclética Química also accepts preprints.

a. Original articles

The manuscript must be organized in sections as follows:

1. Introduction
2. Experimental
3. Results and Discussion
4. Conclusions
References

Sections titles must be written in bold and sequentially numbered; only the first letter should be in uppercase letter. Subsections, numbered as exemplified, should be written in normal and italic letters; only the first letter should be in uppercase letter.

Example:

1. Introduction
1.1 History

2. Experimental
2.1 Surface characterization
2.1.1 Morphological analysis

b. Reviews
Review articles should be original and present state-of-the-art overviews in a coherent and concise form covering the most relevant aspects of the topic that is being revised and indicate the likely future directions of the field. Therefore,

before beginning the preparation of a Review manuscript, send a letter (one page maximum) to the Editor with the subject of interest and the main topics that would be covered in the Review manuscript. The Editor will communicate his decision in two weeks. Receiving this type of manuscript does not imply acceptance to be published in **Eclet. Quim.** It will be peer-reviewed.

c. Short reviews

Short reviews should present an overview of the state-of-the-art in a specific topic within the scope of the journal and limited to 5,000 words. Consider a table or image as corresponding to 100 words. Before beginning the preparation of a Short Review manuscript, send a letter (one page maximum) to the Editor with the subject of interest and the main topics that would be covered in the Short Review manuscript.

d. Communications

Communications should cover relevant scientific results and are limited to 1,500 words or three pages of the journal, not including the title, authors' names, figures, tables and references. However, Communications suggesting fragmentation of complete contributions are strongly discouraged by Editors.

e. Technical notes

Descriptions of methods, techniques, equipment or accessories developed in the authors' laboratory, as long as they present chemical content of interest. They should follow the usual form of presentation, according to the peculiarities of each work. They should have a maximum of 25 pages, including figures, tables, diagrams, etc.

f. Articles in education in chemistry and chemistry-correlated areas

Research manuscript related to undergraduate teaching in Chemistry and innovative experiences in undergraduate and graduate education. They should have a maximum of 25 pages, including figures, tables, diagrams, and other elements.

3. Special issues

Special issues with complete articles dedicated to Symposia and Congresses and to special themes or in honor of scientists with relevant contributions in Chemistry and correlate areas can be published by **Eclet. Quim.** under the condition that a previous agreement with Editors is established. All the guides of the journal must be followed by the authors.

4. Approval

Ensure all authors have seen and approved the final version of the article prior to submission. All authors must also approve the journal you are submitting to.

ETHICAL GUIDELINES

Before starting the submission process, please be sure that **all ethical aspects mentioned below were followed**. Violation of these ethical aspects may preclude authors from submitting or publishing articles in **Eclet. Quim.**

a. Coauthorship: The corresponding author is responsible for listing as coauthors only researchers who have really taken part in the work, for informing them about the entire manuscript content and for obtaining their permission to submit and publish it.
Two Corresponding authors for an article may be accepted provided both have equivalent contribution to the article, being one of them permanent in the Institution.

b. Nonauthors: Explicit permission of a nonauthor who has collaborated with personal communication or discussion to the manuscript being submitted to **Eclet. Quim.** must be obtained before being cited.

c. Unbiased research: Authors are responsible for carefully searching for all the scientific work relevant to their reasoning irrespective of whether they agree or not with the presented information.

d. Citation: Authors are responsible for correctly citing and crediting all data taken from other sources. This requirement is not necessary only when the information is a result of the research presented in the manuscript being submitted to **Eclet. Quim.**

e. Direct quotations: The word-for-word reproduction of data or sentences as long as placed between quotation marks and correctly cited is not considered ethical deviation when indispensable for the discussion of a specific set of data or a hypothesis.

f. Do not cite: Master's Degree dissertations and PhD theses are not accepted; instead, you must cite the publications resulted from them.

g. Plagiarism: Plagiarism, self-plagiarism, and the suggestion of novelty when the material was already published are unaccepted by **Eclet. Quim.** Before reviewing a manuscript, the **Turnitin antiplagiarism software** will be used to detect any ethical deviation.

h. Simultaneous submissions: of the same manuscript to more than one journal is considered an ethical deviation and is conflicted to the declaration has been done below by the authors.

i. Studies with humans or other animals: Before submitting manuscripts involving human beings, materials from human or animals, the authors need to confirm that the procedures established, respectively, by the institutional committee on human experimentation and Helsinki's declaration, and the recommendations of the animal care institutional committee were followed. Editors may request complementary information on ethical aspects.

COPYRIGHT NOTICE

PUBLICATION CHARGES

Eclética Química is supported by the Institute of Chemistry/UNESP and publication is free of charge for authors.

MANUSCRIPT PREPARATION

COVER LETTER

We provide a template to help you prepare your cover letter. To download it, click **here**.

The cover letter MUST include:

1. Identification of authors

a. The authors' full names (they must be written in full and complete, separated by comma)

João M. José	Incorrect
J. M. José	Incorrect
João Maria José	Correct!

b. E-mail addresses and affiliations (**neither more nor less than two instances**) of all authors;
c. ORCID ID links;
d. A plus sign (+) indicating the corresponding author and your contact phone number.

Example:

Author Full Name[1+], Author Full Name[2]

1. University, Faculty or Institute, City, Country.
2. Company, Division or Sector or Laboratory, City, Country.

+ Author 1: address@mail.com, ORCID: https://orcid.org/xxxx-xxxx-xxxx-xxxx, Phone: +xx xxxxxxxx
Author 2: address@mail.com, ORCID: https://orcid.org/xxxx-xxxx-xxxx-xxxx, Phone: +xx xxxxxxxx

2. Authors' contribution

We request authors to include author contributions according to CRediT taxonomy standardized contribution descriptions. CRediT (Contributor Roles Taxonomy) is a high-level taxonomy, including 14 roles, that can be used to represent the roles typically played by contributors to scientific scholarly output. The roles describe each contributor's specific contribution to the scholarly output.

a. Please, visit this link (https://casrai.org/credit/) to find out which role(s) the authors fit into;
b. Do not modify the role names; do not write "all authors" in any role. Do not combine two or more roles in one line.
c. If there are any roles that no author has engaged in (such as funding in papers that were not funded), write "Not applicable" in front of the name of the role;
d. Write the authors' names according to the **American Chemistry Society (ACS) citation style**.

Example:

Conceptualization: Foster, J. C.; O'Reilly, R. K.
Data curation: Varlas, S.; Couturaud, B.; Coe, J.; O'Reilly, R. K.
Formal Analysis: Foster, J. C.; Varlas, S.
Funding acquisition: Not applicable.
Investigation: Foster, J. C.; O'Reilly, R. K.
Methodology: Coe, J.; O'Reilly, R. K.

Project administration: O'Reilly, R. K.
Resources: Coe, J.
Software: Not applicable.
Supervision: O'Reilly, R. K.
Validation: Varlas, S.; Couturaud, B.
Visualization: Foster, J. C.
Writing – original draft: Foster, J. C.; Varlas, S.; Couturaud, B.; Coe, J.; O'Reilly, R. K.
Writing – review & editing: Foster, J. C.; Varlas, S.; Couturaud, B.; Coe, J.; O'Reilly, R. K.

3. Indication of reviewers

We kindly ask the authors to suggest **five** suitable reviewers, providing full name, affiliation, and email.

4. Other information

a. The authors must write one paragraph remarking the novelty and relevance of the work;
b. The corresponding author must declare, on behalf of the other authors, that the manuscript being submitted is original and its content has not been published previously and is not under consideration for publication elsewhere;
c. The authors must inform if there is any conflict of interest.

5. Acknowledgements and funding

Acknowledgements and funding information will be requested after the article is accepted for publication.

6. Data availability statement

A data availability statement informs the reader where the data associate with your published work is available, and under what conditions they can be accessed. Therefore, authors must inform if:

Data will be available upon request;
All dataset were generated or analyzed in the current study; or
Data sharing is not applicable.

MANUSCRIPT

We provide a template to help you prepare your manuscript. To download it, click **here**.

1. General rules

Only manuscripts written in English are accepted. British or American usage is acceptable, but they should not be mixed. Non-native English speakers are encouraged to have their manuscripts professionally revised before submission.

Manuscripts must be sent in editable files as *.doc, *.docx or *.odt. The text must be typed using font style Times New Roman and size 12. Space between lines should be 1.5 mm and paper size A4, top and bottom margins 2.5 cm, left and right margins 2.0 cm.

All contributions must include an **abstract** (170 words maximum), t**hree to five keywords** and a **graphical abstract** (8 cm wide × 8 cm high).

Appendix should be included at the end of the main text of the manuscript.

Supplementary information: all type of articles accepts supplementary information (SI) that aims at complementing the main text with material that, for any reason, cannot be included in the article.

TITLE

The title should be concise, explanatory and represent the content of the work. The title must have only the first letter of the sentence in uppercase. The following are not allowed: acronyms, abbreviations, geographical location of the research, en or em dashes (which must be replaced by a colon). Titles do not have full point.

ABSTRACT

Abstract is the summary of the article. The abstract must be written as a running text not as structured topics, but its content should present background, objectives, methods, results, and conclusion. It cannot contain citations. The text should be written in a single paragraph with a **maximum of 170 words**.

KEYWORDS

Keywords are intended to make it easier for readers to find the content of your text. As fundamental tools for database indexing, they act as a gateway to the text. The correct selection of keywords significantly increases the chances that a document will be found by researchers on the topic, and consequently helps to promote the visibility of an article within a myriad of publications.

FIGURES, TABLES AND EQUATIONS

Figures, tables and equations must be written with initial capital letter followed by their respective number and period, in bold, without adding zero "**Table 1**", preceding an explanatory title. Tables, Figures and Equations should appear after the first citation and should be numbered according to the ascending order of appearance in the text (1, 2, 3...).

Figures, tables, schemes and photographs already published by the same or different authors in other publications may be reproduced in manuscripts of **Eclet. Quim.** only with permission from the editor house that holds the copyright.

Nomenclature, abbreviations, and symbols should follow IUPAC recommendations.

DATA AVAILABILITY STATEMENT

The data availability statement informs the reader where the data associate with your work is available, and under what conditions they can be accessed. They also include links (where applicable) to the data set.

    a. The data are available in a data repository (cite repository and the DOI of the deposited data);
    b. The data will be available upon request;
    c. All data sets were generated or analyzed in the current study;
    d. Data sharing is not applicable (in cases where no data sets have been generated or analyzed during the current study, it should be declared).

GRAPHICAL ABSTRACT

The graphical abstract must summarize the manuscript in an interesting way to catch the attention of the readers. As already stated, it must be designed with 8 cm wide $\times$ 8 cm high, and a 900-dpi resolution is mandatory for this journal. It must be submitted as *.jpg, *.jpeg, *.tif or *.ppt files as supplementary file.

We provide a template to help you prepare your GA. To download it, click **here**.

SUPPLEMENTARY INFORMATION

When appropriate, important data to complement and a better comprehension of the article can be submitted as Supplementary File, which will be published online and will be made available as links in the original article. This might include additional figures, tables, text, equations, videos or other materials that are necessary to fully document the research contained in the paper or to facilitate the readers' ability to understand the work.

Supplementary material should be presented in appropriate .docx file for text, tables, figures and graphics. All supplementary figures, tables and videos should be referred in the manuscript body as "Table S1, S2…", "Fig. S1, S2…" and "Video S1, S2 …".

At the end of the main text the authors must inform: This article has supplementary information.

Supplementary information will be located following the article with a different DOI number from that of the article, but easily related to it.

CITATION STYLE GUIDE

From 2021 on, the journal will follow the **ACS citation style**.

Indication of the sources is made by authorship and date. So, the reference list is organized alphabetically by author.

Each citation consists of two parts: the in-text citation, which provides brief identifying information within the text, and the reference list, a list of sources that provides full bibliographic information.

We encourage the citation of primary research over review articles, where appropriate, in order to give credit to those who first reported a finding. Find out more about our commitments to the principles of San Francisco Declaration on Research Assessment (DORA).

What information you must cite?

 a. Exact wording taken from any source, including freely available websites;
 b. Paraphrases of passages;
 c. Summaries of another person's work;
 d. Indebtedness to another person for an idea;
 e. Use of another researchers' work;
 f. Use of your own previous work.

You do not need to cite **common knowledge**.

Example:
Water is a tasteless and odorless liquid at room temperature (common knowledge, no citation needed)

In-text citations
You can choose the cite your references within or at the end of the phrase, as showed below.

Within the cited information:
 One author: Finnegan (2004) states that the primary structure of this enzyme has also been determined.
 Two authors: Finnegan and Roman (2004) state that the structure of this enzyme has also been determined.
 Three or more authors: Finnegan *et al.* (2004) state that the structure of this enzyme has also been determined.
 PREPRINT Reference: Finnegan et al. (2004, PREPRINT) state that the structure of this enzyme has also been determined.

At the end of the cited information:
 One author: The primary structure of this enzyme has also been determined (Finnegan, 2004).
 Two authors: The primary structure of this enzyme has also been determined (Finnegan and Roman, 2004).
 Three or more authors: The primary structure of this enzyme has also been determined (Finnegan *et al.*, 2004).
 PREPRINT Reference: The primary structure of this enzyme has also been determined (Finnegan *et al.*, 2004, PREPRINT).

If you need to cite more than one reference in the same brackets, separate them with semicolon and write them in alphabetic order:

The primary structure of this enzyme was determined (Abel *et al.*, 2011; Borges, 2004; Castro *et al.*, 2021).

Bibliographic references

Article from scientific journals
Foster, J. C.; Varlas, S.; Couturaud, B.; Coe, J.; O'Reilly, R. K. Getting into Shape: Reflections on a New Generation of Cylindrical Nanostructures' Self-Assembly Using Polymer Building Block. *J. Am. Chem. Soc*. **2019**, *141* (7), 2742−2753. https://doi/10.1021/jacs.8b08648

Book
Hammond, C. *The Basics of Crystallography and Diffraction*, 4th ed.; International Union of Crystallography Texts on Crystallography, Vol. 21; Oxford University Press, 2015.

Book chapter
Hammond, C. Crystal Symmetry. In *The Basics of Crystallography and Diffraction*, 4th ed.; International Union of Crystallography Texts on Crystallography, Vol. 21; Oxford University Press, 2015; pp 99−134.

Book with editors
Mom the Chemistry Professor: Personal Accounts and Advice from Chemistry Professors Who Are Mothers, 2nd ed.; Woznack, K., Charlebois, A., Cole, R. S., Marzabadi, C. H., Webster, G., Eds.; Springer, 2018.

Website
ACS Publications Home Page. https://pubs.acs.org/ (accessed 2019-02-21).

Document from a website
American Chemical Society, Committee on Chemical Safety, Task Force for Safety Education Guidelines. *Guidelines for Chemical Laboratory Safety in Academic Institutions*. American Chemical Society, 2016. https://www.acs.org/content/dam/acsorg/about/governance/committees/chemicalsafety/publications/acs-safety-guidelines-academic.pdf (accessed 2019-02-21).

Conference proceedings
Nilsson, A.; Petersson, F.; Persson, H. W.; Jönsson, H. Manipulation of Suspended Particles in a Laminar Flow. In Micro Total Analysis Systems 2002, Proceedings of the μTAS 2002 Symposium, Nara, Japan, November 3−7, 2002; The Netherlands, 2002; pp 751−753. https://doi.org/10.1007/978-94-010-0504-3_50

Governmental and legislation information
Department of Commerce, United States Patent and Trademark Office. Section 706.02 Rejection of Prior Art [R-07.2015]. *Manual of Patent Examining Procedure (MPEP)*, 9th ed., rev. 08.2017, last revised January 2018. https://www.uspto.gov/web/offices/pac/mpep/s706.html#d0e58220 (accessed 2019-03-20).

PREPRINT
Fugivara, C. S.; Guilherme, L. H.; Benedetti, A. V. Microstructure of a passive film galvanostatically grown on stainless steel. ChemRxiv. [PREPRINT] September 20, 2021. https://doi.org/10.26434/chemrxiv.xxxxxx.v1 (accessed 2021-12-19).

Patent
Lois-Caballe, C.; Baltimore, D.; Qin, X.-F. Method for Expression of Small RNA Molecules within a Cell. US 7 732 193 B2, 2010.

Streaming data
American Chemical Society. Game of Thrones Science: Sword Making and Valyrian Steel. *Reactions*. YouTube, April 15, 2015. https://www.youtube.com/watch?v=cHRcGoje4j4 (accessed 2019-02-28).

For more information, you can access the ACS Style Quick Guide and the Williams College LibGuides.

SUBMITTING YOUR MANUSCRIPT

The corresponding author should submit the manuscript online by clicking **here**. If you are a user, register by clicking **here**.

At the **User home** page, click in **New submission**.

In Step 1, select a section for your manuscript, verify one more time if you followed all these rules in **Submission checklist**, add Comments for the Editor if you want to, and click Save and continue.

In Step 2, you will **upload your manuscript**. Remember it will pass through a double-blind review process. So, do not provide any information on the authorship.

In Step 3, enter **submission's metadata**: authors' full names, valid e-mail addresses and ORCID ID links (with "http" not "https"). Add title, abstract, contributors and supporting agencies, and the list of references.

In Step 4, upload the **cover letter**, the **graphical abstract** and other **supplementary material** you want to include in your manuscript.

In Step 5, you will be able to check all submitted documents in the **File summary**. If you are certain that you have followed all the rules until here, click in **Finish submission**.

REVIEW PROCESS

The time elapsed between the submission and the first response of the reviewers is around three months. The average time elapsed between submission and publication is around seven months.

Resubmission (manuscripts "rejected in the present form" or subjected to "revision") must contain a letter with the responses to the comments/criticism and suggestions of reviewers/editors should accompany the revised manuscript.

All modifications made to the original manuscript must be highlighted.

If you want to check our Editorial process, click **here**.

EDITOR'S REQUIREMENTS

Authors who have a manuscript accepted in **Eclet. Quim.** may be invited to act as reviewers.

Only the authors are responsible for the correctness of all information, data and content of the manuscript submitted to **Eclet. Quim.** Thus, the Editors and the Editorial Board cannot accept responsibility for the correctness of the material published in **Eclet. Quim.**

Proofs

After accepting the manuscript, **Eclet. Quim.** technical assistants will contact you regarding your manuscript page proofs to correct printing errors only, i.e., other corrections or content improvement are not permitted. The proofs shall be returned in three working days (72 h) via email.

Appeal

Authors may only appeal once about the decision regarding a manuscript. To appeal against the Editorial decision on your manuscript, the corresponding author can send a rebuttal letter to the editor, including a detailed response to any comments made by the reviewers/editor. The editor will consider the rebuttal letter, and if dimmed appropriate, the manuscript will be sent to a new reviewer. The Editor decision is final.

Contact

If you have any question, please contact our team:

Prof. Assis Vicente Benedetti
Editor-in-Chief
assis.v.benedetti@unesp.br

Letícia Amanda Miguel
Technical support
ecletica@ctrlk.com.br

SUMMARY

ARTICLES IN EDUCATION IN CHEMISTRY AND CHEMISTRY-CORRELATED AREAS

ORIGINAL ARTICLES

Chemical variability of phenolic compounds in *Phyllanthus niruri*

Ingrid Albrecht[1] ✉, Natália Coelho da Silva[1] ✉, Flávio Alexandre Carvalho[1] ✉, Fernando Bombarda Oda[1] ✉, André Gonzaga dos Santos[1+]

1. São Paulo State University, School of Pharmaceutical Sciences, Araraquara, Brazil.

+Corresponding author: André Gonzaga dos Santos, **Phone:** +55 16 33016994, **Email address:** andre.gonzaga@unesp.br

ABSTRACT: *Phyllanthus niruri* L. has been used in folk medicine to treat hepatitis, diabetes, urinary tract disorders, and renal calculi. Here, the chemical differences among its organs and the seasonal chemical variability in the aerial parts were evaluated. The chromatographic profile and gallic acid, corilagin, and ellagic acid contents were determined by ultrahigh performance liquid chromatography with photodiode array ultraviolet (UHPLC-PDA/UV) method, which showed adequate resolution and a short analysis time. The contents of gallic acid, corilagin and ellagic acid in the leaf extract were 2.8, 6.7 and 7.9%, respectively, whilst their contents in the stem and root extracts were lower ($< 0.2\%$). Thus, using the whole plant or aerial parts for herbal medicines can produce different biological responses. The chemical profile of the aerial parts showed only quantitative variation over 12 months. The seasonal content of gallic acid showed no correlation with monthly rainfall, but the contents of corilagin and ellagic acid were positively correlated with rainfall.
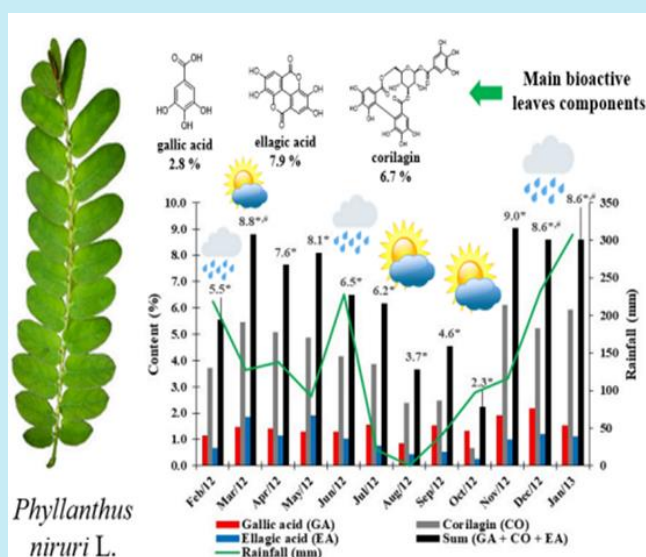
1. Introduction

Phyllanthus niruri Linn. (Euphorbiaceae) is an herbaceous plant found in subtropical and tropical areas in Latin America and Asia and known as *quebra-pedra* in Brazil or *chanca-piedra* in Latin America (Klein-Junior *et al*., 2017; Moreira *et al*., 2013). In folk medicine, it is mainly used to treat hepatitis, diabetes, and urinary tract disorders (bladder and kidney), especially for removing kidney stones (Bagalkotkar *et al*., 2006; Santos *et al*., 1995; Wang *et al*., 1995). The traditional use of its aerial parts in urolithiasis treatment and the results of preclinical and clinical trials using its aqueous extract have confirmed its action in preventing the formation of calcium oxalate renal stones. In addition, its extracts also presented antispasmodic, antihyperalgesic, anti-Alzheimer's disease, antioxidant, hepatoprotective, hypoglycemic, anti-inflammatory, antiviral, and antimicrobial activities (Bagalkotkar *et al*., 2006; Barros *et al*., 2006; Moreira *et al*., 2013; Pathania *et al*., 2022; Rajamanickam and Manju, 2022).

Thus, literature data support its therapeutic use as herbal medicine. The Brazilian Health Surveillance Agency (ANVISA, 2021) included aqueous and ethanolic preparations of its dried aerial parts or the whole plant in the *Brazilian Herbal Medicines Form* (2nd edition), indicated for the treatment of urinary disorders.

P. niruri secondary metabolites (Fig. 1) include flavonoids as quercetin (**1**) and quercitrin (**2**), hydrolysable tannins as corilagin (**3**) and geraniin (**4**), phenolic acids as gallic acid (**5**) and ellagic acid (**6**), securinine-type alkaloids as nirurine (**7**) and securinine (**8**), lignans as phyllanthin (**9**) and phyltetralin (**10**), monoterpenes as *p*-cymene (**11**) and limonene (**12**), and triterpenes as lupeol (**13**) and phyllantheol (**14**) (Kumar *et al*., 2017).

Seasonality is one of the essential factors in the variability of secondary plant metabolism since the amount and, sometimes, even the nature of the secondary metabolites are variable during the year, including their bioactivity. The chemical differences among plant organs are also well-established for many species (Gobbo-Neto and Lopes, 2007; Kiazolu *et al*., 2016).

Seasonality, the circadian cycle, organ type, location, environmental factors, temperature, rainfall, soil composition, relative humidity, and processing are essential factors that influence the secondary plant metabolites content, and consequently, their bioactivity (Carvalho *et al*., 2021; Gobbo-Neto and Lopes, 2007; Kiazolu *et al*., 2016). This work aimed to contribute to the standardization of *P. niruri* herbal medicines, through the evaluation of the seasonal dynamics of its phenolic compounds and the comparison of the chemical composition of its different organs, including the quantification of the pharmacopeial chemical markers corilagin (main tannin) and gallic acid (ANVISA, 2021). The chemical analyzes were performed by a developed ultrahigh performance liquid chromatography with photodiode array ultraviolet (UHPLC-PDA/UV) method.
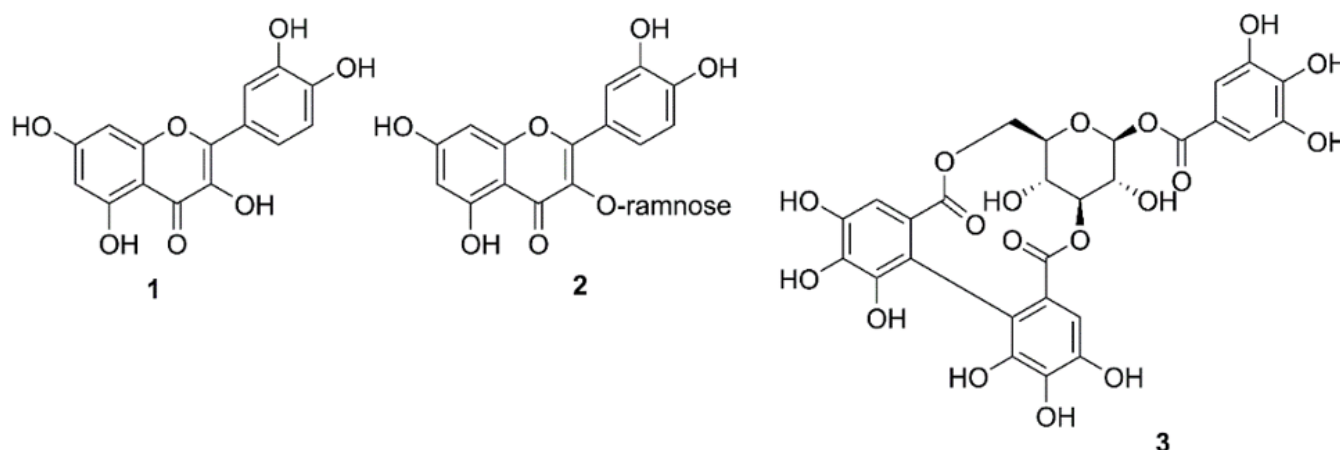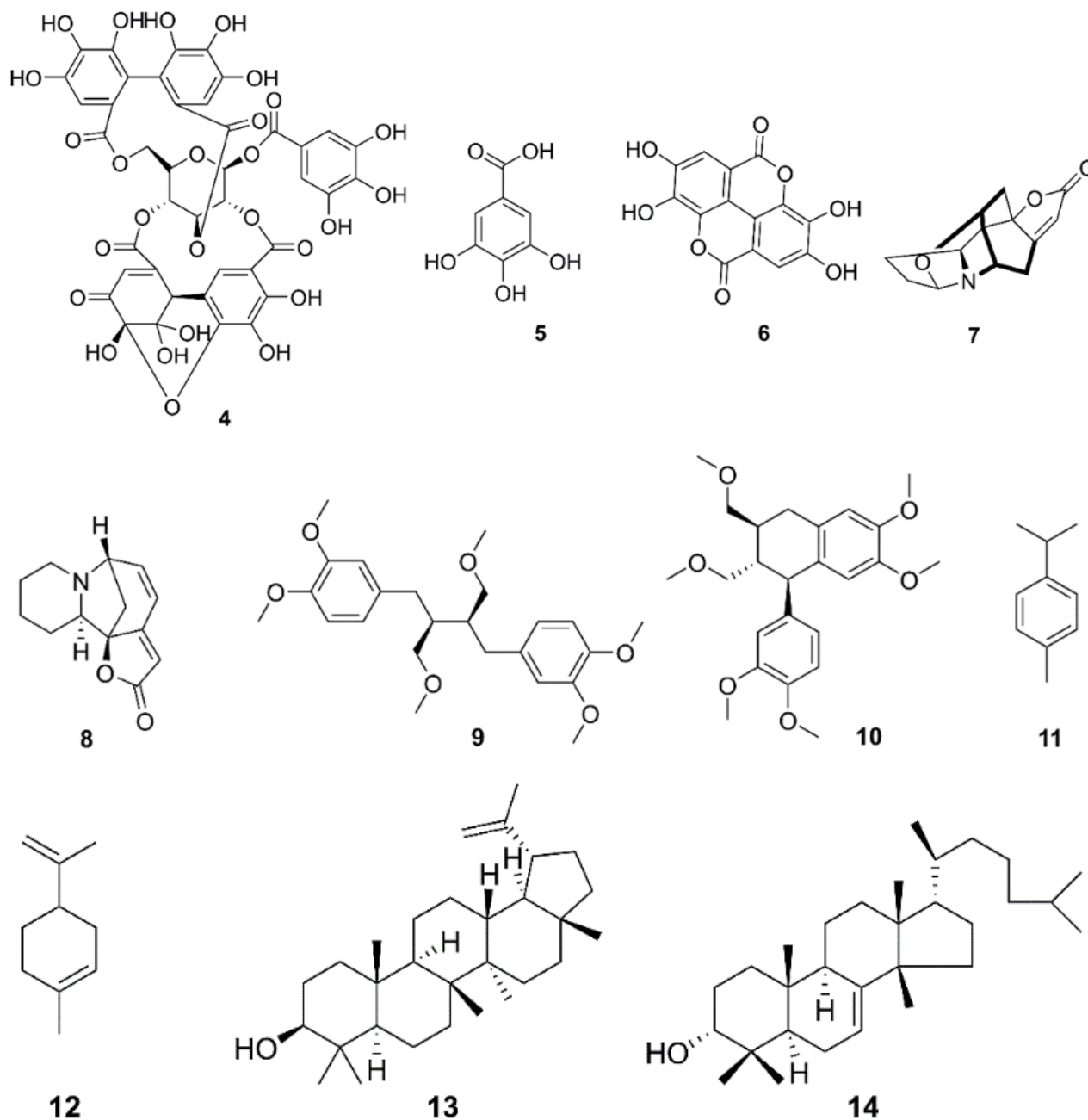
Figure 1. Chemical structure of main components identified in *P. niruri* aerial parts.

2. Experimental

2.1 Reagents and solutions

Ultrapure water (Elga System, Brazil) was used in this work. Acetonitrile and methanol HPLC-grade were purchased from Merck (Germany). Chromatographic standards: gallic acid, corilagin (Chromadex, USA), ellagic acid (Sigma Aldrich, Brazil), and rutin (United States Pharmacopoeia, USA).

2.2 Plant material and extracts

The aerial parts (leaf plus stems) from six specimens of *P. niruri* were harvested monthly between February 2012 and January 2013 at Anidro Extrações do Brasil Ltda, Centroflora Group (Botucatu city, São Paulo state, Brazil, 22°87'33"6 S, 48°48'10"7 W). Leaves, stems, and roots were collected in August 2012 from the same specimens for comparison between the organs. This study was registered in the National System for the Management of Genetic Heritage and Associated

Traditional Knowledge of Brazil (SisGen) under the code AEFB157. Climatic data were acquired from the Meteorological Institute (INMET, 2013). The plant material was dried in an oven with air circulation at 60 °C for 5 days (Fanem 320 SE, Brazil), and the dried material was powdered in a knife mill (Tecnal TE-650, Brazil).

The dried and powdered *P. niruri* aerial parts (10.0 g) were extracted with deionized water (100.0 mL) at 65 °C for 1 h, in a stainless-steel extractor shaking every 10 min. The extractive solutions were concentrated at 60 °C under reduced pressure (Tecnal, Brazil).

2.3 Ultrahigh performance liquid chromatography with UHPLC-PDA/UV analysis

The leaf, stems, and roots extracts pretreatment (10.0 mg mL^{-1}, methanol: water 50:50) was performed by solid phase extraction using a C18 cartridge (500 mg; 6 mL; Perkin Elmer) and eluting with 4.0 mL of methanol: water 50:50 (high polar interfering compounds), and 5.0 mL of methanol: water 95:05 (sample concentrated in the phenolic compounds). After drying, 1.0 mL of the samples generated (2.0 mg mL^{-1}, methanol: water 60:40) were filtered through 0.22 µm membrane filters (Merck Millipore, Germany) for injection into the chromatographic system. The aerial part (leaf plus stems) extracts for seasonal evaluation (10.0 mg mL^{-1}, methanol: water 60:40) were only filtered through 0.22 µm membrane filters (Merck Millipore, Germany).

Chromatographic analyses were performed on a UPLC H-Class Acquity system (Waters, USA) equipped with a quaternary pump QSM, an FTN autosampler (20 µL-loop), column oven, and PDA detector, controlled with Empower 3 software. The analytical method was developed based on the transfer of HPLC chromatographic parameters (Colombo *et al.*, 2009) to UHPLC conditions according to the Acquity UPLC Columns Calculator software. The chromatographic resolution was improved through the experimental mobile and stationary phase modifications. Chromatographic conditions: HSS T3 column (100 × 2.1 mm i.d., 1.8 µm, Waters, USA) at 30 ± 1 °C; segmented linear gradient with acetic acid 0.1% (v/v) (solvent A) and acetonitrile (solvent B), 0–4.80 min 13–37% B, 4.81–5.20 min 37–100% B, 5.21–6.00 min 100% B, 6.01–6.40 min 100–13% B; 6.41–8.00 min 13% B; flow rate of 0.150 mL min^{-1};

samples were kept at 25 ± 1 °C, the pre injection volume was 346 µL and sample injection volume was 1.7 µL; monitoring detection at 267 nm.

Gallic acid, corilagin, and ellagic acid were quantified (triplicate) in the extract by the standard analytical curve using gallic acid (4.0–8.0 µg mL^{-1}), corilagin (15.0–150.0 µg mL^{-1}), and ellagic acid (7.0–63.0 µg mL^{-1}) in a UHPLC-PDA/UV. Theoretical limits of detection (LOD) and quantification (LOQ) were determined through the analytical curve equations (ANVISA, 2017). Gallic acid, ellagic acid, and corilagin contents were expressed as percentages (%, w/w) on a dry weight basis.

2.4 Data analysis

The UHPLC-PDA/UV results were presented as average ± standard error. Statistical analyses were performed through statistical software (GraphPad Prism, Version 3, USA) using analysis of variance followed by Tukey's post-test being *p*-values less than 0.05 significant, and Pearson correlation analysis being *p*-values less than 0.05 significant.

3. Results and discussion

Despite the relevance of harvesting medicinal plants (Gobbo-Neto and Lopes, 2007) and the extensive therapeutic use of *P. niruri*, there is only one report on seasonal variations of secondary metabolites in *P. niruri* described in the scientific literature (Couto *et al.*, 2013a). Here, the qualitative and quantitative chemical profiles of aqueous extracts from *P. niruri* aerial parts (six specimens) harvested during 12 months were determined. As well as the differences among plant organs.

The extract yield was higher in the aerial parts (15.8%), followed by the stems (6.2%) and roots (4.7%). Higher extract yields (w/w) were observed in February (14.3%), April (13.9%), and June (12.9%), whilst the lowest ones were observed in October, December (6.5%), January (7.5%), and September (8.0%). The extract yield monthly (Fig. 2) average was 10 ± 3%, and, according to the literature data, the aqueous extract yield of *P. niruri* ranged from 1.8 to 26.2% (Asare *et al.*, 2011; Giribabu *et al.*, 2014; Markom *et al.*, 2007). The monthly average temperature and rainfall did not correlate with the extract yield over the 12 months and thus did not influence the extract yield.
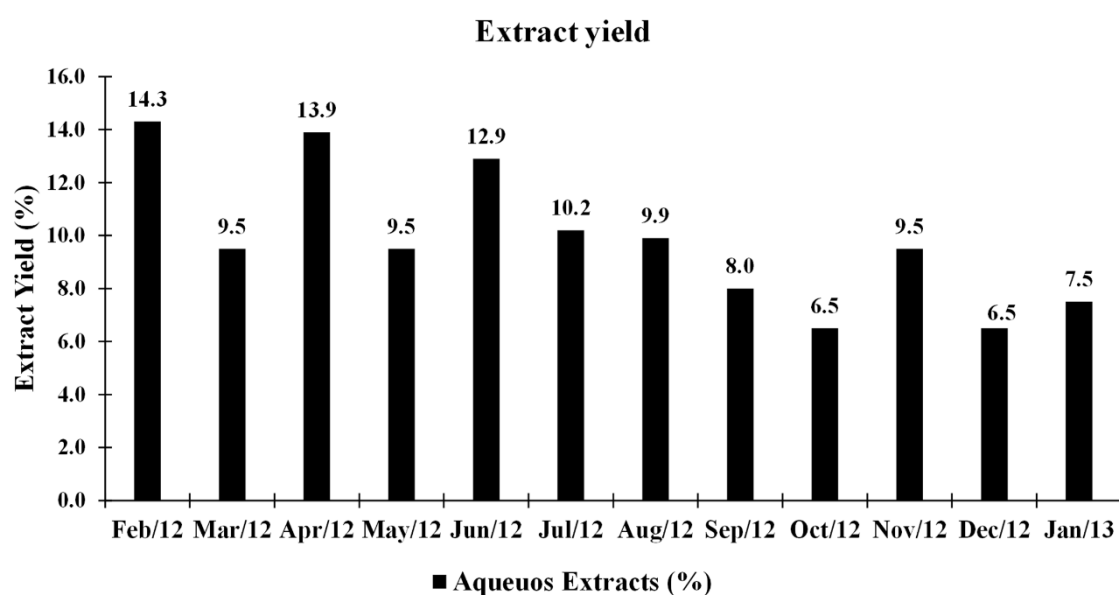
Figure 2. Seasonal variability of the yields (w/w, %) of the aqueous extracts of the aerial parts of *P. niruri* (six specimens mixed).

The phenolic compounds gallic acid, ellagic acid, and corilagin have demonstrated biological activities and may be related to the pharmacological activities of *P. niruri* extracts. According to the 6th edition of the *Brazilian Pharmacopeia* (ANVISA, 2019), gallic acid (minimum content 0.15%) and tannins (minimum content 6.5%) are the analytical markers for quality control of *P. niruri* aerial parts. The developed UHPLC-PDA/UV method showed suitable resolution (Rs > 1.5) for these compounds and others in a short analysis time, 6 min (plus 2 min of conditioning time). Linear regression analysis presented a good fit for gallic acid and corilagin according to r values greater than 0.99 (Table 1). Except for the *r* values of ellagic acid, the other values are in accordance with the minimum required for method validation by the National Health Surveillance Agency (ANVISA, 2017).

Table 1. Data from analytical curves of gallic acid, ellagic acid, and corilagin.

Patterns	Regression equation	r	LOD (µg/L)	LOQ (µg/L)
Gallic acid	$y = 3.28 \times 10^4 x + 2.82 \times 10^4$	0.9990	0.459	1.530
Corilagin	$y = 2.03 \times 10^4 x - 1.37 \times 10^4$	0.9996	0.946	3.153
Ellagic acid	$y = 3.35 \times 10^4 x - 1.89 \times 10^5$	0.9813	1.460	4.867

LOD: Limit of detection, LOQ: Limit of quantification, and *r*: Coefficient of correlation.

The UHPLC-PDA/UV analyzes determined the contents of gallic acid, corilagin, and ellagic acid in the leaf's aqueous extract as 2.8 ± 0.1, 6.7 ± 0.3, and 7.9 ± 0.4%, w/w in dry basis (Fig. 3a). The aqueous extract of the stems (Fig. 3b) showed content for gallic acid < 0.10 ± 0.05% and for corilagin 0.1 ± 0.0%; however, ellagic acid was not detected. In the root aqueous extract (Fig. 3c), only corilagin (0.2 ± 0.1%) was detected. The root's chemical profile was previously described as different from other organs (Couto *et al.*, 2013b).

The chemical variability between the organs may produce different pharmacological responses, which is a concern for herbal medicines (Gobbo-Neto and Lopes, 2007; Kiazolu *et al.*, 2016). Considering the contents of the analytical markers corilagin (tannin) and gallic acid, the leaves or aerial parts must be preferred instead of the whole plant to comply with the pharmacopeial specifications (ANVISA, 2021).

21
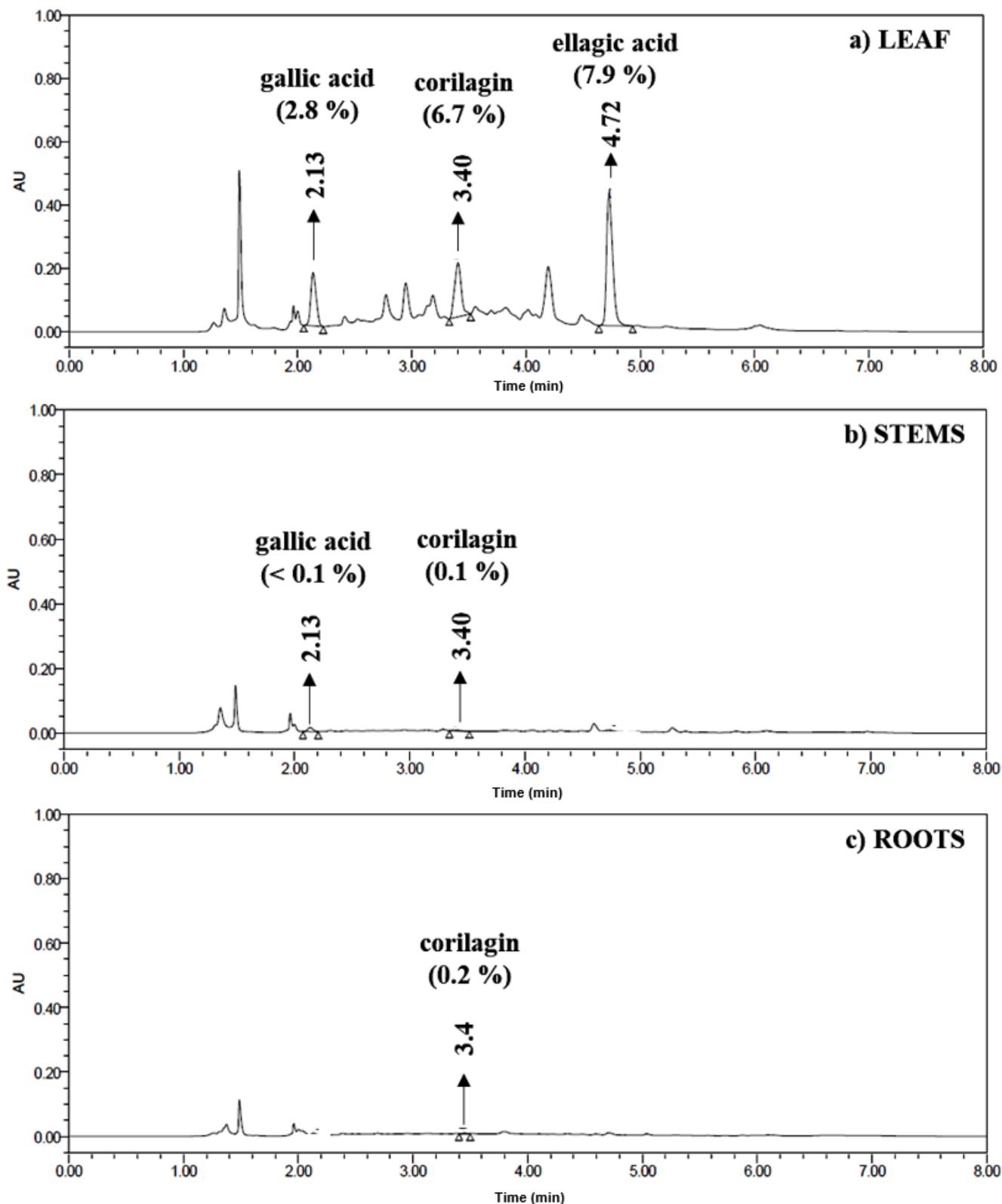
Figure 3. Chromatograms (UHPLC-PDA/UV) of *P. niruri* aqueous extracts: **(a)** leaf, **(b)** stems and **(c)** roots. Gallic acid, corilagin, and ellagic acid contents in the extracts were expressed as w/w (%) in dry basis. Chromatographic conditions: HSS T3 column (100 × 2.1 mm i.d., 1.8 μm) at 30 °C; segmented linear gradient with acetic acid aqueous solution 0.1% (A) and acetonitrile (B), 0–4.80 min 13–37% B, 4.81–5.20 min 37–100% B, 5.21–6.00 min 100% B, 6.01–6.40 min 100–13% B; 6.41–8.00 min 13% B; flow rate 0.150 mL min^{-1}; monitoring detection at 267 nm.

The UHPLC-PDA/UV chromatograms of the leaves presented identical qualitative profiles (t_R) in the seasonal chemical variability evaluation, except for minor peaks in some months (Fig. 4). For the time course analyzed here, the identified compounds in the extracts were gallic acid, corilagin, rutin, and ellagic acid (t_R: 2.1, 3.3, 4.0, and 4.7 min, respectively). The monthly extract contents of gallic acid, ellagic acid, and corilagin and the associated climatic factors data (monthly average rainfall) are shown in Fig. 5. The lower contents of these three compounds were observed from August to October 2012. Higher ellagic acid and corilagin contents were observed in December, January, and March to June, while the higher gallic acid content was noted in November and December. On the other hand, the gallic acid content was higher in *P. niruri* leaves in the dry season (winter), which was associated with pruning fluence (Couto *et al.*, 2013b).

The gallic acid monthly content presented no correlation with the monthly average rainfall through the Pearson correlation ($r = –0.3366$; $p > 0.05$). However, the contents of corilagin ($r = 0.6077$; $p < 0.05$), ellagic acid ($r = 0.7550$; $p < 0.01$), and the sum of these three compounds (SUM; $r = 0.7067$; $p < 0.05$) presented a positive correlation with the monthly average rainfall. We verified that corilagin and ellagic acid contents as well as sum showed significative ($p > 0.05$) decrease from August to October (2.3–4.6%), which may be due to lower rainfall index (< 100 mm), supporting the Pearson correlation and suggesting seasonal variability (Gobbo-Neto and Lopes, 2007; Kiazolu *et al.*, 2016). These results were similar to literature data, which reported a positive correlation between tannins/phenolic compounds and the rainy season for the leaves of *Eugenia uniflora* L. (Santos *et al.*, 2011). Moreover, the lowest contents of total tannins (condensed tannins) and total phenols in the *Stryphnodendron adstringens* (Mart.) Coville bark collected in Goiânia city, Goiás state (Brazil), were observed for months with the lowest rainfall (< 100 mm), which corroborates this study (Santos *et al.*, 2006). The Pearson correlation showed that the contents of gallic acid ($r = –0.2871$; $p > 0.05$), corilagin ($r = 0.0510$; $p > 0.05$), ellagic acid ($r = 0.2212$; $p > 0.05$), and sum ($r = 0.1663$; $p > 0.05$) did not demonstrate correlation with the monthly average temperature.
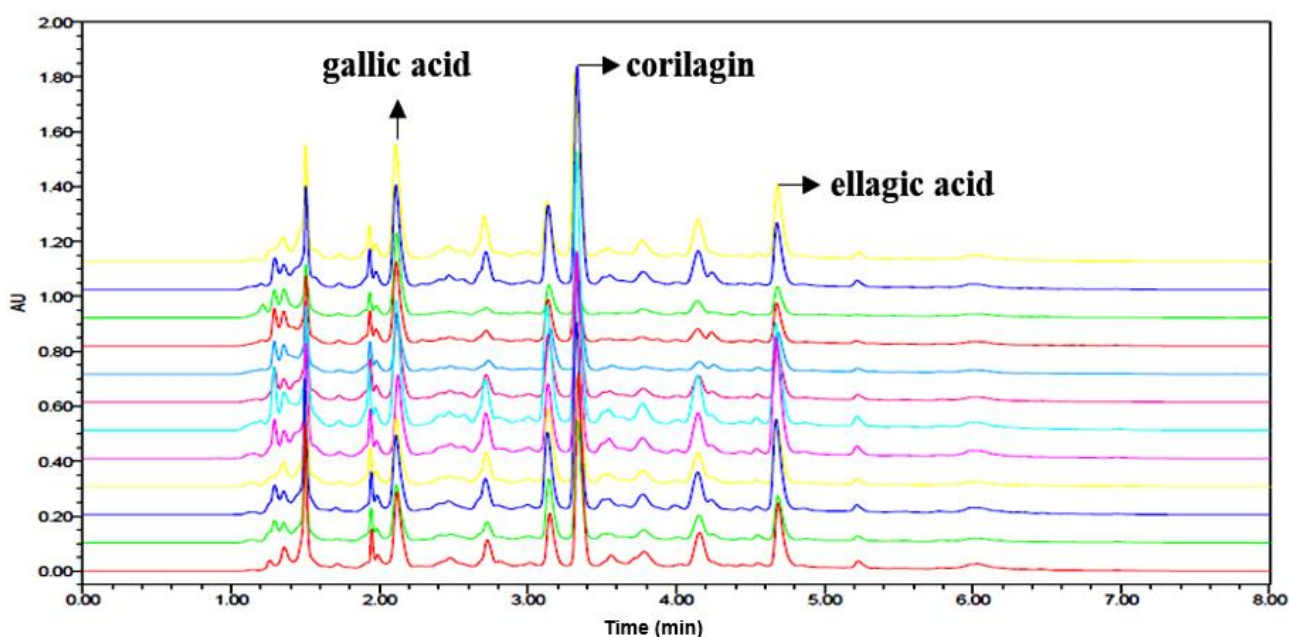

Figure 4. Chromatograms (UHPLC-PDA/UV) of *P. niruri* aqueous extracts of the aerial parts (six specimens) overlaid from February 2012 to January 2013 (t_R: gallic acid = 2.1 min, corilagin = 3.3 min, and ellagic acid = 4.7 min). Gallic acid, corilagin, and ellagic acid contents in the extracts were expressed as w/w (%) in dry basis. Chromatographic conditions: HSS T3 column (100 × 2.1 mm i.d., 1.8 μm) at 30 °C; segmented linear gradient with acetic acid aqueous solution 0.1% (A) and acetonitrile (B), 0–4.80 min 13–37% B, 4.81–5.20 min 37–100% B, 5.21–6.00 min 100% B, 6.01–6.40 min 100–13% B; 6.41–8.00 min 13% B; flow rate 0.150 mL min^{-1}; monitoring detection at 267 nm.
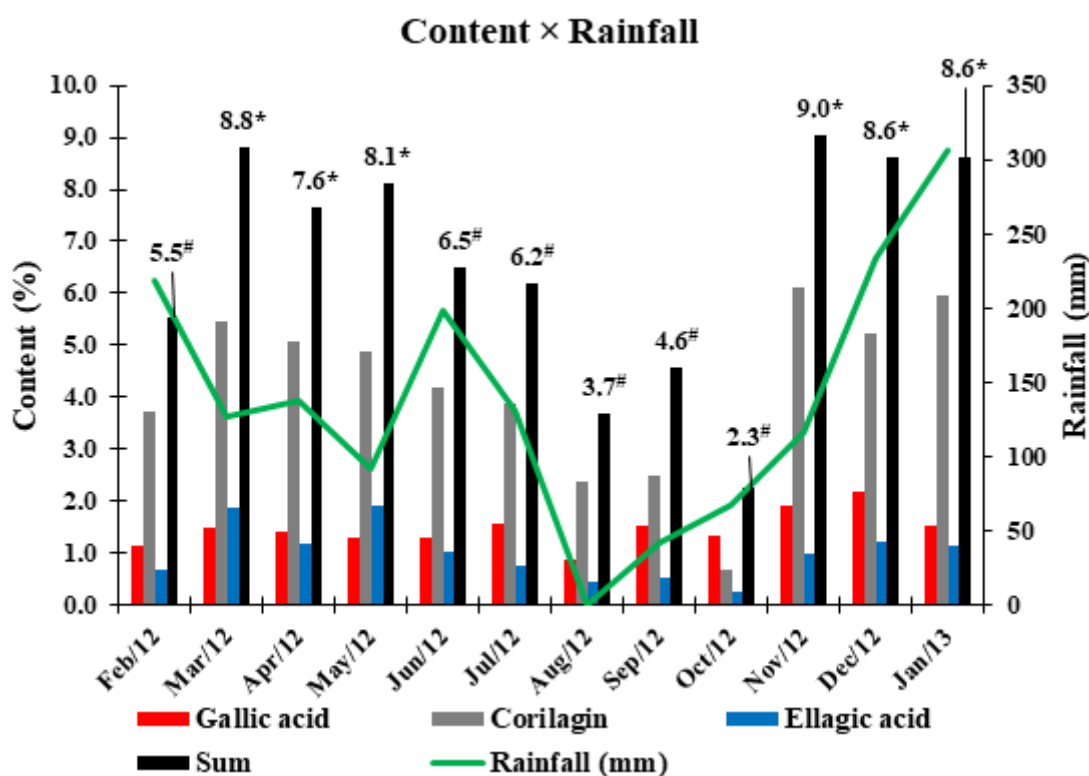
Figure 5. Seasonal variability of gallic acid (**5**), corilagin (**3**), ellagic acid (**6**) contents (w/w,%), and the sum of their contents of the aqueous extracts of the aerial parts of *P. niruri* (six specimens mixed) and climatic factors data - monthly average rainfall (mm). Samples were harvested from February 2012 to January 2013.
*Present statistical significance when compared with other months: $p < 0.05$, and #did not present statistical significance between themselves: $p > 0.05$.

4. Conclusions

The developed UHPLC-PDA/UV method showed adequate resolution and short analysis time, useful for research and quality control, following green chemistry principles. The qualitative and quantitative chemical profiles of the organs (leaves, stems, and roots) of *P. niruri* were different, showing that the use of the leaves, aerial parts (leaves plus stems), or whole plant (aerial parts plus roots) can produce different biological responses. According to the contents of the analytical markers in *P. niruri* leaves, stems, and roots, we suggest that the use of leaves or aerial parts is better than the whole plant, because only the leaves contents comply with the Brazilian pharmacopeial specifications, and the stems and roots have low contents of these compounds, or they were not detected.

The seasonal chemical profile of aerial parts showed only quantitative variation. The higher contents of ellagic acid and corilagin in November to January and March to June may be influenced by the rainy season, whilst gallic acid showed higher contents in November and December without correlation with the rainfall rate.

Authors' contribution

Conceptualization: Santos, A. G.
Data curation: Albrecht, I.; Silva, N. C.; Carvalho, F. A.; Oda, F. B.; Santos, A. G.
Formal Analysis: Carvalho, F. A.; Oda, F. B.; Santos, A. G.
Funding acquisition: Not applicable.
Investigation: Albrecht, I.; Silva, N. C.
Methodology: Albrecht, I.; Silva, N. C.
Project administration: Santos, A. G.
Resources: Albrecht, I.; Silva, N. C.; Santos, A. G.
Software: Albrecht, I.
Supervision: Santos, A. G.
Validation: Albrecht, I.; Oda, F. B.
Visualization: Santos, A. G.
Writing – original draft: Carvalho, F. A.; Oda, F. B.; Santos, A. G.
Writing – review & editing: Carvalho, F. A.; Oda, F. B.; Santos, A. G.

Data availability statement

Funding

Acknowledgments

References

Agência Nacional de Vigilância Brasileira (ANVISA). *Resolução da Diretoria Colegiada RDC Nº 166, de 24 de julho de 2017*. Dispõe sobre a validação de métodos analíticos e dá outras providências. Ministério da Saúde, 2017. http://antigo.anvisa.gov.br/documents/10181/2721567/RDC_166_2017_COMP.pdf/d5fb92b3-6c6b-4130-8670-4e3263763401 (accessed 2021-03-20).

Agência Nacional de Vigilância Brasileira (ANVISA). Resolução da Diretoria Colegiada - RDC Nº 298, de 12 de agosto de 2019. Dispõe sobre a aprovação da Farmacopeia Brasileira, 6ª edição. Ministério da Saúde, 2019. https://www.gov.br/anvisa/pt-br/assuntos/farmacopeia/farmacopeia-brasileira/arquivos/7984json-file-1 (accessed 2021-03-20)

Agência Nacional de Vigilância Brasileira (ANVISA). *Formulário de Fitoterápicos*: Farmacopeia Brasileira; ANVISA, 2021. https://www.gov.br/anvisa/pt-br/assuntos/farmacopeia/formulario-fitoterapico/arquivos/2021-fffb2-final-c-capa2.pdf (accessed 2021-03-20)

Asare, G.; Addo, P.; Bugyei, K.; Gyan, B.; Adjei, S.; Otu-Nyarko, L.; Wiredu, E.; Nyarko, A. Acute toxicity studies of aqueous leaf extract of *Phyllanthus niruri*. *Interdiscip. Toxicol*. **2011**, *4* (4), 206–210. https://doi.org/10.2478/v10102-011-0031-9

Bagalkotkar, G.; Sagineedu, S. R.; Saad, M. S.; Stanslas, J. Phytochemicals from *Phyllanthus niruri* Linn. and their pharmacological properties: a review. *J. Pharm. Pharmacol*. **2006**, *58* (12), 1559–1570. https://doi.org/10.1211/jpp.58.12.0001

Barros, M. E.; Lima, R.; Mercuri, L. P.; Matos, J. R.; Schor, N.; Boim, M. A. Effect of extract of *Phyllanthus niruri* on crystal deposition in experimental urolithiasis. *Urol. Res*. **2006**, *34* (6), 351–357. https://doi.org/10.1007/s00240-006-0065-1

Carvalho, F. A.; Oda, F. B.; Crevelin, E. J.; Crotti, A. E. M.; Santos, A. G. *Casearia sylvestris* Essential Oil Degradation Products Generated by Leaf Processing. *Chem. Biodivers*. **2021**, *18* (6), e2000880. https://doi.org/10.1002/cbdv.202000880

Colombo, R.; Batista, A. N. L.; Teles, H. L.; Silva, G. H.; Bomfim, G. C. C.; Burgos, R. C. R.; Cavalheiro, A. J.; Bolzani, V. S.; Silva, D. H. S.; Pelícia, C. R. Validated HPLC method for the standardization of *Phyllanthus niruri* (herb and commercial extracts) using corilagin as a phytochemical marker. *Biomed. Chromatogr*. **2009**, *23* (6), 573–580. https://doi.org/10.1002/bmc.1155

Couto, A. G.; Kunzler, M. L.; Spaniol, B.; Magalhães, P. M.; Ortega, G. G.; Petrovick, P. R. Chemical and technological evaluation of the *Phyllanthus niruri* aerial parts as a function of cultivation and harvesting conditions. *Rev. Bras. Farmacogn*. **2013a**, *23* (1), 36–43. https://doi.org/10.1590/S0102-695X2013005000002

Couto, A. G.; Kassuya, C. A. L.; Calixto, J. B.; Petrovick, P. R. Anti-inflammatory, antiallodynic effects and quantitative analysis of gallic acid in spray dried powders from *Phyllanthus niruri* leaves, stems, roots and whole plant. *Rev. Bras. Farmacogn*. **2013b**, *23* (1), 124–131. https://doi.org/10.1590/S0102-695X2012005000133

Giribabu, N.; Rao, P. V.; Kumar, K. P.; Muniandy, S.; Rekha, S. S.; Salleh, N. Aqueous extract of *Phyllanthus niruri* leaves displays *in vitro* antioxidant activity and prevents the elevation of oxidative stress in the kidney of streptozotocin-induced diabetic male rats. *Evid. Based Complement. Altern. Med*. **2014**, *2014*, 834815 https://doi.org/10.1155/2014/834815

Gobbo-Neto, L.; Lopes, N. P. Plantas medicinais: fatores de influência no conteúdo de metabólitos secundários. *Quim. Nova*. **2007**, *30* (2), 374–381. https://doi.org/10.1590/S0100-40422007000200026

Instituto Nacional de Meteorologia (INMET). *Ministério da agricultura, pecuária e abastecimento*. 2013. https://www.gov.br/agricultura/pt-br/assuntos/inmet?r=bdmep/bdmep (accessed 2013-01-15).

Kiazolu, J. B.; Intisar, A.; Zhang, L.; Wang, Y.; Zhang, R.; Wu, Z.; Zhang, W. Phytochemical screening and chemical variability in volatile oils of aerial parts of

Morinda morindoides. *Nat. Prod. Res*. **2016**, *30* (19), 2249–2252. https://doi.org/10.1080/14786419.2016.1154058

Klein-Júnior, L. C.; Silva, L. M.; Boeing, T.; Somensi, L. B.; Beber, A. P.; Rocha, J. A. R.; Henriques, A. T.; Andrade, S. F.; Cechinel-Filho, V. The Protective Potential of *Phyllanthus niruri* and Corilagin on Gastric Lesions Induced in Rodents by Different Harmful Agents. *Planta Med*. **2017**, *83* (01/02), 30–39. https://doi.org/10.1055/s-0042-107356

Kumar, S.; Singh, A.; Bajpai, V.; Singh, B.; Kumar, B. Development of a UHPLC-MS/MS method for the quantitation of bioactive compounds in *Phyllanthus* species and its herbal formulations. *J. Sep. Sci*. **2017**, *40* (17), 3422–3429. https://doi.org/10.1002/jssc.201601361

Markom, M.; Hasan, M.; Daud, W. R. W.; Singh, H.; Jahim, J. M. Extraction of hydrolysable tannins from *Phyllanthus niruri* Linn.: Effects of solvents and extraction methods. *Sep. Purif. Technol*. **2007**, *52* (3), 487–496. https://doi.org/10.1016/j.seppur.2006.06.003

Moreira, J.; Klein-Júnior, L. C.; Cechinel Filho, V.; Campos-Buzzi, F. Anti-hyperalgesic activity of corilagin, a tannin isolated from *Phyllanthus niruri* L. (Euphorbiaceae). *J. Ethnopharmacol*. **2013**, *146* (1), 318–323. https://doi.org/10.1016/j.jep.2012.12.052

Pathania, R.; Najda, A.; Chawla, P.; Kaushik, R.; Khan, M. A. Low-energy assisted sodium alginate stabilized *Phyllanthus niruri* extract nanoemulsion: Characterization, *in vitro* antioxidant and antimicrobial application. *Biotechnol. Rep*. **2022**, *33*, e00711. https://doi.org/10.1016/j.btre.2022.e00711

Rajamanickam, G.; Manju, S. L. Bio-guided isolation of anti-Alzheimer's compounds from *Phyllanthus niruri* and role of niruriflavone in the reversal of aluminum chloride-induced neurobehavioral and biochemical changes in an animal model. *Med. Chem. Res*. **2022**, *31* (10), 1740–1753. https://doi.org/10.1007/s00044-022-02944-5

Santos, A. R. S.; Valdir Filho, C.; Yunes, R. A.; Calixto, J. B. Analysis of the mechanisms underlying the antinociceptive effect of the extracts of plants from the genus Phyllanthus. *Gen. Pharmac*. **1995**, *26* (7), 1499–1506. https://doi.org/10.1016/0306-3623(95)00030-5

Santos, S. C.; Costa, W. F.; Batista, F.; Santos, L. R.; Ferri, P. H.; Ferreira, H. D.; Seraphin, J. C. Seasonal variation in the content of tannins in barks of barbatimão species. *Rev. Bras. Farmacogn*. **2006**, *16* (4), 552–556. https://doi.org/10.1590/S0102-695X2006000400019

Santos, R. M.; Oliveira, M. S.; Ferri, P. H.; Santos, S. C. Seasonal variation in the phenol content of *Eugenia uniflora* L. leaves. *Rev. Bras. Plantas Med*. **2011**, *13* (11), 85–89. https://doi.org/10.1590/S1516-05722011000100013

Wang, M.; Cheng, H.; Li, Y.; Meng, L.; Zhao, G.; Mai, K. Herbs of the genus Phyllanthus in the treatment of chronic hepatitis B: observations with three preparations from different geographic sites. *J. Lab. Clin. Med*. **1995**, *126* (4), 350–352.

The potency of cooperative integrated reading and composition in building chemistry students' scientific literacy and self-regulated learning

Habiddin Habiddin[1+] , Cyndi Yanis Saputri[1] , Aman Santoso[1]

1. State University of Malang, Faculty of Mathematics and Natural Sciences, Malang, East Java, Indonesia.

+Corresponding author: Habiddin Habiddin, **Phone:** +62 81333886762, **Email address:** habiddin_wuni@um.ac.id

ABSTRACT: The effect of the Cooperative Integrated Reading and Composition (CIRC) approach on scientific literacy and students' regulated learning in colligative properties of solution was explored. The contribution of the CIRC approach was measured by investigating whether the improvement in scientific literacy and regulated learning of the CIRC students are more significant than the improvement for students with the Direct Instructional Teaching Method (DITM) after experiencing two different teaching approaches. Two groups of students (experiment and comparison) from a public senior high school in East Java, Indonesia, were involved. The experimental group experienced the colligative properties of solution with the CIRC teaching approach, while the comparison group experienced the DITM one. We found that scientific literacy and self-regulated learning of students with CIRC are higher than students with DITM, implying the potency of this approach to be applied to other chemistry topics. This study indicates that CIRC could be used to improve students' scientific literacy and self-regulated learning for other chemistry topics. The implication of this study for teaching colligative properties of solution is also discussed.
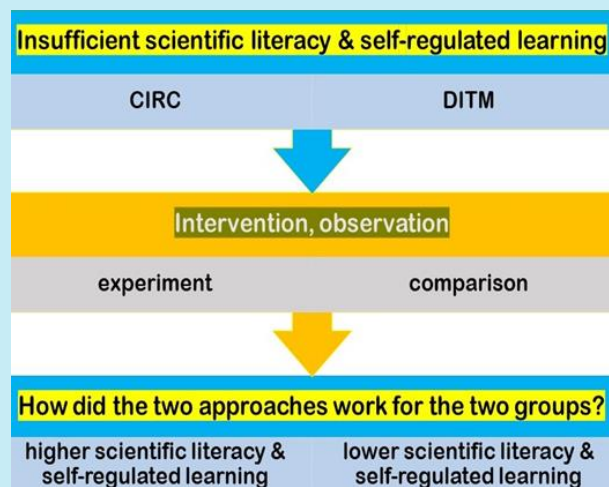
1. Introduction

Educational institutions in the current era are demanded to provide a learning environment supporting the development of students' soft skills that meet the 21st-century skills requirement. Soft skills, also known as behavioural skills, play a crucial role in personal growth that is more nebulous than hard skills (Almeida and Morais, 2021). Their definition is contested, but Cimatti (2016) links them to empathy and problem-solving, such as emotional intelligence, teamwork, time management, resilience, and intuitive thinking. Although their roles in the academic field have not been systematically uncovered, the pivotal support in other aspects of life has been confirmed (Feraco et al., 2022). Several soft skills have been considered essential to be mastered by students, including scientific/chemical literacy ability (Cigdemoglu et al., 2017; Kohen et al., 2020; Suwono et al., 2022; Wei and Lin, 2022), communication skill (Chung et al., 2016; Kleckner and Butz, 2022; Skagen et al., 2018), collaborative skill (Heeg et al., 2020; Kumar et al., 2022; Reid et al., 2022), and self-regulated learning (Austin et al., 2018; Eklund and Prat-Resina, 2014; Seibert et al., 2021).

Scientific literacy is the capacity to use scientific knowledge, identify questions and draw evidence-based conclusions to understand and help make decisions about the natural world and its changes through human activity (PISA, 2004). It is also defined as the capacity to comprehend scientific processes and interact meaningfully with everyday scientific information (Fives et al., 2014). The United Nations Educational, Scientific and Cultural Organization (UNESCO) has emphasised that all educational institutions should cultivate students' scientific literacy (Nogueira et al., 2021). Building students' chemical literacy should be the paramount goal of science education teaching in this era (Kohen et al., 2020). Scientific literacy should also emphasise the character and values that lead students to make the right decisions for a sustainable planet and the protection of fundamental human rights for all (Choi et al., 2011). Remarkably, the significant contribution of scientific literacy skills to foster the economic growth of a developing country like Indonesia is highly considered (Laugksch, 2000). These statements imply that scientific literacy is an essential skill to be held by students.

With the ultimate goal of arriving at the golden generation by 2045, Indonesia should ensure that current Indonesian students exhibit sufficient scientific literacy skills. Human resources in this generation will hold sufficient soft skills to contribute optimally to the country's development. However, the lack of students' scientific literacy has challenged science learning in Indonesia (Sari et al., 2017). The current Programme for International Student Assessment (PISA) survey in 2018 put Indonesian scientific literacy ability within the lower rank (70) among 78 participant countries (PISA, 2018). The result of this survey fits with the findings of several studies in this area. Adnan et al. (2021) found that secondary school students in South Sulawesi, Indonesia, demonstrated low scientific literacy skills. Even first-year students have shown only a moderate level of chemical literacy (Djaen et al., 2021). Islami et al. (2020) compared the level of scientific literacy skills between novice Indonesian and Thailand science teachers and found that Thai teachers demonstrated a slightly higher performance. This result is supported by the evidence that Indonesian students' mastery of the content, processes and contexts of scientific phenomena is considered insufficient (Rochman, 2015). The domination of the Direct Instructional Teaching Method (DITM) in many chemistry classes in Indonesia may contribute to this issue (Fuadi et al., 2020).

Another valuable skill for students is the ability to learn independently or through self-regulated learning. In some literature, self-regulated learning is also called learning autonomy (Eklund and Prat-Resina, 2014). Such ability allows students to monitor, control and regulate their cognition, motivation, and behaviour (Saribas and Bayram, 2009; Schunk, 2011). Self-regulated learning is characterised by the reflective application of suitable techniques in each learning circumstance, as well as motivational and metacognitive regulation on the side of the students (Seibert et al., 2021). Students are intrinsically driven to study in order to self-regulate; this is a fundamental component of theories on self-regulated learning (Austin et al., 2018). Several studies uncovering the role of self-regulated learning are found in the literature. Hermanns and Schmidt (2019) found that the stepped tool effectively improved students' self-regulated learning and ability to solve chemistry questions. Another study involving thousands of students taking organic chemistry found that those with self-regulated learning demonstrated higher achievement (Austin et al., 2018). Talanquer (2010) summarised a slightly different perspective in which students who generate explanations for themselves while studying or solving problems can gain a deeper understanding of the subject matter and improve knowledge transfer. We firmly believe that self-generated explanation is also connected to self-generated learning. This claim is built upon the consideration that self-directed students successfully transfer their knowledge and abilities to new contexts (Sperling et al., 2016).

In considering the essential role of self-regulated learning, some efforts to promote it have been found. Using inquiry based-learning, Seibert *et al.* (2021) promoted students' self-regulated with Multitouch Experiment Instructions in School Laboratories. In other studies, the stepped tool was also employed to facilitate self-regulated learning in organic chemistry classes (Hermanns and Schmidt, 2019); a virtual lab with inquiry-based learning enhanced scientific literacy in optics and light (Putri *et al.*, 2021); and problem-based learning was also applied to improve students' problem-solving and learning autonomy (Kurniawati, 2022).

Chemistry teaching should be carried out in a way to promote students' scientific/chemical literacy and self-regulated learning. Cigdemoglu and Geban (2015) revealed the effectiveness of a context-based approach in improving students' scientific literacy on the topic of chemical thermodynamics. Scrum methodology could also enhance students' scientific literacy (Vogelzang *et al.*, 2020). Inquiry based-learning has been applied to promote students' self-regulated learning (Kurniawati, 2022; Putri *et al.*, 2021). Drawing a conclusion from the previous strategies indicates that some strategies could be employed to improve students' scientific literacy and self-regulated learning. As the interactive compensatory learning model suggests, no single skill can completely support or obstruct self-regulated learning (Hubbard *et al.*, 2019).

In this study, we implemented a Cooperative Integrated Reading and Composition (CIRC) approach to promote students' scientific literacy and self-regulated learning on colligative properties of solutions. CIRC is a methodology in which students are divided into groups to cooperatively learn the relevant concepts (Mubarok and Sofiana, 2017). This model is designed to develop reading and writing abilities essential for supporting scientific literacy skills (Durukan, 2011). Even though this strategy is mainly implemented in the area of social science and literature, its contribution to the area of science education has also been uncovered. Ristanto *et al.* (2021) revealed that CIRC effectively improved students' conceptual understanding of the excretory system. In chemistry, implementing CIRC also improved students' achievement and motivation (Masnaini *et al.*, 2018). In addition, improving reading skills, one of the advantages of using this strategy helps to improve students' understanding and scientific literacy. To sum up, the primary purpose of this study is to investigate the difference in scientific literacy and self-regulated learning between CIRC and DITM students.

2. Experimental

2.1 Research Design

This *quasi-experimental design* employed a *post-test-only control group design* and involved two groups of students (67 in total). The students were chosen because they will embark on the colligative properties of solution class. The group that experienced the CIRC teaching approach is the experimental group, while the other with DITM is the comparison group. The two groups of students were selected using the convenience sampling technique. The school provided two groups without allowing the authors to choose other groups. Such a procedure in which respondents cannot be randomly obtained is called convenience sampling (Fraenkel *et al.*, 2011). Post-test aiming to measure the improvement of students' scientific literacy was performed after finishing the interventions (CIRC and DITM) for the two groups. The assigning procedure for the experiment and comparison groups was determined randomly after considering that the initial ability of the two groups was equal. Normality employing Kolmogorov-Smirnov and *Independent Sample T-Tests* were applied to confirm the equal initial ability of the two groups. Calculating the two tests were carried out using the software SPSS for Windows. Students' average chemistry grade from the previous term was the basis for determining students' initial ability.

2.2 Instrumentation

Scientific literacy in colligative properties of solution test (SC-CPST) was applied in the post-test to measure the improvement of students' scientific literacy after interventions. Meanwhile, students' self-regulated learning was identified using an observation sheet assessment during the interventions. Meanwhile, students' Self-Regulated Learning-Observation Sheet Assessment (SGL-OSA) was identified during the interventions. Both instruments were developed by the authors and were validated before being used for data collection. The instruments have not been used in any previous study. The validation covered content, construct, and face validities involving the chemistry lecturer and school chemistry teacher. They provided feedback on the content, its relevance to secondary school students' cognitive level, and the language. Their feedback was taken into account for refining the final instrument for data collection. The interventions (CIRC and DITM) were carried out for three meetings with

100 min each. The post-test was conducted three days after the last meeting of the interventions for 90 min.

2.3 Data Analysis

Students' scientific literacy in the topic of colligative properties of solution for the two groups was measured using the SC-CPST instrument at the post-test. The students' scientific literacy level was classified according to the Organisation for Economic Co-operation and Development (OECD) parameter presented in Table 1 (PISA, 2016). The difference in scientific literacy level between the two groups was measured using the *independent sample t-test* after meeting the normality test as a prerequisite procedure.

Table 1. The three domains for classifying students' scientific literacy levels.

Domains	Indicators
Explaining the phenomenon scientifically	Identify, offer, and evaluates the explanation of various natural and technological phenomena.
Evaluating and designing scientific questions	Describe and assesses scientific investigations and propose ways of answering questions scientifically.
Interpret data and evidence scientifically.	Analyse and evaluate data, claims and arguments in various representations and draw appropriate scientific conclusions.

Source: Retrieved from PISA (2016).

Meanwhile, students' self-regulated learning was observed during the interventions that involved seven well and equal trained observers. The parameter to classify it is presented in Table 2 (Azwar, 2009). An observation sheet with five Likert scales contains five indicators: initiative, creativity, innovation, improvisation, and proactiveness. The complete instrument is available on request.

Table 2. Students' self-regulated learning parameter.

Score Interval	Category
$X < Mi - 1.5\,SDi$	Very Low
$Mi - 1.5\,SDi < X \leq Mi - 0.5\,SDi$	Low
$Mi - 0.5\,SDi < X \leq Mi + 0.5\,SDi$	Medium
$Mi + 0.5\,SDi < X \leq Mi + 1.5\,SDi$	High
$Mi + 1.5\,SDi < X$	Very High

Note: $Mi = (X_{max} + X_{min})\frac{1}{2}$; $SDi = (X_{max} - X_{min})\frac{1}{6}$

Source: Elaborated by the authors using data from Azwar (2009).

3. Results and discussion

3.1 Comparing students' science literacy between the two groups

To determine whether the CIRC is influential in improving students' scientific literacy, the gained scientific literacy scores between the two groups were compared. The higher contribution of the CIRC teaching method in improving students' scientific literacy compared to DITM is indicated by the different scores when answering SC-CPST questions. The average score of CIRC students was 82.06, which is higher than that of DITM students with 64.00. The statistical procedure (independent t-test) confirms the difference of 0.000 significance value. Masnaini *et al.* (2018) found the superiority of CIRC to DITM in improving chemistry students' achievement. In teaching the excretory system in Biology class, CIRC students also demonstrate better performance than DITM students (Ristanto *et al.*, 2021). This difference implies that CIRC is more potent in improving students' scientific literacy. In addition, this study also indicates that CIRC applies not only to social and language literature but also to basic science disciplines, including chemistry, biology, and physics. Therefore, for basic science fields, we encourage the implementation of this strategy for teaching a topic with coverage of many factual information and rules, such as hydrocarbon.

The discrepancy in scientific literacy between both groups can also be identified from their responses explaining the sugar solution's increase in the boiling point. Figure 1 depicts how CIRC students explain why the boiling point of sugar solution is higher than its pure solvent (water, H_2O). The CIRC student explained that (*in English translation*) "the sugar molecules prevent the process of water evaporation from equalizing the external pressure, so a bigger temperature is required for it." His/her answer (Fig. 1) reflects that he/she harboured a scientific literacy domain, "explaining phenomena scientifically." Describing or interpreting phenomena scientifically, predicting changes, and identifying appropriate descriptions, explanations, and predictions are all aspects of this framework (Tsai, 2015). Figure 1 depicts that the student can explain the presence of solute molecules ($C_6H_{12}O_6$) inhibiting the evaporation of solvents (H_2O) and strengthen by stating that a higher temperature is needed to reach its boiling point.

Figure 1. A CIRC student's explanation regarding the boiling point of sugar solution.

The different phenomena are shown by the answers of DITM students, as presented in Fig. 2. The students stated (*in English translation*) that "the increase in viscosity of solution causes the increase boiling point of a solution." The student correctly recognized that the boiling point of sugar solution is higher than that of pure water but failed to support his/her answer with scientific argumentation. The student also can calculate the increase in the boiling point of the sugar solution using mathematical equations, but again, presenting the supporting scientific explanation is missing. The student can only explain the cause from the macroscopic aspect related to viscosity. This result reflects the insufficient scientific literacy domain, particularly "explaining phenomena scientifically."

Figure 2. A DITM student's explanation regarding the boiling point of sugar solution.

The improvement of students' ability in improving their scientific literacy is also demonstrated by some students participating in special education in mathematics and science in Thailand. At the beginning of the intervention, their ability in this aspect was considered low as they argued that "polyethylene glycol 600's benefits to the environment include its low toxicity, ability to protect seeds, and low absorption into the human body." After the intervention (Science, Technology, Society, and Environment), students provided a better explanation, as presented in the following sentences: "Since it is a non-toxic water-soluble chemical to plants and the environment, physostigmine can be used instead of glyphosate products. The potential for this method to produce acidic soil is a major drawback. Soil acidification is easily remedied by amending it with lime (CaO)" (Chanapimuk et al., 2018).

Another CIRC student (Fig. 3) explained (*in English translation*) that attractive interaction between water and sugar molecules hinders the vaporization of water molecules leading to higher temperatures for the solution to hit the boiling point. Meanwhile, other DITM students only mentioned that the sugar molecules affect the

boiling point of the sugar solution without providing a further explanation to support it. The result of this study is in line with previous studies regarding the impact of several interventions in improving students; scientific literacy, including a context-based approach (Cigdemoglu and Geban, 2015), scrum methodology (Vogelzang *et al.*, 2020), and argumentative practice (Cigdemoglu *et al.*, 2017).

Figure 3. Another example of a CIRC student's explanation regarding the boiling point of sugar solution.

It is essential to regularly test students' scientific literacy throughout their academic careers to see if *the seeds of literacy* have taken root in their brains (Shwartz *et al.*, 2006). Even during the emergence of COVID-19, Ramachandran *et al.* (2021) put effort into utilizing a collaborative-based learning approach, problem-solving, and understanding applied scientific data for strengthening scientific literacy through the cultivation of analytical, problem-solving, and teamwork abilities. Tsai (2015) found that students in the experimental group might have improved their PISA science competencies, including scientific literacy, after being exposed to online argumentation, which included argumentation instruction and activities. Students may benefit from learning how to use deductive and inductive reasoning through the process of constructing and defending an argument.

3.2 Students' self-regulated learning between the two groups

Students' self-regulated learning for both groups is derived from the observation sheet. Table 3 shows the significant advantages of CIRC in promoting self-regulated learning over the DITM for all indicators. The number of CIRC students demonstrating self-regulated learning behaviours is more than 20% higher than DITM students in each indicator. An enormous gap is observed in the initiative indicator. Self-regulated learning occurrences for CIRC students are about 82% on average.

Table 3. The self-regulated learning occurrences between CIRC and DITM students for each indicator.

Category	Percentage	
	CIRC	DITM
Initiative	82.07	58.45
Creativity	81.10	61.35
Innovation	81.61	62.89
Improvisation	84.17	61.98
Pro-Activeness	82.52	62.49

For five self-regulated learning indicators, CIRC students also demonstrated better self-regulated learning. Table 4 describes that almost 80% of CIRC students demonstrated very high self-regulated learning, while none of the DITM students did so. Meanwhile, only about 61% of DITM students exhibited high self-regulated learning. The self-regulated learning of DITM students ranges from very low to medium, with an almost equal number between categories. On the contrary, none of the CIRC students exhibited a very low category of self-regulated learning. Only a tiny portion of CIRC students hold a low and medium level of self-regulated learning. These results indicate that the CIRC teaching method supports the formation of students' self-regulated learning.

Table 4. The comparison of self-regulated learning levels between CIRC and DITM students.

Category	Percentage	
	CIRC	DITM
Very Low	0	35.29
Low	12.12	26.47
Medium	9.09	38.23
High	0	0
Very High	78.78	0

The better self-regulated learning of CIRC students may explain why their scientific literacy ability is better than that of DITM students. Compared to students in the comparison group (DITM), those in the experimental group (CIRC) used metacognitive strategies more frequently; these strategies are linked to self-regulated learning and, as a result, leading to higher achievement outcomes (i.e., more correct responses and/or more thorough scientific explanations) (Kadioglu-Akbulut and Uzuntiryaki-Kondakci, 2021).

A similar finding was revealed from the study covering 2,648 organic chemistry students in which those with high achievement hold self-regulated learning (Austin *et al.*, 2018). Another study employing problem-based learning teaching approach also improved students' self-regulated learning (Kurniawati, 2022). Putri *et al.* (2021) reported the effectiveness of virtual labs with inquiry-based learning in enhancing students' scientific literacy.

The essential role of self-regulated learning has been found even beyond its contribution to the student's conceptual understanding. A study involving hundreds of Taiwanese undergraduate students uncovered the link between professional development and confidence in one's own marketability is mediated by the ability to engage in self-regulated learning (Hsu *et al.*, 2022). Individuals' optimistic outlooks on self-improvement, driven by intrinsic motivation, are aided by motivational self-regulated learning processes (Pintrich, 1999). A person's effort and persistence in learning are more likely to be exemplary when they are driven by their intrinsic motivation rather than by external pressures or rewards (Ryan and Deci, 2000). Motivated students positively view their abilities and take responsibility for their learning (Zimmerman, 1986). Students with high levels of self-efficacy (those who are confident in their abilities to succeed) may view themselves as highly employable and, as a result, have a better chance of securing a job in the future (Berntson *et al.*, 2008). Students with high levels of self-efficacy believe they can successfully complete all course requirements and view obstacles as exciting opportunities to growth (Caprara *et al.*, 2008). Uzuntiryaki-Kondakci *et al.* (2017) suggest that colleges and universities should give future educators ample chances to hone their professional content knowledge and self-regulation skills in the classroom.

4. Conclusions

This study reveals that students with the CIRC approach improved scientific literacy and self-regulated learning more than those with the DITM approach. Regarding scientific literacy, CIRC students exhibited a better performance in all three indicators, as reflected in their answers to the colligative properties of solution questions. CIRC students' explanations reflect the mastery of scientific literacy, particularly in explaining phenomena scientifically. CIRC also contributes more to students' self-regulated learning in the occurrence number and its level. Almost all the CIRC students performed self-regulated learning behaviours for each indicator.

Meanwhile, only more than half of DITM students demonstrated these behaviours for each indicator. The level of self-regulated learning for CIRC students was also mostly in the very high category, while DITM students ranged from very low to medium, and none between high and very high. The results indicate that CIRC could potentially improve students' scientific

literacy, self-regulated learning, and other 21st-century skills. We realise that involving two groups of students is insufficient to offer a general conclusion; however, these results could be a pilot for a future study involving broader respondents and various chemistry topics. Considering the type of CIRC, it may sound like a reasonable exercise to expand this strategy for improving students' scientific literacy and self-regulated learning in chemistry topics involving many chemical facts and rules. Hydrocarbon, matter and measurements, colloidal systems, additive and food chemistry, and other similar topics are examples of chemistry topics that may suit the CIRC strategy. The result of this study also implies that students' scientific literacy and self-regulated learning can be promoted using several active learning such as a collaborative-based learning approach. Future studies to explore this suggestion will be interesting.

Authors' contribution

Conceptualization: Habiddin, H.
Data curation: Saputri, C. Y.
Formal Analysis: Saputri, C. Y.
Funding acquisition: Habiddin, H.
Investigation: Saputri, C. Y.
Methodology: Habiddin, H.
Project administration: Habiddin, H.; Saputri, C. Y.
Resources: Habiddin, H.; Saputri, C. Y.
Software: Not applicable.
Supervision: Habiddin, H.; Santoso, A.
Validation: Santoso, A.
Visualization: Saputri, C. Y.
Writing – original draft: Habiddin, H.; Saputri, C. Y.; Santoso, A.
Writing – review & editing: Habiddin, H.

Data availability statement

All data sets were generated or analyzed in the current study.

Funding

Acknowledgments

References

Adnan; Mulbar, U.; Sugiarti; Bahri, A. Scientific literacy skills of students: Problem of biology teaching in junior high school in South Sulawesi, Indonesia. *Int. J. Instr.* **2021**, *14* (3), 847–860. https://doi.org/10.29333/iji.2021.14349a

Almeida, F.; Morais, J. Strategies for developing soft skills among higher engineering courses. *J. Educ.* **2021**, *203* (1), 103–112. https://doi.org/10.1177/00220574211016417

Austin, A. C.; Hammond, N. B.; Barrows, N.; Gould, D. L.; Gould, I. R. Relating motivation and student outcomes in general organic chemistry. *Chem. Educ. Res. Pract.* **2018**, *19* (1), 331–341. https://doi.org/10.1039/C7RP00182G

Azwar, S. *Metode penelitian (cetakan kesembilan)*; Pustaka Pelajar, 2009.

Berntson, E.; Näswall, K.; Sverke, M. Investigating the relationship between employability and self-efficacy: A cross-lagged analysis. *Eur. J. Work Organ. Psychol.* **2008**, *17* (4), 413–425. https://doi.org/10.1080/13594320801969699

Caprara, G. V.; Fida, R.; Vecchione, M.; Del Bove, G.; Vecchio, G. M.; Barbaranelli, C.; Bandura, A. Longitudinal analysis of the role of perceived self-efficacy for self-regulated learning in academic continuance and achievement. *J. Educ. Psychol.* **2008**, *100*, 525–534. https://doi.org/10.1037/0022-0663.100.3.525

Chanapimuk, K.; Sawangmek, S.; Nangngam, P. Using Science, Technology, Society, and Environment (STSE) Approach to Improve the Scientific Literacy of Grade 11 Students in Plant Growth and Development. *J. Sci. Learn.* **2018**, *2* (1), 14–20. https://doi.org/10.17509/jsl.v2i1.11997

Choi, K.; Lee, H.; Shin, N.; Kim, S.; Krajcik, J. Re-conceptualization of scientific literacy in South Korea for the 21st century. *J. Res. Sci. Teach.* **2011**, *48* (6), 670–697. https://doi.org/10.1002/tea.20424

Chung, Y.; Yoo, J.; Kim, S.-W.; Lee, H.; Zeidler, D. L. Enhancing students' communication skills in the science classroom through socioscientific issues. *Int. J. Sci. Math. Educ.* **2016**, *14* (1), 1–27. https://doi.org/10.1007/s10763-014-9557-6

Cigdemoglu, C.; Geban, O. Improving students' chemical literacy levels on thermochemical and thermodynamics concepts through a context-based approach. *Chem. Educ. Res. Pract.* **2015**, *16* (2), 302–317. https://doi.org/10.1039/C5RP00007F

Cigdemoglu, C.; Arslan, H. O.; Cam, A. Argumentation to foster pre-service science teachers' knowledge, competency, and attitude on the domains of chemical literacy of acids and bases. *Chem. Educ. Res. Pract.* **2017**, *18* (2), 288–303. https://doi.org/10.1039/C6RP00167J

Cimatti, B. Definition, development, assessment of soft skills and their role for the quality of organisations and enterprises. *Int. J. Qual. Res.* **2016**, *10* (1), 97–130. https://doi.org/10.18421/IJQR10.01-05

Djaen, N.; Rahayu, S.; Yahmin, Y.; Muntholib, M. Chemical literacy of first year students on carbon chemistry. *J-PEK.* **2021**, *6* (1), 41–62. https://doi.org/10.17977/um026v6i12021p041

Durukan, E. Effects of cooperative integrated reading and composition (CIRC) technique on reading-writing skills. *Educ. Res. Rev.* **2011**, *6* (1), 102–109.

Eklund, B.; Prat-Resina, X. ChemEd X Data: Exposing students to open scientific data for higher-order thinking and self-regulated learning. *J. Chem. Educ.* **2014**, *91* (9), 1501–1504. https://doi.org/10.1021/ed500316m

Feraco, T.; Resnati, D.; Fregonese, D.; Spoto, A.; Meneghetti, C. Soft skills and extracurricular activities sustain motivation and self-regulated learning at school. *J. Exp. Educ.* **2022**, *90* (3), 550–569. https://doi.org/10.1080/00220973.2021.1873090

Fives, H.; Huebner, W.; Birnbaum, A. S.; Nicolich, M. Developing a measure of scientific literacy for middle school students. *Sci. Educ.* **2014**, *98* (4), 549–580. https://doi.org/10.1002/sce.21115

Fraenkel, J.; Wallen, N.; Hyun, H. *How to design and evaluate research in education*; McGraw-Hill, 2011.

Fuadi, H.; Robbia, A. Z.; Jamaluddin, J.; Jufri, A. W. Analisis Faktor Penyebab Rendahnya Kemampuan Literasi Sains Peserta Didik. *Jurnal Ilmiah Profesi Pendidikan* **2020**, *5* (2), 108–116. https://doi.org/10.29303/jipp.v5i2.122

Heeg, J.; Hundertmark, S.; Schanze, S. The interplay between individual reflection and collaborative learning – seven essential features for designing fruitful classroom practices that develop students' individual conceptions. *Chem. Educ. Res. Pract.* **2020**, *21* (3), 765–788. https://doi.org/10.1039/C9RP00175A

Hermanns, J.; Schmidt, B. Developing and applying stepped supporting tools in organic chemistry to promote students' self-regulated learning. *J. Chem. Educ.* **2019**, *96* (1), 47–52. https://doi.org/10.1021/acs.jchemed.8b00565

Hsu, A. J. C.; Chen, M. Y.-C.; Shin, N.-F. From academic achievement to career development: Does self-regulated learning matter? *Int. J. Educ. Vocat. Guidance.* **2022**, *22* (2), 285–305. https://doi.org/10.1007/s10775-021-09486-z

Hubbard, B. A.; Jones, G. C.; Gallardo-Williams, M. T. Student-generated digital tutorials in an introductory organic chemistry course. *J. Chem. Educ.* **2019**, *96* (3), 597–600. https://doi.org/10.1021/acs.jchemed.8b00457

Islami, R. A. Z.; Nuangchalerm, P. Comparative study of scientific literacy: Indonesian and Thai pre-service science teachers report. *Int. J. Eval. Res. Educ.* **2020**, *9* (2), 261–268. https://doi.org/10.11591/ijere.v9i2.20355

Kadioglu-Akbulut, C.; Uzuntiryaki-Kondakci, E. U. Implementation of self-regulatory instruction to promote students' achievement and learning strategies in the high school chemistry classroom. *Chem. Educ. Res. Pract.* **2021**, *22* (1), 12–29. https://doi.org/10.1039/C9RP00297A

Kleckner, M. J.; Butz, N. T. Developing entry-level communication skills: A comparison of student and employer perceptions. *Bus. Prof. Commun. Q.* **2022**, *85* (2), 192–221. https://doi.org/10.1177/23294906221078300

Kohen, Z.; Herscovitz, O.; Dori, Y. J. How to promote chemical literacy? Online question posing and communicating with scientists. *Chem. Educ. Res. Pract.* **2020**, *21* (1), 250–266. https://doi.org/10.1039/C9RP00134D

Kumar, A.; Mantri, A.; Singh, G.; Kaur, D. P. Impact of AR-based collaborative learning approach on knowledge gain of engineering students in embedded system course. *Educ. Inf. Technol.* **2022**, *27* (5), 6015–6036. https://doi.org/10.1007/s10639-021-10858-9

Kurniawati, I. L. The effect of problem-based learning on students' problem-solving and self-learning abilities in acid-base. *J-PEK.* **2022**, *7* (1), 44–48. https://doi.org/10.17977/um026v7i12022p044

Laugksch, R. C. Scientific literacy : A conceptual overview. *Sci. Educ.* **2000**, *84* (1), 71–94. https://doi.org/10.1002/(SICI)1098-237X(200001)84:1<71::AID-SCE6>3.0.CO;2-C

Masnaini; Copriady, J.; Osman, K. Cooperative integrated reading and composition (CIRC) with mind mapping strategy and its effects on chemistry achievement and motivation. *Asia-Pacific Forum on Science Learning and Teaching* **2018**, *9* (1), 2.

Mubarok, H.; Sofiana, N. Cooperative integrated reading and composition (CIRC) and reading motivation: Examining the effect on students' reading ability. *Lingua Cultura* **2017**, *11* (2), 121–127. https://doi.org/10.21512/lc.v11i2.1824

Nogueira, B. A.; Silva, A. D.; Mendes, M. I. P.; Pontinha, A. D. R.; Serpa, C.; Calvete, M. J. F.; Rocha-Gonçalves, A.; Caridade, P. J. B. S.; Rodrigues, S. P. J. Molecular school – A pre-university chemistry school. *Chemistry Teacher International* **2021**, *3* (3), 257–268. https://doi.org/10.1515/cti-2020-0013

Pintrich, P. R. The role of motivation in promoting and sustaining self-regulated learning. *Int. J. Educ. Res.* **1999**, *31* (6), 459–470. https://doi.org/10.1016/S0883-0355(99)00015-4

Programme for International Student Assessment (PISA). *The PISA 2003*: Assessment framework – Mathematics, reading, science and problem-solving knowledge and skills; OECD, 2004. https://www.oecd.org/education/school/programmeforinternationalstudentassessmentpisa/33694881.pdf (accessed 2022-09-12)

Programme for International Student Assessment (PISA). *PISA 2015*: Assessment and analytical framework – Science, reading, mathematic and financial literacy; OECD, 2016. https://doi.org/10.1787/9789264255425-en

Programme for International Student Assessment (PISA). *PISA 2018 results*: What students know and can do (Volume I); OECD, 2018. https://doi.org/10.1787/5f07c754-en

Putri, L. A.; Permanasari, A.; Winarno, N.; Ahmad, N. J. Enhancing students' scientific literacy using virtual lab activity with inquiry-based learning. *J. Sci. Learn.* **2021**, *4* (2), 173–184. https://doi.org/10.17509/JSL.V4i2.27561

Ramachandran, R.; Bernier, N. A.; Mavilian, C. M.; Izad, T.; Thomas, L.; Spokoyny, A. M. Imparting scientific literacy through an online materials chemistry general education course. *J. Chem. Educ.* **2021**, *98* (5), 1594–1601. https://doi.org/10.1021/acs.jchemed.1c00138

Reid, J. W.; Gunes, Z. D. K.; Fateh, S.; Fatima, A.; Macrie-Shuck, M.; Nennig, H. T.; Quintanilla, F.; States, N. E.; Syed, A.; Cole, R.; Rushton, G. T.; Shah, L.; Talanquer, V. Investigating patterns of student engagement during collaborative activities in undergraduate chemistry courses. *Chem. Educ. Res. Pract.* **2022**, *23* (1), 173–188. https://doi.org/10.1039/D1RP00227A

Ristanto, R. H.; Rahayu, S.; Mutmainah, S. Conceptual understanding of excretory system: Implementing cooperative integrated reading and composition based on scientific approach. *Particip. Educ. Res.* **2021**, *8* (1), 28–47. https://doi.org/10.17275/per.21.2.8.1

Rochman, C. Penerapan Pembelajaran Berbasis Scientific Approach Model 5M dan Analisis Kemampuan Literasi Sains Peserta Didik pada Sekolah Mitra Universitas Islam Negeri Sunan Gunung Djati Bandung. *Seminar Kontribusi Fisika* **2015**, *1* (2), 435–440.

Ryan, R. M.; Deci, E. L. Intrinsic and extrinsic motivations: Classic definitions and new directions. *Contemp. Educ. Psychol.* **2000**, *25* (1), 54–67. https://doi.org/10.1006/ceps.1999.1020

Sari, Y. A.; Bahar, A.; Rohiat, S. Studi Perbandingan Pembelajaran Kooperatif Menggunakan Media Kartu Pintar Dan Kartu Kemudi Pintar. *Alotrop.* **2017**, *1* (1), 44–48. https://doi.org/10.33369/atp.v1i1.2716

Saribas, D.; Bayram, H. Is it possible to improve science process skills and attitudes towards chemistry through the development of metacognitive skills embedded within a motivated chemistry lab?: A self-regulated learning approach. *Procedia Soc. Behav. Sci.* **2009**, *1* (1), 61–72. https://doi.org/10.1016/j.sbspro.2009.01.014

Schunk, D. H. *Learning theories*: An educational perspective; Pearson, 2011.

Seibert, J.; Heuser, K.; Lang, V.; Perels, F.; Huwer, J.; Kay, C. W. M. Multitouch experiment instructions to promote self-regulation in inquiry-based learning in school laboratories. *J. Chem. Educ.* **2021**, *98* (5), 1602–1609. https://doi.org/10.1021/acs.jchemed.0c01177

Shwartz, Y.; Ben-Zvi, R.; Hofstein, A. The use of scientific literacy taxonomy for assessing the development of chemical literacy among high-school students. *Chem. Educ. Res. Pract.* **2006**, *7* (4), 203–225. https://doi.org/10.1039/B6RP90011A

Skagen, D.; McCollum, B.; Morsch, L.; Shokoples, B. Developing communication confidence and professional identity in chemistry through international online collaborative learning. *Chem. Educ. Res. Pract.* **2018**, *19* (2), 567–582. https://doi.org/10.1039/C7RP00220C

Sperling, R. A.; Ramsay, C. M.; Reeves, P. M.; Follmer, D. J.; Richmond, A. S. Supporting students' knowledge construction and self-regulation through the use of elaborative processing strategies. *Middle Sch. J.* **2016**, *47* (3), 25–32. https://doi.org/10.1080/00940771.2015.1135099

Suwono, H.; Maulidia, L.; Saefi, M.; Kusairi, S.; Yuenyong, C. The development and validation of an instrument of prospective science teachers' perceptions of scientific literacy. *EURASIA J. Math. Sci. Tech. Ed.* **2022**, *18* (1), em2068. https://doi.org/10.29333/ejmste/11505

Talanquer, V. Exploring dominant types of explanations built by general chemistry students. *Int. J. Sci. Educ.* **2010**, *32* (18), 2393–2412. https://doi.org/10.1080/09500690903369662

Tsai, C.-Y. Improving students' PISA scientific competencies through online argumentation. *Int. J. Sci. Educ.* **2015**, *37* (2), 321–339. https://doi.org/10.1080/09500693.2014.987712

Uzuntiryaki-Kondakci, E.; Demirdöğen, B.; Akın, F. N.; Tarkin, A.; Günbatar, S. A. Exploring the complexity of teaching: the interaction between teacher self-regulation and pedagogical content knowledge. *Chem. Educ. Res. Pract.* **2017**, *18* (1), 250–270. https://doi.org/10.1039/C6RP00223D

Vogelzang, J.; Admiraal, W. F.; van Driel, J. H. Effects of Scrum methodology on students' critical scientific literacy: the case of Green Chemistry. *Chem. Educ. Res. Pract.* **2020**, *21* (3), 940–952. https://doi.org/10.1039/D0RP00066C

Wei, B.; Lin, J. Manifestation of three visions of scientific literacy in a senior high school chemistry curriculum: A content analysis study. *J. Chem. Educ.* **2022**, *99* (5), 1906–1912. https://doi.org/10.1021/acs.jchemed.2c00013

Zimmerman, B. J. Becoming a self-regulated learner: Which are the key subprocesses? *Contemp. Educ. Psychol.* **1986**, *11* (4), 307–313. https://doi.org/10.1016/0361-476X(86)90027-5

Novel organophosphorus Schiff base ligands: Synthesis, characterization, ligational aspects, XRD and biological activity studies

Yasmin Mos'ad Jamil[1+], Fathi Mohammed Al-Azab[1], Nedhal Abdulmawla Al-Selwi[1]

1. Sana'a University, Faculty of Science, Sana'a, Yemen.

+Corresponding author: Yasmin Mos'ad Jamil, **Phone:** +967 771952842, **Email address:** y.jamil@su.edu.ye

ABSTRACT: Six complexes have been synthesized from Cu(II), Ni(II), and Co(II) with new bidentate N_2 donor Schiff base ligand (2-methoxybenzalidene-1-phenylsemicarbazide **L₁**) and tridentate N_2O donor organophosphorus Schiff base ligand (2-methoxybenzalidenediphenylphosphate-1-phenylsemicarbazide **L₂**). Both ligands were synthesized and characterized by metal analysis, infrared (IR), ultraviolet visible (UV-Vis), and nuclear magnetic resonance (NMR) spectral studies. The chemical structures of the synthesized complexes were characterized using their metal analysis, magnetic susceptibility, molar conductance, IR, and UV-Vis spectra. According to molar ratio studies, the complexes have the composition of ML_2 for **L₁** and ML for **L₂**. The X-ray diffraction (XRD) studies showed that the particle size of ligands and **L₁** complexes were in nano-range. The ligands and their metal complexes have been screened for their antioxidant, antibacterial and antifungal activity.
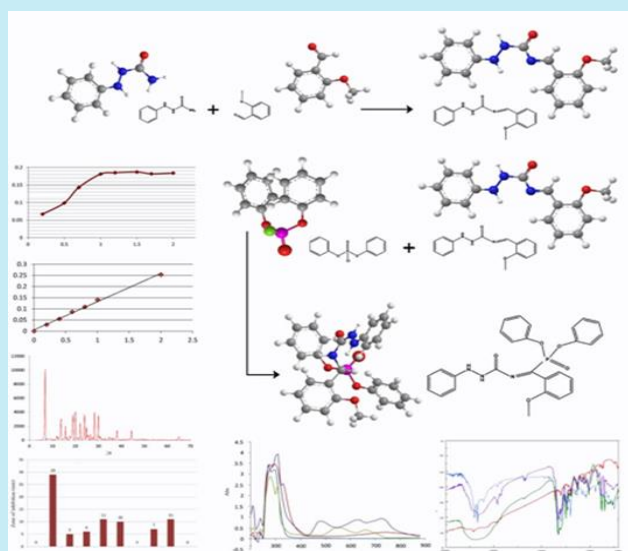
1. Introduction

Schiff base compounds are commonly used as ligands in inorganic chemistry to create stable complexes with different transition metal ions (Abu-Dief *et al.*, 2021). They are prepared by a condensation reaction of aromatic/aliphatic aldehydes and amines to form an azomethine group (CH=N) (Abu-Yamin *et al.*, 2022). In previous research, many biological activities of Schiff base compounds have been documented including antibacterial, antifungal, antimalarial, antiproliferative, analgesic, anti-inflammatory, antiviral, antipyretic, and anticancer properties (Camellia *et al.*, 2022; Ceramella *et al.*, 2022; Ibeji *et al.*, 2022; Jamil *et al.*, 2023; Kaczmarek *et al.*, 2018; Kafi-Ahmadi and Marjani, 2019; Song *et al.*, 2020). A survey of the literature reveals a work devoted to the synthesis, characterization, and biological activities of many metal complexes of Schiff base from 2-methoxybenzaldyde (Camellia *et al.*, 2022; Ibeji *et al.*, 2022; Sani and Iliyasu, 2018; Yusof *et al.*, 2015) In addition, organophosphorus compounds with transition metal ions have been the subject of several studies since complexes of such compounds exhibit biological activity (Abd El-Wahab and El-Sarrag, 2004; Brzezińska-Błaszczyk *et al.*, 1996; El-khazandar, 1997; Ochocki *et al.*, 1995). Hence, in the present study, a new Schiff base of 2-methoxybenzaldyde and 1-phenylsemicarbazide, its organophosphorus Schiff base, and their complexes with Cu^{2+}, Ni^{2+}, and Co^{2+} were prepared and characterized. The biological activities were investigated for these compounds, such as their antibacterial and antioxidant.

2. Experimental

2.1 Materials

The chemicals, 1-phenylsemicarbazide (Riedel-de Haën), 2-methoxybenzaldyde (Aldrich), diphenyl chlorophosphate (Riedel-de Haën), Triethyl amine (Riedel-de Haën), bipyridine (Aldrich), ferric chloride (Aldrich), ascorbic acid (BDH), sodium acetate trihydrate (BDH), glacial acetic acid (BDH) and metals chloride hydrate ($CuCl_2.2H_2O$, $NiCl_2.6H_2O$, and $CoCl_2.6H_2O$) were purchased from BDH. The solvents used were of spectroscopic grade.

2.2 Physical measurements

Elemental analysis for C, H, and N was performed with a Vario EL Fab. CHN Nr, at Central Laboratory, Faculty of Science, Cairo University, Giza, Egypt. Conductivity measurements were done with a Jenway conductivity meter model 4510 in dimethylformamide (DMF). The magnetic moments were determined by Gouy's method using a magnetic susceptibility balance from Johnson Metthey and Sherwood model. Ultraviolet visible (UV-vis) spectra were measured with (Specord200, Analytilk Jena, Germany) in the range of 200–900 nm, at Sana'a University. Fourier-transform infrared (FT-IR) spectra were recorded in transmission mode by an (FT/IR-140, Jasco, Japan) spectrophotometer in the wavenumber range of 4000–400 cm^{-1} (KBr was used as a matrix material for pellets). ^1H and ^{13}C NMR spectra for ligands were performed in d$_6$-DMSO solvent using tetramethylsilane as an internal standard, at Cairo University, Giza, Egypt. All melting points reported for the compounds are measured in glass capillary tubes in Celsius degrees. Chloride was determined gravimetrically by silver nitrate (Vogel, 1961). The amount of coordinated and uncoordinated water molecules was determined gravimetrically using the weight loss method (Vogel, 1961). The X-ray diffraction (XRD) patterns were obtained using XD-2 (Shimadzu ED-720) powder X-ray diffractometer at a voltage of 35 kV and a current of 20 mA using CuK(α) radiation in the range of 5° < 2θ < 70° at 1° min^{-1} scanning rate and a wavelength 1.54056 Å at Yemen Geological Survey and Mineral Resources Board.

2.3 Synthesis of ligands

2.3.1 Synthesis of Schiff base (2-methoxybenzalidene-1-phenylsemicarbazide L₁)

The reaction mixture, including an ethanolic solution of amine (1-phenylsemicarbazide) (7.55 g, 0.05 mol) with an ethanolic solution of aldehyde (2-methoxybenzaldyde) (6.80 g, 0.05 mol) was refluxed on hot reflux under constant stirring for 2–3 h, then the product was separated on cooling, it was filtered, washed several times with ethanol and ether, then the obtained crystals product was recrystallized by ethanol to give the corresponding Schiff base. The reaction is given in Fig. 1.
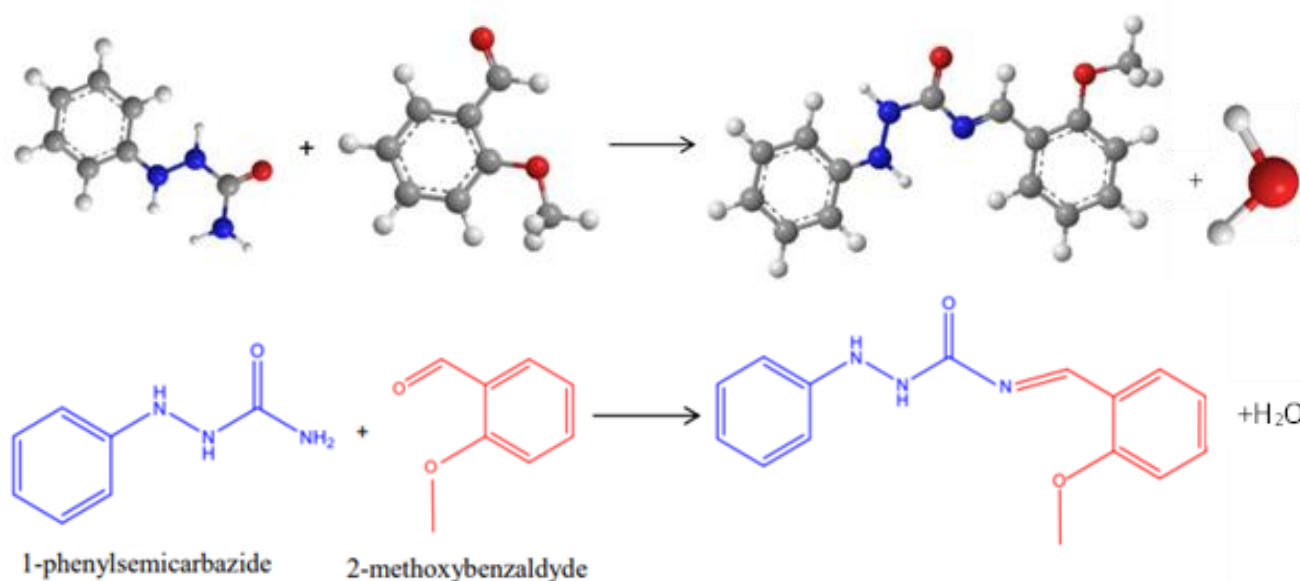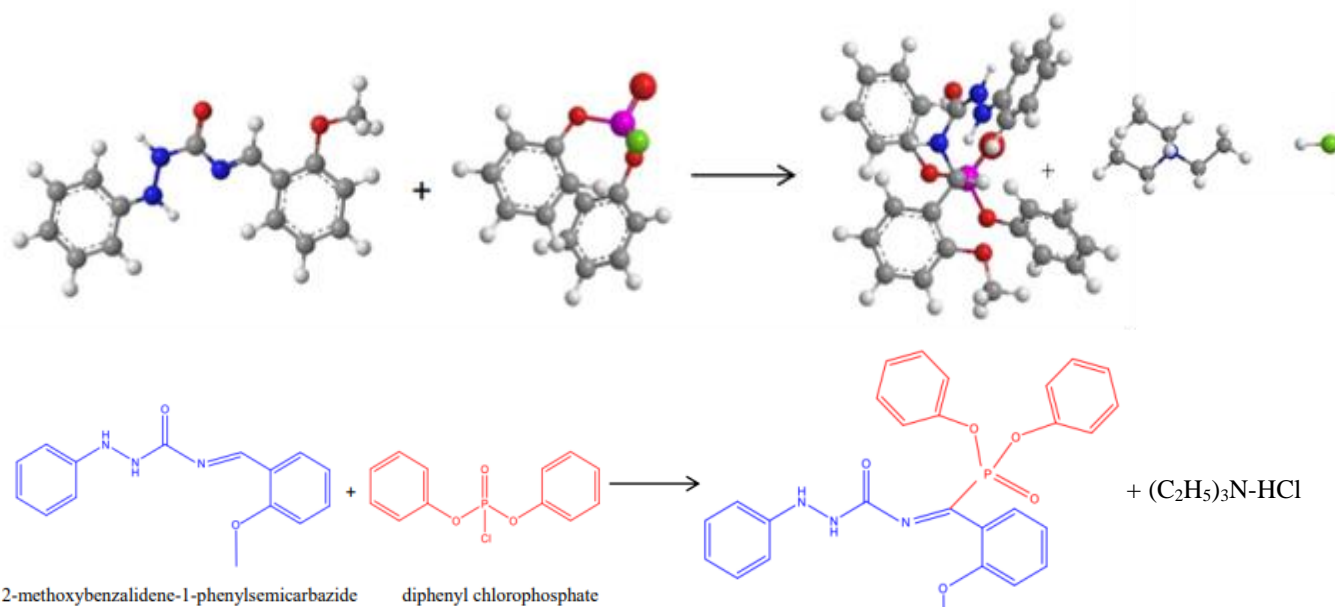
Figure 1. Preparation of Schiff base 2-methoxybenzalidene-1-phenylsemicarbazide **L₁**.

2.3.2 Synthesis of organophosphorus Schiff base (2-methoxybenzalidenediphenylphosphate-1-phenylsemicarbazide L₂)

The organophosphorus Schiff base **L₂** was prepared by condensation between a solution of Schiff base (4.03 g, 0.015 mol) in dry benzene (50 mL) with a solution of diphenyl chlorophosphate (3.69 g, 0.015 mol) in dry benzene (50 mL) in 1:1 molar ratio in presence of triethyl amine (Fig. 2). After complete addition, the reaction mixture was heated under reflux for 2 h. The formed solid (triethyl amine hydrochloride) was filtered and the product was obtained after evaporation in a water bath.

Figure 2. Preparation of organophosphorus Schiff base 2-methoxybenzalidenediphenylphosphate-1-phenylsemicarbazide **L₂**.

2.4 Synthesis of metal complexes

2.4.1 Synthesis of Schiff base metal complexes

A hot ethanolic solution of metal chloride was added dropwise to an ethanolic solution of Schiff base (2 L:1 mol L^{-1}) molar ratio. The mixture was refluxed on a hot plate with stirring for 2–3 h. After evaporation of the solvent, the solid product was washed several times with ethanol and dried over anhydrous CaCl$_2$.

2.4.2 Synthesis of organophosphorus Schiff base metal complexes

A solution of metal chloride in 20 mL absolute ethanol was added dropwise to the solution of organophosphorus Schiff base in warm absolute ethanol (1 L: 1 mol L^{-1}). After the addition, the mixture was heated under hot reflux for three hours. The solution was evaporated, and the solid complexes were collected using ether.

2.5 Determination of the stoichiometry of the formed complexes of molecular structure (Molar ratio method)

The molar ratio method was described by the Molar ratio method (Yoe and Jones, 1944). The concentrations of metal ions (Cu^{2+}, Ni^{2+}, and Co^{2+}) were kept constant at (1×10^{-3} mol L^{-1}) in methanol and the concentration of ligands (**L$_1$** and **L$_2$**) was regularly varied in methanol. The absorbance of the prepared solutions was measured at the constant wavelength (λ_{max}). The absorbance values were plotted versus the molar ratio [ligand] / [metal ion]. The intersections of the obtained straight lines indicate the molar ratio of the stable complexes.

2.6 Crystallinity and particle size from XRD

The percentage of crystallinity, XC (%) was calculated based on the integrated peak areas of the principal peaks (Shah et al., 2006). The crystallinity of the complexes is calculated relative to the crystallinity of the ligands as a ratio (Eq. 1):

$$X_C \ (\%) = \frac{A_{complex}}{A_{ligand}} \times 100 \tag{1}$$

where $A_{complex}$ and A_{ligand} are the areas under the principal peaks of the complex and ligand sample, respectively.

X-ray diffraction was also used to determine the average particle size (D) which was estimated by the Scherrer equation (Akhtar et al., 2015; Patterson, 1939) (Eq. 2):

$$D = \frac{K \lambda}{\beta \cos\theta} \tag{2}$$

where K is Scherrer constant and equals 0.94, λ is the X-ray wavelength of Cu-Kα radiations (1.5405 Å), β is full width at half maximum (FWHM) and θ is Bragg diffraction angle in degrees.

2.7 Antioxidant activity

The total antioxidant activity of the compounds has been studied using ferric-bipyridine reducing capacity (FBRC) (Al-Azab et al., 2023). It was taken (1 mL, 10^{-2} mol L^{-1} FeCl$_3$.6H$_2$O) to 10 mL volumetric flask different volumes of the standard antioxidant ascorbic acid (0.1 g L^{-1}) were added (0.01, 0.02, 0.04, 0.06, 0.08, 0.1, 0.2 mL). This was followed by 2.0 mL 0.3 mol L^{-1} acetate buffer (pH 4) and 1.0 mL bipyridine (6.4 × 10^{-3} mol L^{-1}). The volume was completed to the mark with deionized water. After 10 min of incubation at room temperature, the absorbance was recorded against a blank at 535 nm. The absorbance values were plotted against the concentration of the various antioxidant solutions (Fig. 3). Similarly, 0.02 mL of (0.1 mg mL^{-1} methanol) of each tested compound was reacted with 1 mL, 10^{-2} mol L^{-1} FeCl$_3$.6H$_2$O solution, (6.4 × 10^{-3} mol L^{-1}) bipyridine and 2.0 mL 0.3 mol L^{-1} acetate buffer (pH 4). This mixture was diluted to 10 mL with deionized water for the antioxidant assay. The fixed reaction time and fixed state measurement method were used to find out the antioxidant activity of these compounds in methanol as a solvent. All spectrophotometric measurements were measured using UV-vis spectrophotometer (Specord200, Analytikjena, Germany) at Sana'a University.
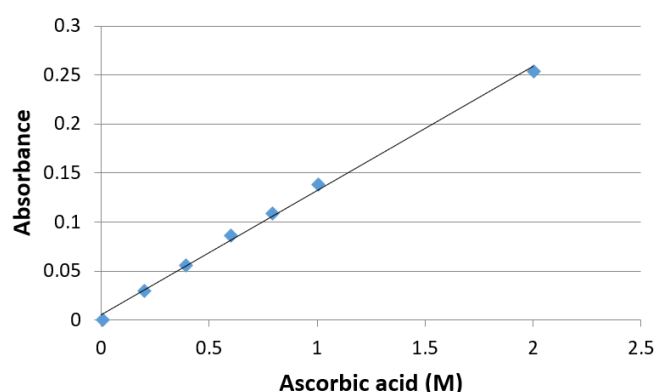

Figure 3. Calibration curve of ascorbic acid with Fe-Bp complex.

2.8 Antimicrobial activity

The synthesis compounds were exanimated for their antimicrobial activity in the Laboratory of Microbiology at Sana'a University. They Germinated four types of bacteria (*Staphylococcus aureus*, *Bacillus subtilis*, *Escherichia coli*, and *Pseudomonas aeruginosa*) and one fungus (*Candida albicans*) on nutrient agar and Sabouraud agar solid media respectively. Using the filter paper disc method (Ericsson *et al.*, 1960), it was prepared one concentration from each compound (1000 µg mL^{-1}) in DMSO. Then added (100 µL) from each prepared compound on a filter paper (Whatman No. 1 filter paper, 5 mm diameter) which contained the bacteria with agar solid media, all the Petri dishes were put in an incubation period at 37 °C for 24 h. Gentamicin 120 µg mL^{-1} was used as a reference substance for bacteria and Mycostatin 30 µg mL^{-1} for fungi. The results were registered by calculating the diameter of the inhibition zone (mm).

3. Results and discussion

The Schiff base ligand (**L$_1$**) was prepared by the condensation of 1-phenylsemicarbazide with 2-methoxybenzaldyde in the molar ratio 1:1. The organophosphorus ligand (**L$_2$**) was prepared by the condensation of diphenylchlorophosphate with the prepared Schiff base (**L$_1$**) in the molar ratio 1:1. The ligand ratio of (**L$_1$**) with Cu(II), Ni(II), and Co(II) complexes was found to be 1:2, and the ligand ratio of (**L$_2$**) with Cu(II), Ni(II), and Co(II) complexes were found to be 1:1. The molar conductance data of the complexes of **L$_1$** are 18.44, 20.31, and 21.09 Ω^{-1} cm^2 mol^{-1} in DMF (1 × 10^{-3} mol L^{-1}). These results show that these complexes are non-electrolytes (Aderoju and Sherifah, 2015; Geary, 1971), so the complexes of **L$_1$** are insoluble in water and common organic solvents but soluble in polar solvents such as DMF and DMSO. The non-electrolytic nature of these complexes suggests that the chloride anions of the three salts have coordinated with the **L$_1$** chelate of metal complexes. The reaction of the synthesized **L$_1$** complexes with silver nitrate have been not given a white precipitate, and after digestion with nitric acid, the silver nitrate test gave a positive result. Furthermore, the results of molar conductance of

L$_2$ complexes (73.75, 84.93, and 77.79) show that these complexes are 1:1 electrolytes in DMF (1 × 10^{-3} mol L^{-1}) (Geary, 1971; Shakdofa *et al.*, 2017). The complexes of **L$_2$** are slightly soluble in water and soluble in common organic solvents. In the case of **L$_2$** complexes, the precipitation was observed upon the addition of silver nitrate to the solution of the complexes (Vogel, 1961).

L$_1$ and **L$_2$** and their complexes were characterized by elemental analyses, FT-IR, ^{1}HNMR, and electronic spectra which are compliant with the proposed structures as shown in Fig. 4a and b. Table 1 lists some physical and analytical data on the ligands and their complexes.
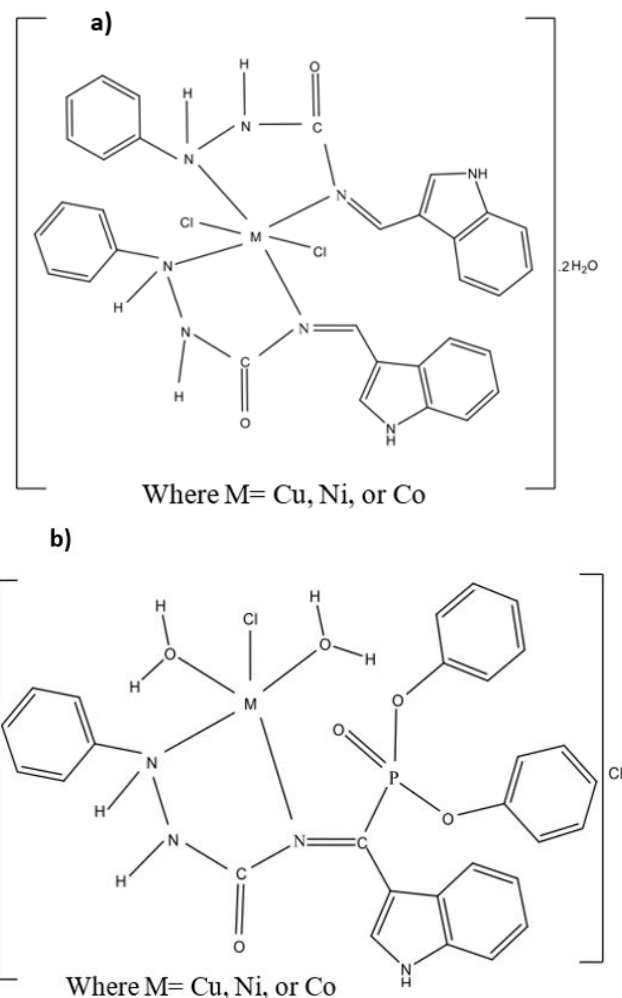

Figure 4. Proposed structure of **(a) L$_1$** complexes; **(b) L$_2$** complexes.

Table 1. Some physical properties and elemental analysis of the ligands and their complexes.

Compound	Color (Yield)	M.P. (°C)	Λm (Ω^{-1} cm^2 mol^{-1})	F.Wt (g mol^{-1})	Elemental analysis calculated% (found)				
					C	H	N	P	M
C$_{12}$H$_{11}$N$_3$O$_2$(L$_1$)	White (70%)	174	-	269.30	66.90 (67.04)	5.61 (5.78)	15.60 (15.27)	-	-
C$_{23}$H$_{10}$N$_3$O$_5$P(L$_2$)	Brown (75%)	153	-	479.36	65.15 (64.96)	2.94 (3.19)	8.76 (8.90)	7.05 (6.89)	-
[Cu(L$_1$)$_2$Cl$_2$]·2H$_2$O	Green (70%)	240	18.44	709.08	50.81 (51.30)	4.83 (4.88)	11.85 (12.08)	-	8.96 (9.00)
[Ni(L$_1$)$_2$Cl$_2$]·2H$_2$O	Green (50%)	250	20.31	704.22	51.16 (50.99)	4.87 (5.02)	11.93 (12.20)	-	8.33 (8.75)
[Co(L$_1$)$_2$Cl$_2$]·2H$_2$O	Dark blue (57%)	220	21.09	704.46	51.14 (51.36)	4.86 (4.33)	11.92 (11.68)	-	8.36 (8.13)
[Cu(L$_2$)Cl (H$_2$O)$_2$].Cl	Dark red (17%)	130	73.75	649.84	48.05 (47.85)	2.79 (2.86)	12.93 (13.18)	4.76 (4.55)	9.77 (9.53)
[Ni(L$_2$)Cl (H$_2$O)$_2$].Cl	Red (19%)	108	84.93	644.98	48.41 (48.47)	2.82 (3.00)	13.02 (12.79)	4.80 (4.70)	9.09 (9.00)
[Co(L$_2$)Cl (H$_2$O)$_2$].Cl	Red (23%)	112	77.79	645.22	48.39 (48.01)	2.81 (2.57)	13.02 (13.24)	4.79 (4.99)	9.13 (8.98)

3.1 Nuclear magnetic resonance spectral studies

3.1.1 ^{1}HNMR spectra of the ligands

The ^{1}HNMR spectra of the ligands **L$_1$** and **L$_2$** (Figs. S1 and S2 see Supplementary Material) exhibited signals which are consistent with the proposed structure. The peaks at 6.019, 6.713, and 5.997, 6.692 ppm are assignable to the protons of the NH groups in the ligands **L$_1$** and **L$_2$** respectively (El-Tabl *et al.*, 2007; Shakdofa *et al.*, 2017). Azomethine proton appeared as a singlet signal at 8.656 ppm (s, 1H) in **L$_1$** (Çakır *et al.*, 2003) and this signal disappeared in the **L$_2$** spectrum due to a replacement reaction on this group with eliminated HCl and forming a P-C bond. The signals at 3.908 and 3.050 were assigned to (s, 3H, OCH$_3$) **L$_1$** and **L$_2$**, respectively (Çakır *et al.*, 2003). The peaks appearing in the range 6.742–7.831 and 6.717–7.842 ppm may correspond to protons of the aromatic hydrogen of **L$_1$** and **L$_2$** respectively (Galil *et al.*, 2015).

3.1.2 ^{13}CNMR Spectra of the ligands

The ^{13}CNMR spectra (Figs. S3 and S4 see Supplementary Material) showed singlet signals at 161.688 and 160.421 ppm that attributed to carbonyl carbon C=O of the ligands **L$_1$** and **L$_2$** respectively (Carrasco *et al.*, 2020; Galil *et al.*, 2015). Also, the spectra exhibited two peaks at δ 149.517 and δ 149.623 ppm that were able to be appointed to azomethine carbon C=N of the ligands **L$_1$** and **L$_2$**, respectively (Shakdofa *et al.*, 2017). The peaks between 111.241–130.917 and 112.189–130.143 ppm is attributed to aromatic carbon in **L$_1$** and **L$_2$**, respectively (Galil *et al.*, 2015). The carbon of

the methoxy group appeared at 55.534 and 45.381 ppm in ligands **L$_1$** and **L$_2$**, respectively (Yusof *et al.*, 2015).

3.2 IR spectra of the ligands and their complexes

Important IR bands of the ligands and their complexes are given in Table 2 and Fig. 5a. The presence of IR bands at 1,655 and 1,602 cm^{-1} of ligand **L$_1$** assigned to υ(C=O) and υ(C=N) respectively (Hossain *et al.*, 2019). The strong bands at 3,334 and 3,397 cm^{-1} are assignable and attributed to υ(NH) of this ligand (Nakamoto, 1998). The bands showed at 3,057, 2,958, and 1,267 cm^{-1} belong to aromatic υ(C-H), aliphatic υ(C-H), and υ(-C-N) stretching mode of vibrations, respectively (Jassem *et al.*, 2013). The band at 2,853 cm^{-1} in its spectrum can be appointed to υ(-O-CH$_3$) (Mohapatra *et al.*, 2011).

The IR spectra of the complexes (Fig. 5a) are characterized by the appearance of broad bands at 3,424, 3,346, and 3,324 cm^{-1} due to the water molecules in L$_1$(Cu), L$_1$(Ni), and L$_1$(Co) complexes, respectively (González-García *et al.*, 2016). In the spectra of all the complexes, no change in the frequency of (C=O) but the 1,602 cm^{-1} band was shifted to a lower frequency indicating the involvement of the N atom of the azomethine group in coordination (Table 2). The bands of υ(NH, NH) disappeared in complexes due to the broad bands of water. New vibrations at 400–600 cm^{-1} that are not present in the free ligand are attributed to the existence of υ(M-N) and υ(M-NH) (Yassin *et al.*, 2020). Based on the observations, it has been suggested that the ligand **L$_1$** acts as bidentate.

Although the presence evidence of υ(M-Cl) could not be brought in the IR data due to instrumental limitation, the insolubility of **L$_1$** complexes in water and their non-

electrolytic nature evinced that 2Cl⁻ coordinated with metal in **L₁** complexes.

In the ligand **L₂** spectrum (Fig. 5b), the bands observed at 1,654 and 1,591 cm⁻¹ corresponds to υ(C=O) and υ(C=N), respectively (Hossain *et al.*, 2019). The presence of υ(P=O) and υ(P-O-C) is indicated by the appearance of bands at 1,188 and 1,072 cm⁻¹, respectively (El-khazandar, 1997).

The coordinated water molecules with metal ions in the complexes were proved by the bands 3,347, 3,407, and 3,312 (Aderoju and Sherifah, 2015). The IR spectra of the metal complexes of ligand **L₂** (Fig. 5b) proposed that this ligand tridentate with the phosphoryl-oxygen, amine-nitrogen, and azomethine-nitrogen due to the shift in the position of υ(P=O), υ(-NH) and υ(C=N) (Table 2).

Table 2. The main IR absorption bands of the ligands and their complexes.

Compound	υ(H₂O)	υ(NH, NH)	υ(-O-CH₃)	υ(C=N)	υ(C=O)	υ(P=O)	υ(P-O-C)	υ(M-N)	υ(M-NH)
C₁₆H₁₄N₄O(L₁)	-	3398 3335	2853	1602	1655	-	-	-	-
C₂₇H₁₃N₄O₄P (L₂)	-	3450 3347	2878	1591	1654	1188	1072	-	-
[Cu(L₁)₂Cl₂]·2H₂O	3424	3424	2850	1580	1651	-	-	527	428
[Ni(L₁)₂Cl₂]·2H₂O	3346	3346	2849	1571	1649	-	-	558	414
[Co(L₁)₂Cl₂]·2H₂O	3324	3324	2855	1577	1653	-	-	574	424
[Cu(L₂)Cl (H₂O)₂].Cl	3421	3467 3452	2866	1560	1650	1165	1072	516	410
[Ni(L₂)Cl (H₂O)₂].Cl	3407	3407	2850	1617	1655	1160	1067	520	458
[Co(L₂)Cl (H₂O)₂].Cl	3312	3365 3312	2846	1603	1651	1161	1068	517	467
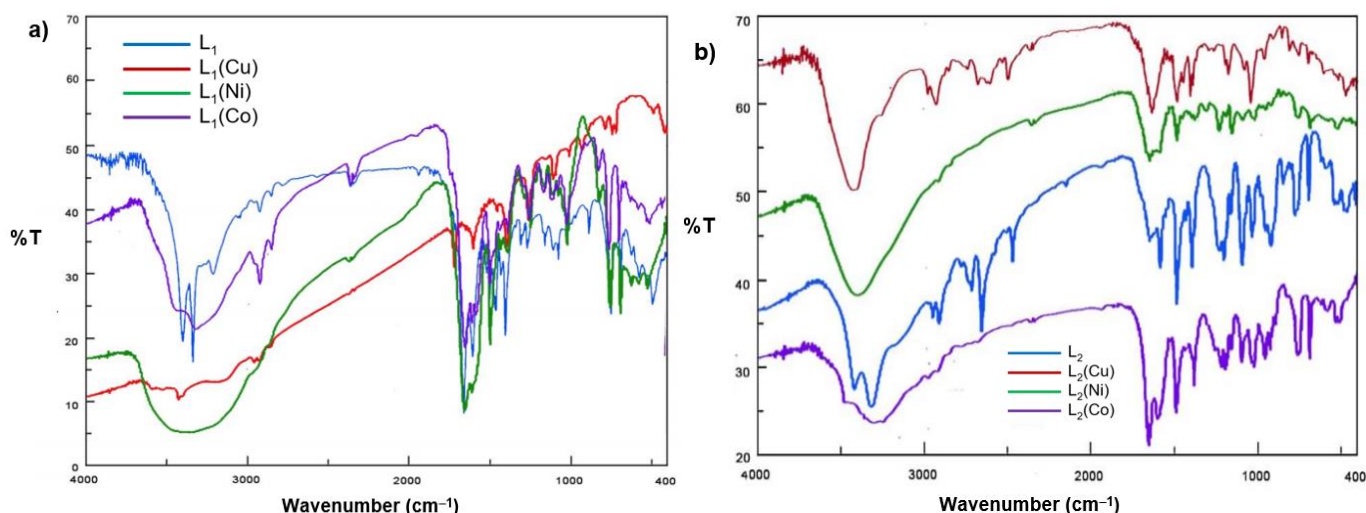
Figure 5. Infrared spectra. **(a) L₁** and its complexes; **(b) L₂** and its complexes.

3.3 Electronic spectra and magnetic measurements

The absorption spectra of the ligands **L₁** and **L₂** and their metal complexes were recorded in DMSO in the range of 200–900 nm (Table 3).

The ligands **L₁** and **L₂** exhibited two absorption bands (Figs. 6a and b) at 37,037.03, 35,714.28 and 33,333.33, 32,258.06 cm⁻¹ that have been allocated for the π-π* and n-π* transitions, respectively (Mohammed *et al.*, 2019). In the metal complexes, the transition of n-π* has been seen but they are shifted to another range. The shift in the transitions has been accounted for by the complexation between ligands with the metal ions.

The Cu complexes of **L₁** and **L₂** exhibited single broad absorption peaks at 13,513.51 and 13,333.33 cm⁻¹ (Figs. 6a and b), respectively, attributable to the ²Eg→²T₂g transition, indicating a distorted octahedral structure (Al-Maydama *et al.*, 2008; Gup and Kirkan, 2005).

The electronic spectra of the **L₁**(Ni) and **L₂**(Ni) complexes (Figs. 5a and b) showed absorption bands at 18,181.81, 15,151.51 and 17,543.85, 15,151.51 cm⁻¹, respectively, attributable to the ³A₂g → ³T₁g(P) and ³A₂g → ³T₁g(F) transitions, which is compatible with this complex having the octahedral structure (Gup and Kirkan, 2005).

The electronic spectra of the **L₁** and **L₂** complexes with Co (Figs. 6a and b) exhibited characteristic bands at 20,833.33, 15,873.01, 13,888.88 and 21,739.13, 20,000, 17,543.85 cm⁻¹ assigned to $^4T_1g\rightarrow\ ^4T_1g(P)$, $^4T_1g\rightarrow\ ^4A_2g$ and $^4T_1g\rightarrow\ ^4T_2g(F)$ transitions. These bands are associated with the octahedral structures (Gup and Kirkan, 2005).

This information with the effective magnetic moment (**μeff**) data (Table 3) of all complexes helped to support the suggested octahedral geometry (Al-Hakimi *et al.*, 2011; Fouda *et al.*, 2008).

Table 3. Electronic spectral and magnetic moment data of the ligands and their complexes.

Compound	μeff (B.M.)	(π→π*), transition	(n→π*) transition	d-d transition band (cm⁻¹)	Assignments	Supposed structure
C₁₆H₁₄N₄O(L₁)	-	37,037.03	33,333.33	-	-	-
C₂₇H₁₃N₄O₄P(L₂)	-	35,714.28	32,258.06	-	-	-
[Cu(L₁)₂Cl₂].2H₂O	1.88	34,482.75	30,303.03	13,513.51	$^2Eg\rightarrow\ ^2T_2g$	Distorted Octahedral
[Ni(L₁)₂Cl₂]·2H₂O	2.75	35,714.28	32,258.06	18,181.81 15,151.51	$^3A_2g \rightarrow\ ^3T_1g(P)$ $^3A_2g \rightarrow\ ^3T_1g(F)$	Octahedral
[Co(L₁)₂Cl₂]·2H₂O	4.19	35,714.28	32,258.06	20,833.33 15,873.01 13,888.88	$^4T_1g\rightarrow\ ^4T_1g(P)$ $^4T_1g\rightarrow\ ^4A_2g$ $^4T_1g\rightarrow\ ^4T_2g(F)$	Octahedral
[Cu(L₂)Cl (H₂O)₂].Cl	1.61	37,037.03	33,333.33	13,333.33	$^2Eg\rightarrow\ ^2T_2g$	Distorted Octahedral
[Ni(L₂)Cl (H₂O)₂].Cl	2.39	35,714.28	31,250.00	17,543.85 15,151.51	$^3A_2g \rightarrow\ ^3T_1g(P)$ $^3A_2g \rightarrow\ ^3T_1g(F)$	Octahedral
[Co(L₂)Cl (H₂O)₂].Cl	4.77	35,714.28	31,250.00	21,739.13 20,000.00 17,543.85	$^4T_1g\rightarrow\ ^4T_1g(P)$ $^4T_1g\rightarrow\ ^4A_2g$ $^4T_1g\rightarrow\ ^4T_2g(F)$	Octahedral
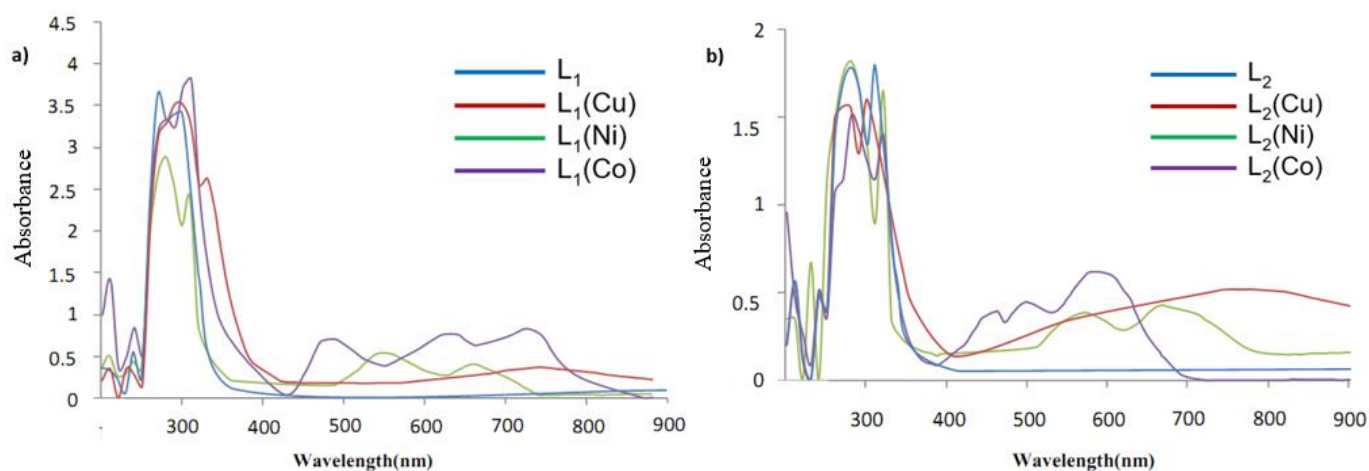
Figure 6. UV-Vis spectra. **(a) L₁** ligand and its complexes; **(b) L₂** ligand and its complexes.

3.4 Molar ratio (stoichiometry) of the studied complexes

Investigation of the molecular structure of the complexes formed between the metal ions of (Cu²⁺, Ni²⁺, and Co²⁺) with ligands in **L₁** and **L₂** in methanol using molar ratio (Figs. 7 and 8) revealed the formation of (1:2) (M:L) complexes for **L₁** and (1:1) (M:L) complexes for **L₂** under investigation. The results are depicted in Table 4.
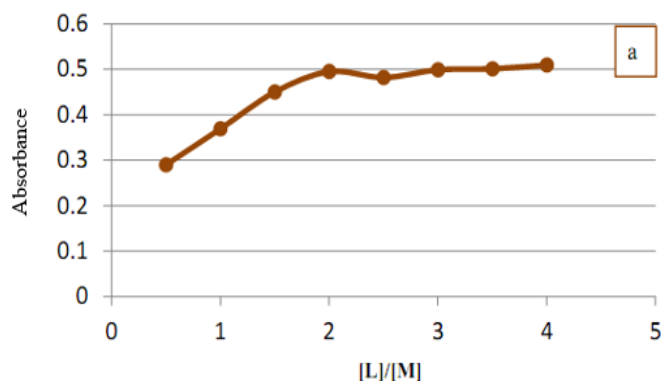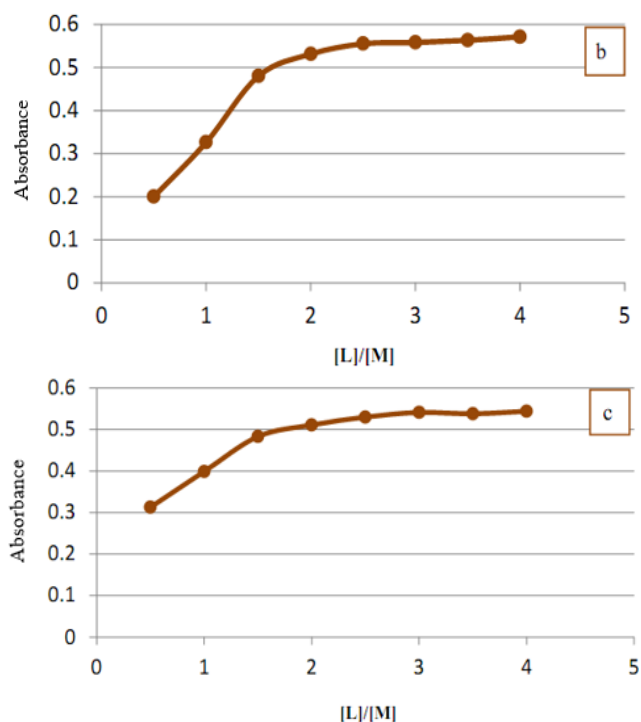
Figure 7. Molar ratio plot for the complexes between metal ions of **(a)** Cu, **(b)** Ni and **(c)** Co with **L₁** in methanol.

Figure 8. Molar ratio plot for the complexes between metal ions of **(a)** Cu, **(b)** Ni and **(c)** Co with **L₂** in methanol.

Table 4. Molar ratios for determination of stoichiometry of the **L₁** and **L₂** complexes in methanol.

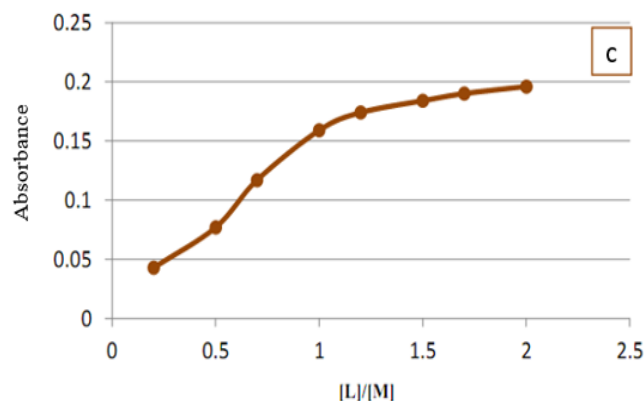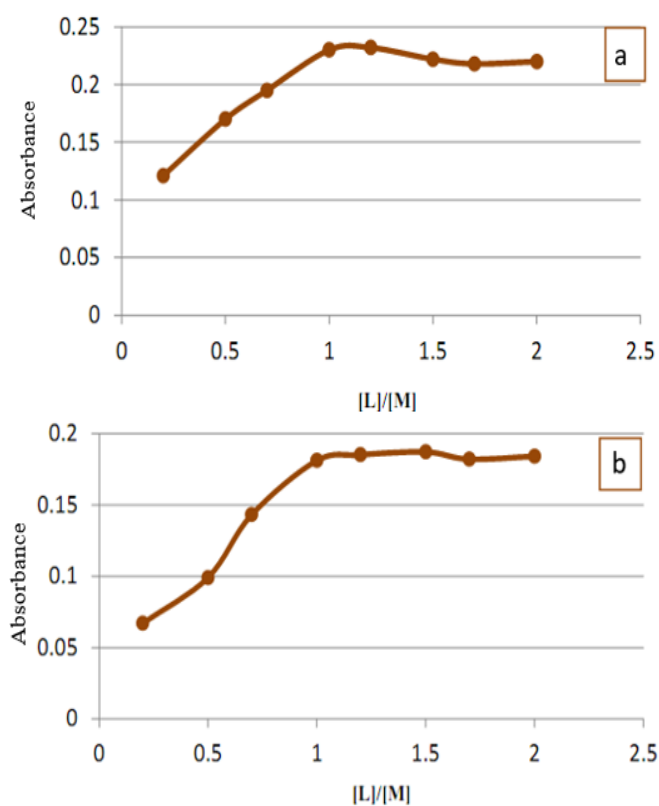| L₁			
	Absorbance of complexes		
[L]/[M]	Cu(II) $\lambda = 330$	Ni(II) $\lambda = 310$	Co(II) $\lambda = 310$
0.5:1	0.121	0.067	0.043
1:1	0.170	0.099	0.077
1.5:1	0.195	0.143	0.117
2:1	0.230	0.181	0.159
2.5:1	0.232	0.185	0.174
3:1	0.222	0.187	0.184
3.5:1	0.218	0.182	0.190
4:1	0.220	0.184	0.196
L₂			
	Absorbance of complexes		
[L]/[M]	Cu(II) $\lambda = 300$	Ni(II) $\lambda = 320$	Co(II) $\lambda = 320$
0.25:1	0.290	0.200	0.313
0.5:1	0.369	0.326	0.399
0.75:1	0.450	0.480	0.483
1:1	0.495	0.531	0.511
1.25:1	0.492	0.555	0.530
1.5:1	0.499	0.558	0.541
1.75:1	0.501	0.563	0.538
2:1	0.509	0.571	0.544

3.5 X-ray diffraction

The XRD patterns of the **L₁** and its complexes are shown in Fig. S5a–d (see Supplementary Material). The decrease of the XRD peak intensities of **L₁** complexes can be attributed to the reduction in crystallinities due to the complexation. This is in good agreement with the lowering in relative crystallinity calculated for these complexes (the crystallinity calculation in Table 5 is based on the integrated area of principal peaks of the complex to the **L₁** ligand obtaining a relative

crystallinity) (Shah *et al.*, 2006). The particle size calculated for L_1 and its complexes (2.074–5.552 nm) in the range of nanoparticle size—the nanoparticle size reported in the literature ranges between 1–100 nm (Boverhof *et al.*, 2015).

The particle size of L_2 ligand was found within nanometric range (10.555 nm), nevertheless its complexes appeared as an amorphous character (Fig. S5e–h, see Supplementary Material). From this change, it is expected to improved properties of L_2 complexes as compared with L_2 ligand.

Table 5. Data of the principal values of intensity of the ligands and L_1 complexes from XRD spectra.

| Compound	2θ	β	D (nm)	Mean D	X_C (%)
L_1	6.780	0.340	4.266	3.991	100
	13.720	0.419	3.480		
	18.880	0.459	3.154		
	19.960	0.405	3.630		
	23.920	0.379	3.905		
	28.220	0.295	5.061		
	29.900	0.337	4.447		
L_2	12.799	0.120	12.142	10.555	100
	16.740	0.153	9.464		
	25.441	0.121	12.268		
	31.040	0.180	8.349		
$[Cu(L_1)_2Cl_2]\cdot 2H_2O$	6.719	0.352	4.120	5.552	10.392
	13.460	0.562	2.576		
	18.599	0.229	6.407		
	20.919	0.237	6.213		
	31.659	0.178	8.455		
$[Ni(L_1)_2Cl_2]\cdot 2H_2O$	16.279	0.439	3.332	5.202	18.506
	32.761	0.240	6.033		
	33.579	0.232	6.241		
$[Co(L_1)_2Cl_2]\cdot 2H_2O$	14.600	0.603	2.421	2.074	3.488
	35.520	0.762	1.995		
	57.199	0.745	2.213		
	57.579	0.868	1.668		

3.6 Antioxidant activity

The ligands and L_2 complexes were investigated using FBRC technique to determine the antioxidant activity (Al-Azab *et al.*, 2023).

Fe(II)-bipyridine complex produced by the reaction of Fe(III) with antioxidant followed by bipyridine exhibited maximum absorption at 535 nm (Fig. 9). Total antioxidant activity is based on the redox reaction between compounds and Fe(III) at room temperature. The initial antioxidant concentration is indicated by the concentration of the oxidizing Fe(III).
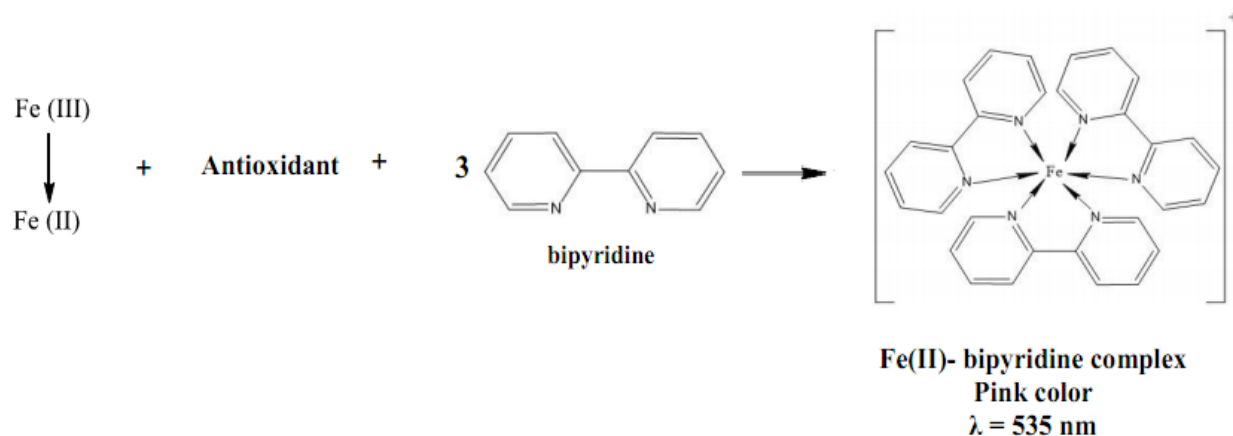
Figure 9. Stoichiometry outline of FBRC method.

The results in Table 6 showed that these compounds were found to possess high potent antioxidant activity due presence of a combination of donor sites such as amide oxygen and imine nitrogen (Kostova and Saso, 2013).

Table 6. FBRC values express antioxidant activity as mg L^{-1} for prepared compounds to 1 mg L^{-1} of ascorbic acid

FBRC (mg L^{-1})	Sample
0.0248 ± 0.0001	**L₁**
0.0281 ± 0.0004	**L₂**
0.0201 ± 0.0002	[Cu(L₂)Cl (H₂O)₂].Cl
0.0183 ± 0.0002	[Ni(L₂)Cl (H₂O)₂].Cl [Ni(L₂)Cl·(H₂O)₂].Cl
0.0187 ± 0.0005	[Co(L₂)Cl (H₂O)₂].Cl [Co(L₂)Cl·(H₂O)₂].Cl

3.7 Antibacterial and antifungal screening for L₁, L₂ and their complexes

The synthetic ligands and their metal complexes havbeen examined for their antibacterial and antifungal activities using the disk diffusion method (Ericsson *et al.*, 1960) against four types of Bacteria (*Staphylococcus aureus*, *Bacillus subtilis*, *Escherichia coli*, *and Pseudomonas aeruginosa*) and one fungus (*Candida albicans*) on nutrient agar and Sabouraud dextrose agar (SDA) solid media, respectively. The inhibition zone diameter of the compounds is shown in Table 7 and Fig. 10a–d. From these results, it was noted that:
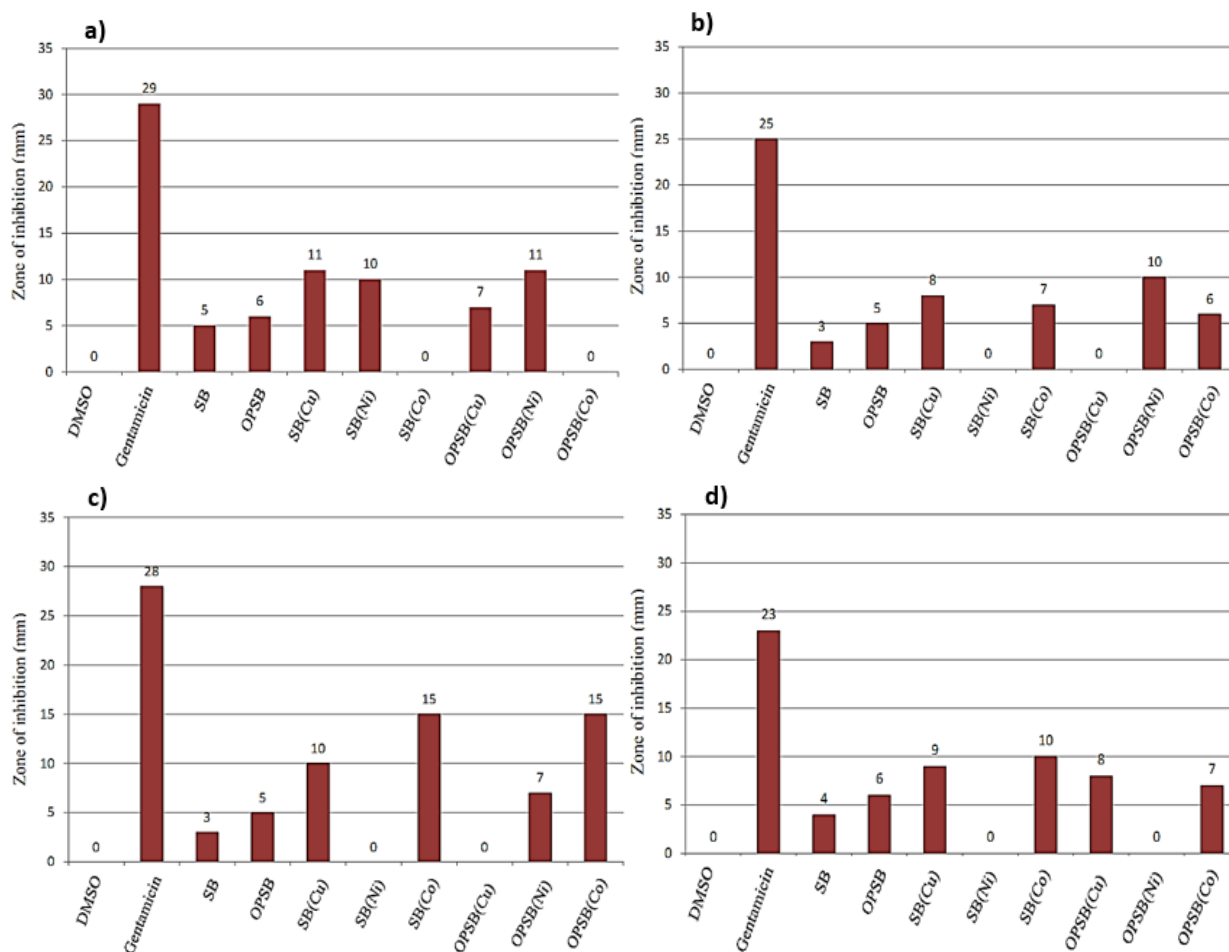
1- No inhibition zone was observed for ligands and their metal complexes against the fungus (*Candida albicans*);
2- The metal complexes are more potent bactericides than the ligands;
3- The order of antibacterial activity for the compounds with *Bacillus subtilis* was **L₁**(Cu) = **L₂**(Ni) > **L₁**(Ni) > **L₂**(Cu) > **L₂** > **L₁** > **L₁**(Co) = **L₂**(Co), with *Staphylococcus aureus* was **L₂**(Ni) > **L₁**(Cu) > **L₁**(Co) > **L₂**(Co) > **L₂** > **L₁** > **L₁**(Ni) = **L₂**(Cu), with *Escherichia Coli* was **L₁**(Co) > **L₁**(Cu) > **L₂**(Cu) > **L₂**(Co) > **L₂** > **L₁** > **L₁**(Ni) = **L₂**(Ni) and with *Pseudomonas aeruginosa* was **L₁**(Co) = **L₂**(Co) > **L₁**(Cu) > **L₂**(Ni) > **L₂** > **L₁** > **L₁**(Ni) = **L₂**(Cu).

In general, the complexes showed good antibacterial compared to the free ligands. Based on the chelation theory (Franklin and Snow, 1989), the increased inhibition activity of the metal complexes may be explained on the basis that their structures mainly possess C=N bonds. Besides, the coordination decreases the polarity of the metal ion due to the partial sharing of its positive charge with donor groups and possible π-electron delocalization inside the chelate ring-shaped during coordination that makes the complexes more lipophilic. This increased lipophilicity enhances the penetration of the metal complexes into lipid membranes, blocks the metal binding sites in the enzymes, and limits the further development of the organisms.

Table 7. Biological activities of the ligands and their metal complexes against bacteria and fungus (zone of inhibition in mm).

Compound (1000/mL⁻¹)	Bacteria				Fungi
	gram-positive		gram-negative		
	Bacillus subtilis	*Staphylococcus aureus*	*Escherichia coli*	*Pseudomonas aeruginosa*	*Candida albicans*
L₁	5	3	4	3	0
L₂	6	5	6	5	0
[Cu(L₁)₂Cl₂].2H₂O	11	8	9	10	0
[Ni(L₁)₂Cl₂].2H₂O	10	0	0	0	0
[Co(L₁)₂Cl₂].2H₂O	0	7	10	15	0
[Cu(L₂)Cl (H₂O)₂].Cl [Cu(L₂)Cl·(H₂O)₂].Cl	7	0	8	0	0
[Ni(L₂)Cl (H₂O)₂].Cl [Ni(L₂)Cl·(H₂O)₂].Cl	11	10	0	7	0
[Co(L₂)Cl (H₂O)₂].Cl [Co(L₂)Cl·(H₂O)₂].Cl	0	6	7	15	0
Gentamicin (120 µg/ml)	29	25	23	28	-
Mycostatin (30 µg/ml)	-	-	-	-	18

Figure 10. Antibacterial activity of the ligands and their metal complexes against gram-positive bacterium **(a)** *Bacillus subtilis*; **(b)** *Staphylococcus aureus*; **(c)** *Pseudomonas aeruginosa*; and gram-negative bacterium **(d)** *Escherichia coli*.

4. Conclusions

In summary, the synthesis and physicochemical analysis were done for new ligands **L₁** and **L₂** with their complexes. In complexes, the ligand **L₁** acts as neutral-bidentate and **L₂** acts as neutral-tridentate around the metallic ion. Electronic properties and magnetic susceptibility suggested octahedral geometry for all complexes. According to XRD, the ligands and **L₁** complexes were in the nanoscale (2.074–10.555 nm). The ligands and **L₂** complexes gave high antioxidant activity using FBRC technique. All compounds have been screened for their antibacterial and antifungal activity.

Authors' contribution

Conceptualization: Jamil, Y. M.; Al-Azab, F. M.
Data curation: Al-Selwi, N. A.
Formal Analysis: Jamil, Y. M.; Al-Selwi, N. A.
Funding acquisition: Not applicable.
Investigation: Jamil, Y. M.; Al-Azab, F. M.; Al-Selwi, N. A.
Methodology: Jamil, Y. M.; Al-Azab, F. M.; Al-Selwi, N. A.
Project administration: Jamil, Y. M.; Al-Azab, F. M.
Resources: Jamil, Y. M.; Al-Azab, F. M.; Al-Selwi, N. A.
Software: Al-Selwi N. A.
Supervision: Jamil, Y. M.; Al-Azab, F. M.
Validation: Jamil, Y. M.; Al-Azab, F. M.
Visualization: Jamil, Y. M.; Al-Azab, F. M.; Al-Selwi, N. A.
Writing – original draft: Al-Selwi, N. A.
Writing – review & editing: Jamil, Y. M.

Data availability statement

All data sets were generated or analyzed in the current study

Funding

Acknowledgments

References

Abd El-Wahab, Z. H.; El-Sarrag, M. R. Derivatives of phosphate Schiff base transition metal complexes: synthesis, studies and biological activity. *Spectrochimica Acta Part A.* **2004**, *60*, 271–277. https://doi.org/10.1016/S1386-1425(03)00216-6

Abu-Dief, A. M.; El-Metwaly, N. M.; Alzahrani, S. O.; Bawazeer, A. M.; Shaaban S.; Adam, M. S. S. Targeting *ct*DNA binding and elaborated in-vitro assessments concerning novel Schiff base complexes: Synthesis, characterization, DFT and detailed in-silico confirmation. *J. Mol. Liq.* **2021**, *322*, 114977. https://doi.org/10.1016/j.molliq.2020.114977

Abu-Yamin, A.; Abduh, M. S.; Saghir, S. A. M.; Al-Gabri, N. Synthesis, characterization and biological activities of new Schiff base compound and its lanthanide complexes. *Pharmaceuticals* **2022**, *15* (4), 454. https://doi.org/10.3390/ph15040454

Aderoju, A. O.; Sherifah, M. W. Synthesis, characterization and antimicrobial activity of some mixed drug trimethoprim-sulfamethoxazole metal drug complexes. *World Appl. Sci. J.* **2015**, *33* (2), 336–342. https://doi.org/10.5829/idosi.wasj.2015.33.02.22206

Akhtar M. S.; Alenad, A.; Malik, M. A. Synthesis of mackinawite FeS thin films from acidic chemical baths. *Mater. Sci. Semicond. Process.* **2015**, *32*, 1–5. https://doi.org/10.1016/j.mssp.2014.12.073

Al-Azab, F. M.; Jamil, Y. M. S.; Al-Gaadbi,A. A. M., Synthesis and Spectroscopic methods on the Complexation of CoII, NiII and CuII with 2-(((1H-indol-3-yl) methylene) amino) acetohydrazide hydrate. Sana'a University J. Appl. Sci. Technol. **2023**, *1* (1), 117–133. https://doi.org/10.59628/jast.v1i1.131

Al-Hakimi, A. N.; Shakdofa, M. M. E.; El-Seidy, A. M. A.; El-Tabl, A. S. Synthesis, Spectroscopic, and biological studies of chromium(iii), manganese(ii), iron(iii), cobalt(ii), nickel(ii), copper(ii), ruthenium(iii), and zirconyl(ii) complexes of N1,N2-Bis(3-((3-hydroxynaphthalen-2-yl)methylene-

amino)propyl)phthalamide. *J. Korean Chem. Soc.* **2011**, *55* (3), 418–429. https://doi.org/10.5012/jkcs.2011.55.3.418

Al-Maydama, H.; Al-Ansi, T. Y.; Jamil, Y. M.; Ali, A. H. Biheterocyclic ligands: synthesis, characterization and coordinating properties of bis(4-amino-5-mercapto-1,2,4-triazol-3-yl)alkanes with transition metal ions and their thermokinetic and biological studies. *Eclét. Quím.* **2008**, *33* (3), 29–42. https://doi.org/10.1590/S0100-46702008000300005

Boverhof, D. R.; Bramante, C. M.; Butala, J. H.; Clancy, S. F.; Lafranconi, M.; West, J.; Gordon, S. C. Comparative assessment of nanomaterial definitions and safety evaluation considerations. *Regul. Toxicol. Pharmacol.* **2015**, *73* (1), 137–150. https://doi.org/10.1016/j.yrtph.2015.06.001

Brzezińska-Błaszczyk, E.; Mińcikiewicz, M.; Ochocki, J. Effect of cisplatin and *cis*-platinum (II) phosphonate complex on murine mast cells. *Eur. J. Pharmacol*. **1996**, *298* (2), 155–158. https://doi.org/10.1016/0014-2999(95)00809-8

Çakır, U.; Temel, H.; Ihan, S.; Uğraş, H. I. Spectroscopic and conductance studies of new transition metal complexes with a Schiff base derived from 4-methoxybenzaldehyde and 1,2-bis(*p*-aminophenoxy)ethane. *Spectrosc. Lett.* **2003**, *36* (5–6), 429–440. https://doi.org/10.1081/SL-120026609

Camellia, F. K.; Ashrafuzzaman, M.; Islam, M. N.; Banu, L. A.; Kudrat-E-Zahan, M. Isoniazid Derived Schiff Base Metal Complexes: Synthesis, Characterization, Thermal Stability, Antibacterial and Antioxidant Activity Study. *Asian J. Chem. Sci.* **2022**, *11* (4), 23-36. https://doi.org/10.9734/ajocs/2022/v11i419131

Carrasco, F.; Hernández, W.; Chupayo, O.; Álvarez, C. M.; Oramas-Royo, S.; Spodine, E.; Tamariz-Angeles, C.; Olivera-Gonzales, P.; Dávalos, J. Z. Indole-3-carbaldehyde semicarbazone derivatives: Synthesis, characterization and antibacterial activities. *J. Chem.* **2020**, *2020*, 7157281. https://doi.org/10.1155/2020/7157281

Ceramella, J.; Iacopetta, D.; Catalano, A.; Cirillo, F.; Lappano, R.; Sinicropi, M. S. A Review on the antimicrobial activity of Schiff bases: data collection and recent studies. *Antibiotics* **2022**, *11* (2), 191. https://doi.org/10.3390/antibiotics11020191

El-khazandar, A. N. Organo-phosphorus Schiff base part (IV): Synthesis and characteristic of some phosphate Schiff-base complexes. *Phosphorus Sulfur Silicon Relat. Elem.* **1997**, *126* (1), 243–255. https://doi.org/10.1080/10426509708043564

El-Tabl, A. S.; El-Saied, F. A.; Al-Hakimi, A. N. Synthesis, spectroscopic investigation and biological activity of metal complexes with ONO trifunctionalalized hydrazone ligand. *Transition Met. Chem.* **2007**, *32* (6), 689–701. https://doi.org/10.1007/s11243-007-0228-0

Ericsson, H.; Tunevall, G.; Wickman, K. The Paper Disc Method for Determination of Bacterial Sensitivity to Antibiotics: Relationship Between the Diameter of the Zone

of Inhibition and the Minimum Inhibitory Concentration. *Scand. J. Clin. Lab. Invest.* **1960**, *12* (4), 414–422. https://doi.org/10.3109/00365516009065406

Fouda, M. F. R.; Abd-Elzaher, M. M.; Shakdofa, M. M.; El-Saied, F. A.; Ayad, M. I.; El Tabl, A. S. Synthesis and characterization of a hydrazone ligand containing antipyrine and its transition metal complexes. *J. Coord. Chem.* **2008**, *61* (12), 1983–1996. https://doi.org/10.1080/00958970701795714

Franklin, T. J.; Snow, G. A. *Biochemistry of Antimicrobial Action*; Springer, 1989. https://doi.org/10.1007/978-94-009-0825-3

Galil, M. S. A.; Al-Hakimi, A. N.; Alshwafy, R. Y.; Al Okab, R. A.; Mutir, A. Synthesis, Structural Studies and Microbial Evaluation of Cu(II), Mn(II) Ni(II), Zn(II), Fe(III), Ru(III), VO(II), UO₂(II) Complexes of Tetradentate Oxime-Hydrazon Ligand. *Chem. J.* **2015**, *1* (3), 95–102.

Geary, W. J. The use of conductivity measurements in organic solvents for characterization of coordination compounds. *Coord. Chem. Rev.* **1971**, *7* (1), 81–122. https://doi.org/10.1016/S0010-8545(00)80009-0

González-García, C.; Mata, A.; Zani, F.; Mendiola M. A.; López-Torres, E. Synthesis and antimicrobial activity of tetradentate ligands bearing hydrazone and/or thiosemicarbazone motifs and their diorganotin (IV) complexes. *J. Inorg. Biochem.* **2016**, *163*, 118–130. https://doi.org/10.1016/j.jinorgbio.2016.07.002

Gup, R.; Kirkan, B. Synthesis and spectroscopic studies of copper(II) and nickel(II) complexes containing hydrazonic ligands and heterocyclic colig and Spectrochim. *Acta Part A Mol. Biomol. Spectrosc.* **2005**, *62* (4–5), 1188–1195. https://doi.org/10.1016/j.saa.2005.04.015

Hossain, M. S.; Camellia, F. K.; Uddin, N.; Kudrat-E-Zahan, M.; Banu, L. A.; Haque, M. M. Synthesis, Characterization and Antimicrobial Activity of Metal Complexes of N-(4-methoxybenzylidene) Isonicotinohydrazone Schiff Base. *Asian J. Chem. Sci.* **2019**, *6* (1), 1–8. https://doi.org/10.9734/ajocs/2019/v6i118987

Ibeji, C. U.; Akintayo, D. C.; Oluwasola, H. O.; Akintemi, E. O. Anti-Corrosion potential of the Ortho and ParaSubstituted Schiff Bases of 2-Methoxybenzaldehyde on Fe (110) surface in acid medium: Synthesis, DFT and Molecular Dynamics Studies. *Research square.* **2022**. [Preprint]. https://doi.org/10.21203/rs.3.rs-1869552/v1

Jamil, Y.M.S.; Al-Azab, A. M.; Al-Azab, F. M.; Al-Selwi, N. A. A. Larvicidal Effects of New Organophosphorus Schiff base compounds against Dengue Fever Vector *Aedes aegypti* (Diptera; Culicidae), *Sana'a University J. Appl. Sci. Technol.* **2023**, *1* (1), 78–87. https://doi.org/10.59628/jast.v1i1.156

Jassem, A. M.; Radhi, W. A.; Jaber, H. A.; Mohammed, F. J. Synthesis and characterization of 1,3,4-Oxadiazoles

Derivatives from 4-Phenyl-Semicarbazide. *J. Basrah Res. Sci.* **2013**, *39* (3), 158–170.

Kaczmarek, M. T.; Zabiszak, M.; Nowak, M.; Jastrzab, R. Lanthanides: Schiff base complexes, applications in cancer diagnosis, therapy, and antibacterial activity. *Coord. Chem. Rev.* **2018**, *370*, 42–54. https://doi.org/10.1016/j.ccr.2018.05.012

Kafi-Ahmadi, L.; Marjani, A. P. Mononuclear Schiff Base Complexes Derived from 5-Azophenylsalicylaldehyde with Co(II), Ni(II) Ions: Synthesis, Characterization, Electrochemical Study and Antibacterial Properties. *S. Afr. J. Chem.* **2019**, *72* (1), 101–107. https://doi.org/10.17159/0379-4350/2019/v72a13

Kostova, I.; Saso, L. Advances in Research of Schiff-Base Metal Complexes as Potent Antioxidants. *Curr. Med. Chem.* **2013**, *20* (36), 4609–4632. https://doi.org/10.2174/09298673113209990149

Mohammed, N. L.; Al-Shawi, J. M. S.; Kadhim, M. J. Synthesis, Characterization and Thermal Studies of Schiff Bases Derived from 2,4-Dihydroxy benzaldehyde and their Complexes with Co(II), Ni (II), Cu(II). *Int. J. Sci. Eng. Res.* **2019**, *7* (1), 31–40.

Mohapatra, R. K.; Mishra, U. K.; Mishra, S. K.; Mahapatra, A.; Dash, D. C. Synthesis and Characterization of Transition Metal Complexes with Benzimidazolyl-2-hydrazones of o-anisaldehyde and Furfural. *J. Korean Chem. Soc.* **2011**, *55* (6), 926–931. https://doi.org/10.5012/jkcs.2011.55.6.926

Nakamoto, K. *Infrared and Raman Spectra of Inorganic and Coordination Compounds*. Part A and Part B; John Wiley & Sons, 1998.

Ochocki, J.; Graczyk, J.; Reedijk, J. Synthesis and antitumor activity of novel Pt(II) diethyl pyridylmethylphosphonate complexes against sarcoma-180. *J. Inorg. Biochem.* **1995**, *59* (2–3), 240. https://doi.org/10.1016/0162-0134(95)97346-R

Patterson, A. L. The Scherrer Formula for X-Ray Particle Size Determination. *Phys. Rev.* **1939**, *56* (10), 978–982. https://doi.org/10.1103/PhysRev.56.978

Sani, U.; Iliyasu, S. M. Synthesis, characterization and antimicrobial studies on Schiff base derived from 2-aminopyridine and 2-methoxybenzaldehyde and its cobalt (II) and nickel (II) complexes. *Bayero J. Pure appl. Sci.* **2018**, *11* (1), 214–219. https://doi.org/10.4314/bajopas.v11i1.35S

Shah, B.; Kakumanu, V. K.; Bansal, A. K. Analytical techniques for quantification of amorphous/crystalline phases in pharmaceutical solids. *J. Pharm. Sci.* **2006**, *95* (8), 1641–1665. https://doi.org/10.1002/jps.20644

Shakdofa, M. M. E.; Al-Hakimi, A. N.; Elsaied, F. A.; Alasbahi, S. O. M.; Alkwlini, A. M. A. Synthesis, Characterization and Bioactivity Zn²⁺, Cu ²⁺, Ni²⁺, Co²⁺, Mn²⁺, Fe³⁺, Ru³⁺, VO²⁺ and UO²⁺ complexes of 2-hydroxy-5-((4-

nitrophnyl(dizenyl)benzylidene)-2-(p-tolylamino)acetohydrazide. *Bull. Chem. Soc. Ethiop.* **2017**, *31* (1), 75–91. https://doi.org/10.4314/bcse.v31i1.7

Song, X.-Q.; Wang, Z.-G.; Wang, Y.; Huang, Y.-Y.; Sun, Y.-X.; Ouyang, Y.; Xie, C.-Z.; Xu, J.-Y. Syntheses, characterization, DNA/HSA binding ability and antitumor activities of a family of isostructural binuclear lanthanide complexes containing hydrazine Schiff base. *J. Biomol. Struct. Dyn.* **2020**, *38* (3), 733–743. https://doi.org/10.1080/07391102.2019.1587511

Vogel, A. I. *Text-book of quantitative inorganic analysis including elementary instrumental analysis*; Longmans, 1961.

Yassin, S. K.; Alshawi J. M. S.; Salih, Z. A. M. Synthesis, characterization and cytotoxic activity study of Cu (II), Co (II), Mn (II), Ni (II) and Cr (III) Metal Complexes with new guanidine Schiff base against the hepatocellular Carcinoma (HCAM) cancer cell. *Egypt. J. Chem.* **2020**, *63* (10), 4005-4016. https://doi.org/10.21608/ejchem.2020.37893.2778

Yoe, J. H.; Jones, A. L. Colorimetric Determination of Iron with Disodium-1,2-dihydroxybenzene-3,5-disulfonate. *Ind. Eng. Chem. Anal. Ed*. **1944**, *16* (2), 111–115. https://doi.org/10.1021/i560126a015

Yusof, E. N. M.; Ravoof, T. B. S. A.; Tiekink, E. R. T.; Veerakumarasivam, A.; Crouse, K. A.; Tahir, M. I. M.; Ahmad, H. Synthesis, Characterization and Biological Evaluation of Transition Metal Complexes Derived from N, S Bidentate Ligands. *Int. J. Mol. Sci.* **2015**, *16* (5), 11034–11054. https://doi.org/10.3390/ijms160511034

Supplementary Materials
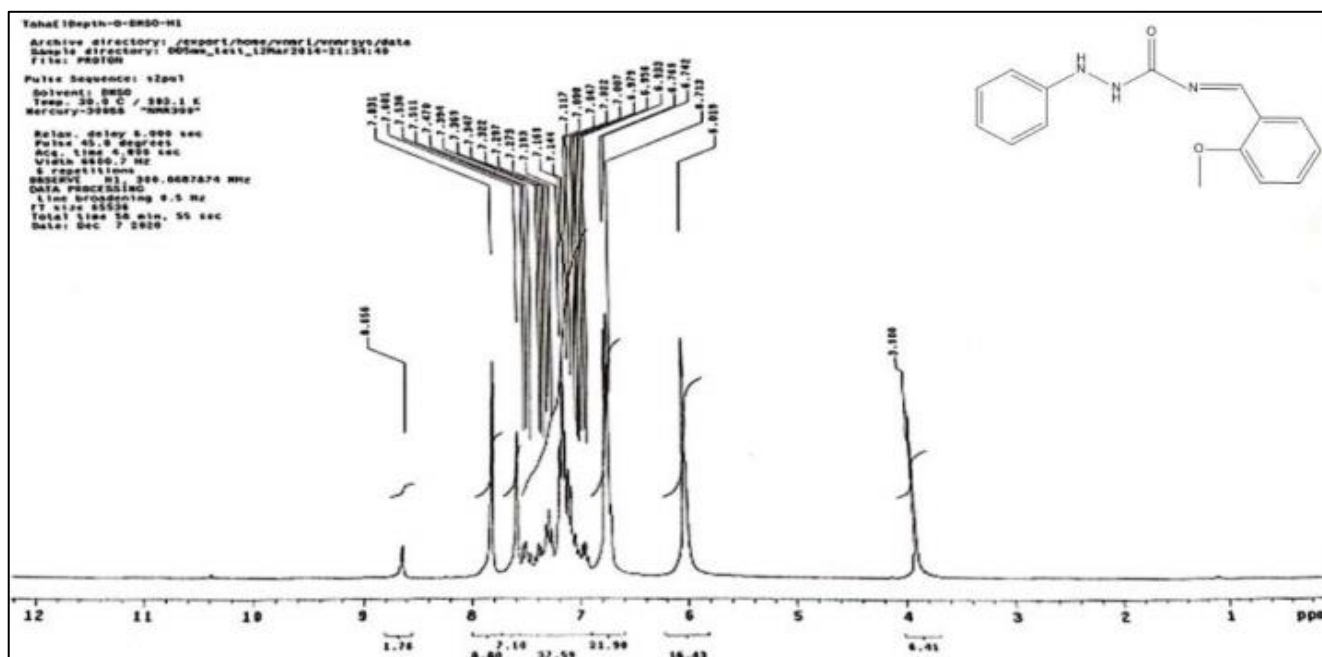
Figure S1. ^{1}HNMR spectrum of **L₁**.
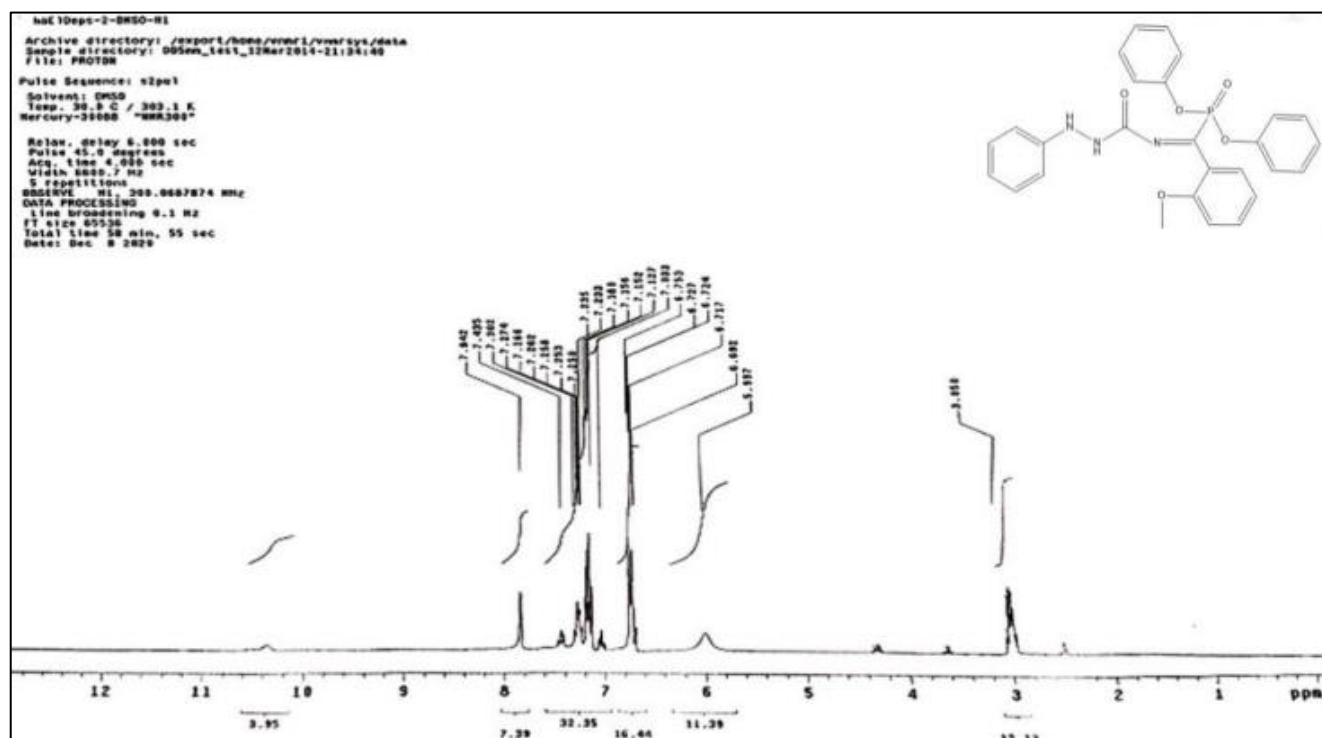
Figure S2. ^{1}HNMR spectrum of **L₂**.
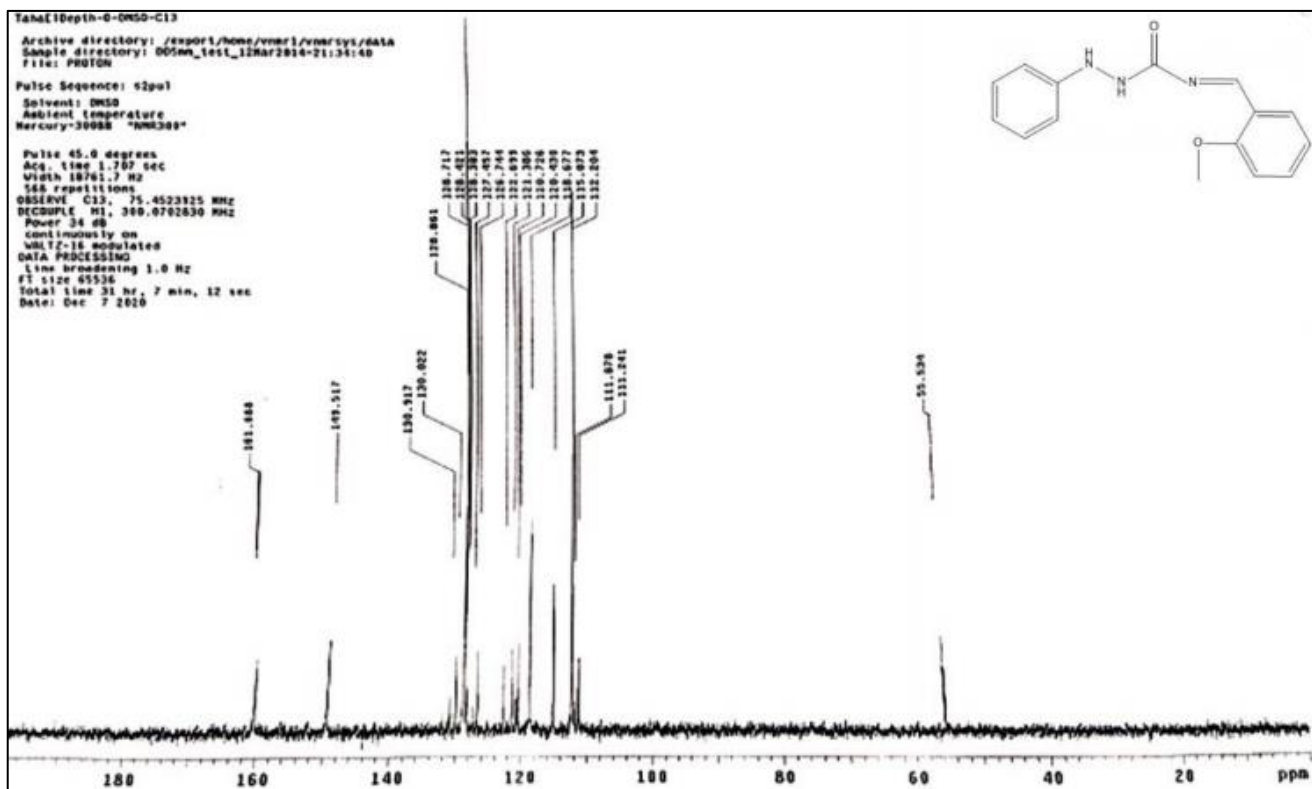
Figure S3. ^{13}CNMR spectrum of **L$_1$**.
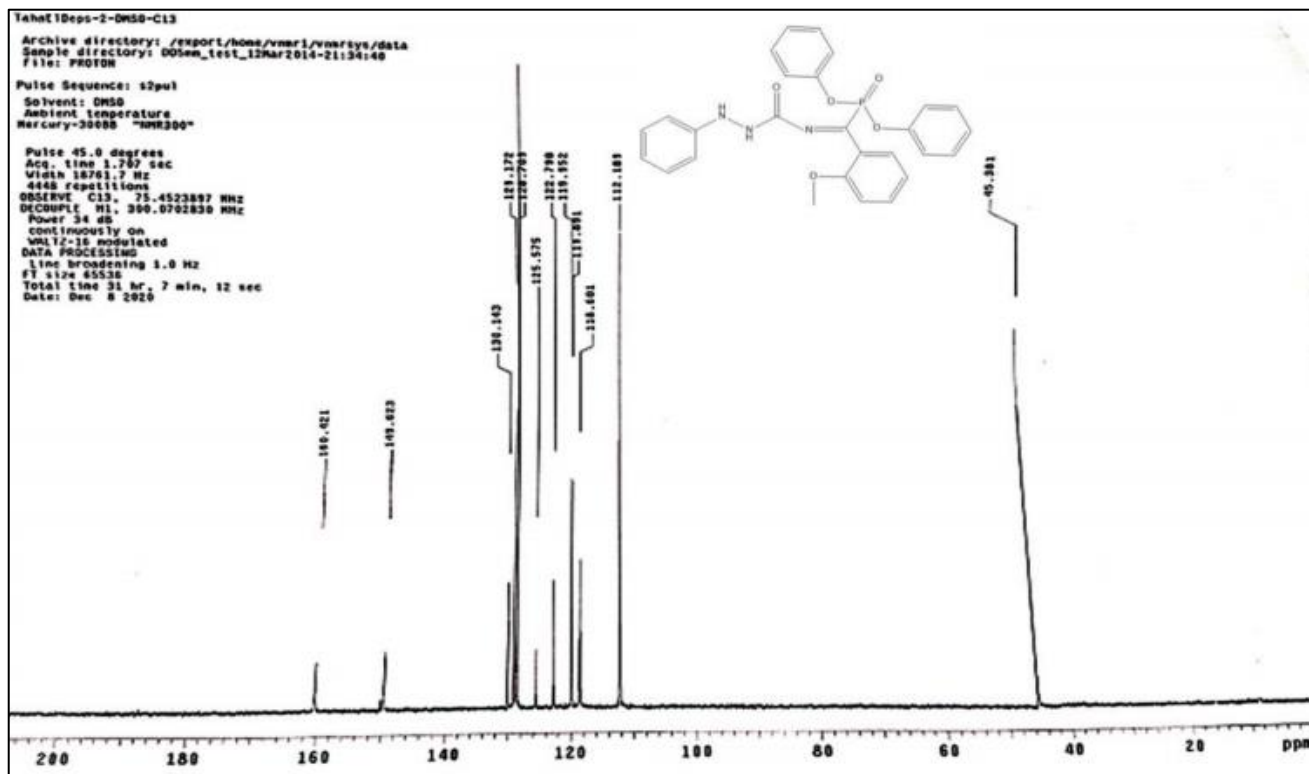
Figure S4. ^{13}CNMR spectrum of **L$_2$**.
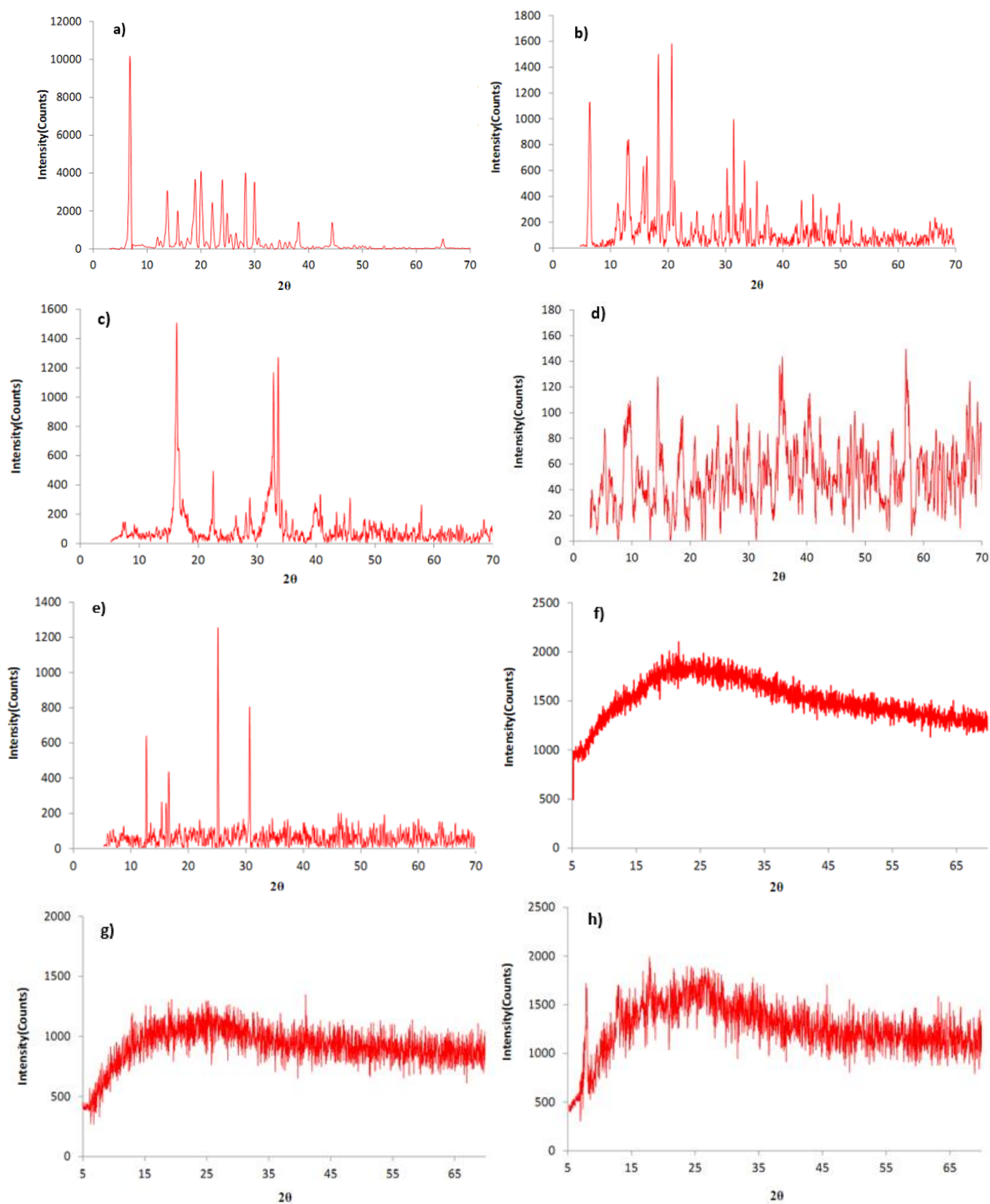
Figure S5. XRD pattern of **(a) L₁**; **(b) L₁(Cu)**; **(c) L₁(Ni)**; **(d) L₁(Co)**; **(e) L₂**; **(f) L₂(Cu)**; **(g) L₂(Ni)**; **(h) L₂(Co)**;

Potential inhibiting activities of phytochemicals in *Scilla natalensis* bulbs against schistosomiasis

Abel Kolawole Oyebamiji[1+], Jonathan Oyebamiji Babalola[2], Kehinde Abraham Odelade[3], Sunday Adewale Akintelu[4], Olubunmi Ayoola Nubi[5], Halleluyah Oluwatobi Aworinde[6], Esther Faboro[1], Emmanuel Temitope Akintayo[1], Banjo Semire[7]

1. Bowen University, Department of Chemistry and Industrial Chemistry, Iwo, Nigeria.
2. University of Ibadan, Department of Chemistry, Ibadan, Nigeria.
3. Federal Polytechnic, Department of Science Laboratory Technology, Ayede, Nigeria.
4. Beijing Institute of Technology, School of Chemistry and Chemical Engineering, Beijing, China.
5. Nigerian Institute for Oceanography & Marine Research, Victoria Island, Nigeria.
6. Bowen University, College of Computing and Communication Studies, Iwo, Nigeria.
7. Ladoke Akintola University of Technology, Department of Pure and Applied Chemistry, Ogbomoso, Nigeria.

+Corresponding author: Abel Kolawole Oyebamiji, **Phone:** +2348032493676, **Email address:** abeloyebamiji@gmail.com

ABSTRACT: Schistosomiasis remains one of the severe ailments that affect both man and woman in South Africa. It is caused by blood fluke, and the rate at which it causes death is alarming in some areas of America, Asia as well as in African countries. It is a neglected tropical disease (NTD) with grave impact on social and economic situation of countries with low sanitation awareness. Thus, the search for lasting solution to this menace, has drawn the attention of many global researchers using phytochemicals from *Scilla natalensis* via *in silico* approach. The studied compounds were optimized using Spartan 14. Docking study was executed via Pymol, Autodock tool, Auto dock vina and discovery studio. Compound **9** with –34.3 kJ mol⁻¹ and –39.3 kJ mol⁻¹ as binding affinity proved to possess highest ability to inhibit glutathione S-transferase and thioredoxin-glutathione reductase than other compounds. Also, ADMET properties for compound **9** and praziquantel were explored and reported. Our findings may open the door for the design of novel drug-like molecules with better
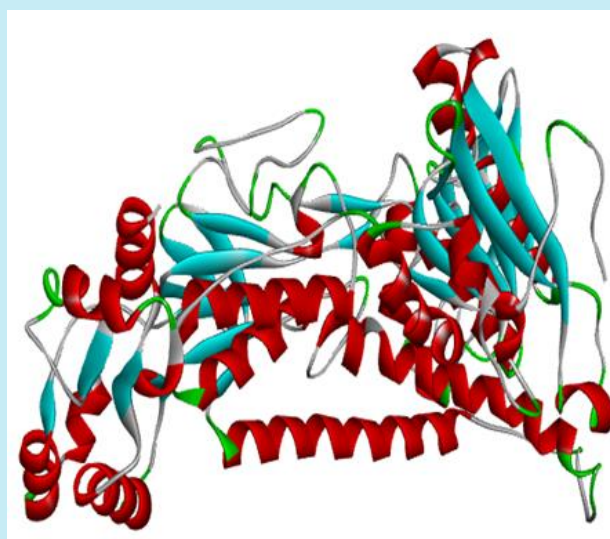
1. Introduction

Neglected tropical diseases (NTDs) are a class of syndromes that occur in tropical and subtropical regions most especially in developing countries (Engels and Zhou, 2020). The continuous spreading and the lingering effects of these types of diseases have been acknowledged to be a function of poverty. According to Ugbe *et al.* (2022), improper treatment of sickness and frequent lack of access to pure water are some of the variables that increase the prevalence of NTDs in local settlements. Series of reports about greater effort to curb diseases, like malaria, tuberculosis, etc., from national and international agencies show that NTDs are completely neglected diseases (Allotey *et al.*, 2010; Molyneux, 2008; 2009). Some of the NTDs are schistosomiasis, Buruli ulcer, trachoma, dengue virus, Guinea worm disease and onchocerciasis (WHO, 2022). The cost of treating NTDs is relatively small in some instances; however, due to poverty or low income, some areas in Africa, America and Asia are still experiencing greatly the effects of NTDs (Reddy *et al.*, 2007).

However, grave operation of schistosomiasis in human has drawn the attention of the World Health Organization (WHO), and it has been categorized as part of the 20 considered NTDs (Colley *et al.*, 2014; WHO, 2020). The name of this disease originated from *Schistosoma*, to which the worm (trematode) that causes it belongs. The taxonomic order of *Schistosoma* is kingdom: Animalia; phylum: Platyhelminthes; order: Diplostomida; subfamilly: Schistosomatinae; genus: *Schitosoma* and species: *haematobium, mansoni, japonicum*, *guineensis*, *intercalatum*, and *mekongi* (Kayuni *et al.*, 2019). Some of these species are the most common disease-causing species, while the remaining ones have lower universal pervasiveness. According to Klohe *et al.* (2021), the effects of schistosomiasis have been recorded in over 70 countries of which over 80% possess moderate to high spread, which requires serious mediation via precautionary chemotherapy. As reported by Porto *et al.* (2021), more than 2 million people have been affected while 800 million people were reported to be at risk of this deadly disease. Despite various efforts to contain this menace, its deadly operation in tropical and subtropical regions requires urgent and rapid intervention by means of potent chemotherapeutic agents.

Scilla natalensis is a bulbous herb with many medicinal features. It is a plant with blue flowers, and it is regarded as one of the well-known plant species with high demand in the South African market (Sparg *et al.*, 2002). As reported by several scientists, *S. natalensis* has been used to treat a series of diseases and infections, such as worms, stomach aches, fractures, boils, veld sores, skin rashes, diarrhea, constipation, dysentery, nausea, and indigestion (Cunningham, 1988; Eloff, 1998; Mander, 1997). Its bulb has the ability to act as laxative for tumors within the body and lumps, male potency enhancer and woman fertility booster. It subdues pain that originated from menstruation, and it eases child delivery for pregnant women (Hutchings, 1989; Hutchings *et al.*, 1996). The extract from *S. natalensis* was screened for anti-inflammatory and anthelmintic activity, and the results showed that the hexane extracts of *S. natalensis* displayed good inhibition against both COX-1 and COX-2 (Sparg *et al.*, 2002).
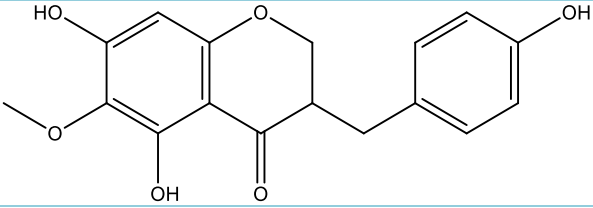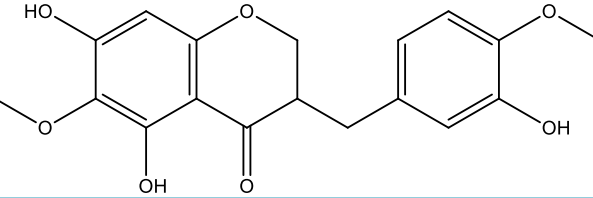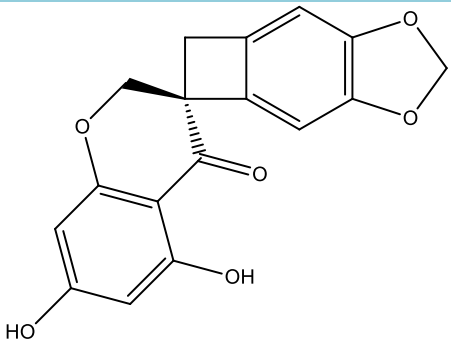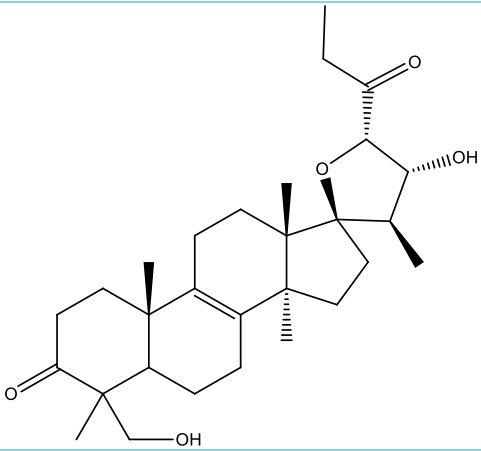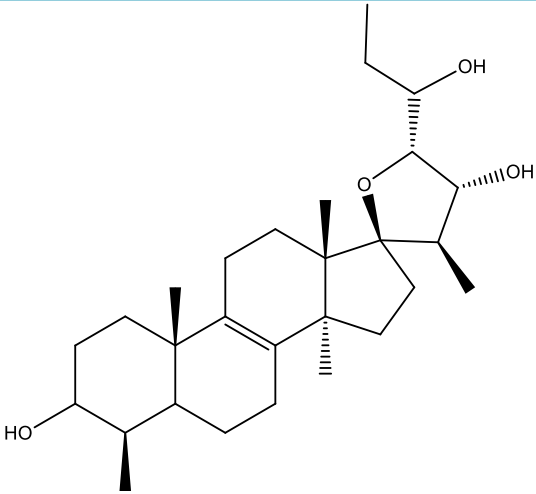
Therefore, the main purpose of this work is to (i) explore theoretical biological features of the selected phytochemicals obtained from *S. natalensis,* (ii) investigate the calculated binding affinity between the selected phytochemicals and the targets, and (iii) theoretically explore the pharmacokinetics of the selected phytochemicals.

2. Materials and methods
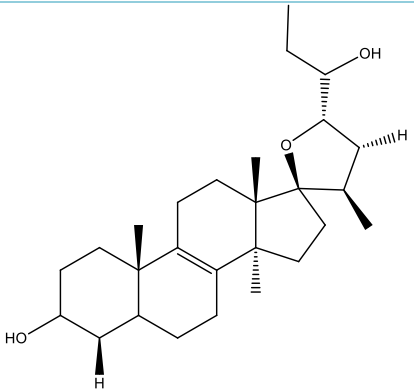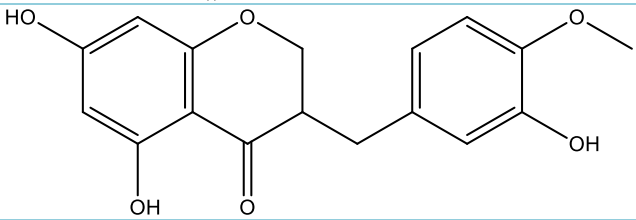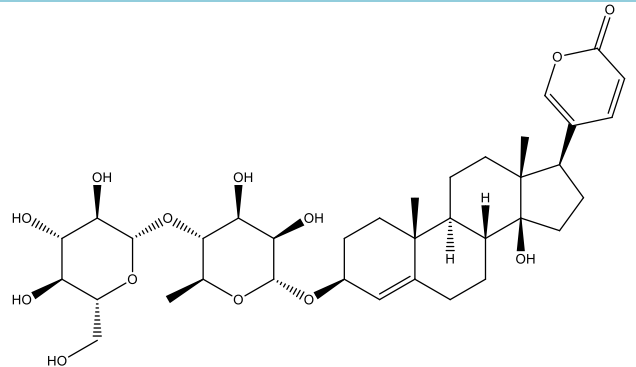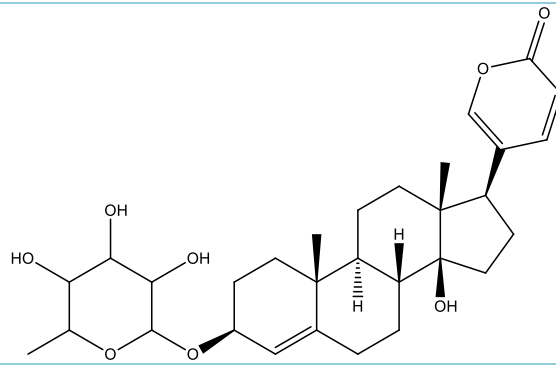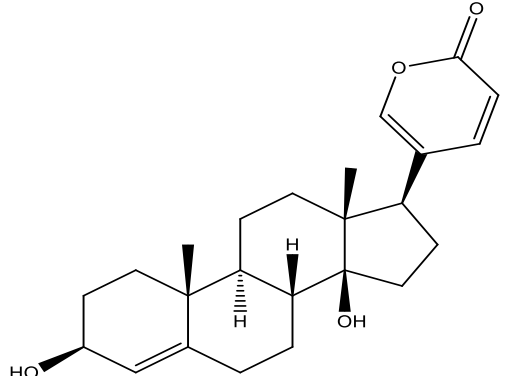
2.1 Structural optimization

The selected compounds from *S. natalensis* bulb were carefully modeled using ChemDraw Ultra 12.0.2 software and saved as MDL SDfile (*.sdf) format (Table 1). The modeled structures were subjected to Spartan'14 software to view a 3D version of the modeled structures and then optimized via energy minimization. The minimization of the studied molecular compounds was executed using Molecular Mechanics Force Field, while the optimization of the compounds was accomplished using density functional theory (DFT) and 6-31G* was used as basis set. The optimized compounds were saved and the calculated descriptors for each molecule were reported (Oyeneyin *et al.*, 2022; Wang *et al.*, 2020).

Table 1. Two-dimensional (2D) structure of the studied compound.

	Chemical structure	IUPAC names
1		5,7-dihydroxy-6-methoxy-3-(4-hydroxybenzyl)chroman-4-one
2		5,7-dihydroxy-6-methoxy-3-(3-hydroxy-4-methoxybenzyl)chroman-4-one
3		(3*R*)-5,7-dihydroxyspiro[2*H*-chromene-3,4'-9,11-dioxatricyclo[6.3.0.0[3,6]]undeca-1(8),2,6-triene]-4-one
4		(22*R*,23*S*)-17α,23-Epoxy-22,29-dihydroxy-27-norlanost-8-en-3,24-dione
5		(22*R*,23*S*)-17α,23-Epoxy-3β,22,24ξ-trihydroxy-27,28-bisnor-lanost-8-ene
		Continue…

6		(23*S*)-17α,23-Epoxy-3*β*,24*ξ*-dihydroxy-27,28,29-trisnorlanost-8-ene
7		5,7 -dihydroxy-3-(3hydroxy-4-methoxybenzyl)chroman-4-one
8		5-[(3*S*,8*R*,9*S*,10*R*,13*R*,14*S*,17*R*)-3-[(2*R*,3*R*,4*S*,5*R*,6*S*)-3,4-dihydroxy-6-methyl-5-[(2*S*,3*R*,4*S*,5*S*,6*R*)-3,4,5-trihydroxy-6-(hydroxymethyl)oxan-2-yl]oxyoxan-2-yl]oxy-14-hydroxy-10,13-dimethyl-1,2,3,6,7,8,9,11,12,15,16,17-dodecahydrocyclopenta[a]phenanthren-17-yl]pyran-2-one
9		5-[(3*S*,8*R*,9*S*,10*R*,13*R*,14*S*,17*R*)-14-hydroxy-10,13-dimethyl-3-(3,4,5-trihydroxy-6-methyloxan-2-yl)oxy-1,2,3,6,7,8,9,11,12,15,16,17-dodecahydrocyclopenta[a]phenanthren-17-yl]pyran-2-one
10		5-[(3*S*,8*R*,9*S*,10*R*,13*R*,14*S*,17*R*)-3,14-dihydroxy-10,13-dimethyl-1,2,3,6,7,8,9,11,12,15,16,17-dodecahydrocyclopenta[a]phenanthren-17-yl]pyran-2-one

Source: Elaborated by the authors using data from Sparg *et al*., (2002).

2.2 Target identification, selection and preparation

Two targets (glutathione S-transferase [PDB ID: 1gtb]) (McTigue *et al.*, 1995) and thioredoxin-glutathione reductase (PDB ID: 3h4k) (Angelucci *et al.*, 2009) were retrieved from protein data bank (Fig. 1a and b). The two receptors were subjected to Pymol software where suitable implements were deployed to treat and prepare glutathione S-transferase (PDB ID: 1gtb) and thioredoxin-glutathione reductase (PDB ID: 3h4k) for docking. The amino acids present in each of the downloaded receptor were carefully checked and any other materials (i.e., crystallographic water and small molecules rooted in each of the receptor) different from amino acids were deleted and saved in *.pdb format.

Also, all the possible missing amino acids in each clean receptor were replaced using Swiss Pdbviewer 4.1.0 version and saved in *.pdb format before identification of the binding site in each receptor using Autodock tool software. The center and size in X, Y and Z directions which show the located binding site for glutathione S-transferase (PDB ID: 1gtb) were 11.97, 45.043 and 32.999 for the center and 50, 52 and 60 for size; and for thioredoxin-glutathione reductase (PDB ID: 3h4k) were 45.78, –0.593 and 16.04 for the center and 80, 90 and 78 for size. The calculation of binding affinity for the studied complex was executed via Autodock vina software and the discovery studio was used to view the interaction between the ligands and the receptors.
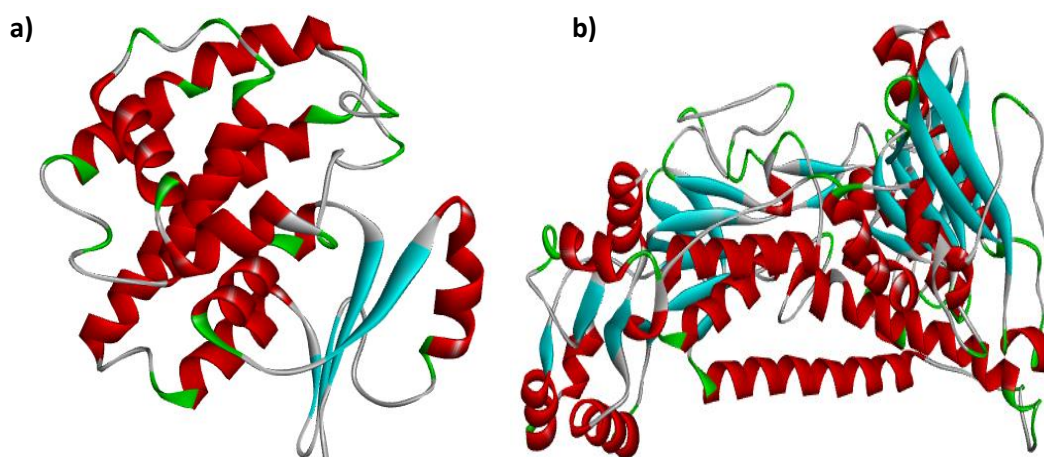
Figure 1. Tree-dimensional (3D) structures of transferase and reductase enzymes: (**a**) 3D structure of glutathione S-transferase and (**b**) 3D structure of thioredoxin-glutathione reductase.

2.3 Computational analysis of pharmacokinetic properties

The study of pharmacokinetics plays a crucial role in drug design and discovery since only chemical compounds with worthy drug-likeness features, as well as outstanding absorption, distribution, metabolism, excretion, and toxicity (ADMET) profiles move into the advance stage of drug production (Lawal *et al.*, 2021). Therefore, 5-[(3*S*,8*R*,9*S*,10*R*,13*R*,14*S*,17*R*)-14-hydroxy-10,13-dimethyl-3-(3,4,5-trihydroxy-6-methyloxan-2-yl)oxy-1,2,3,6,7,8,9,11,12,15,16,17-dodecahydrocyclopenta[a]phenanthren-17-yl]pyran-2-one (**9**) with lower binding affinity value, which indicate better inhibitory activities, was reconnoitered for ADMET study via ADMETlab (https://admetmesh.scbdd.com/), an online ADMET software.

3. Results and discussion

3.1 Calculated descriptors

One of the crucial descriptors calculated from optimized molecular compounds as described by many researchers are the highest occupied molecular orbital energy (E_{HOMO}), and lowest unoccupied molecular orbital energy (E_{LUMO}) (HOMO-LUMO energies). The part taken in overriding vast array of chemical and biological interactions by HOMO-LUMO energies cannot be easily neglected (Saranya *et al.*, 2018). The E_{HOMO} indicates molecule with greater strength to donate electron while E_{LUMO} indicate molecules with greater strength to accept electron from neighboring compounds. In this work, we observed that (3*R*)-5,7-dihydroxyspiro[2*H*-chromene-3,4'-9,11-dioxatricyclo[6.3.0.0^{3,6}]undeca-1(8),2,6-triene]-4-one (**3**) has highest strength to donate and receive electrons

from nearby compounds. Also, lower band gap indicates spontaneous interactions between two molecules (Latona *et al.* 2022a); thus, (3*R*)-5,7-dihydroxyspiro[2*H*-chromene-3,4'9,11-dioxatricyclo[6.3.0.0³,⁶]undeca-1(8),2,6-triene]-4-one (**3**) showed a greater strength to interact with neighboring compounds than other studied compounds (Supplementary Material 1). As we observed in this work, lower number of atoms highly contributed

to high level of interacting ability of compound **3**; this revealed the effectiveness of the combination of the atom as well as the bonds present in (3*R*)-5,7-dihydroxyspiro[2*H*-chromene-3,4'-9,11-dioxatricyclo[6.3.0.0³,⁶]undeca-1(8),2,6-triene]-4-one (**3**). Other descriptors obtained from compounds from *S. natalensis* bulb were also reported in Table 2.

Table 2. The selected descriptors obtained from compounds from *S. natalensis* bulb.

	E_{HOMO}	E_{LUMO}	BG	MW	LogP	HBD	HBA
1	−5.76	−1.48	4.28	316.30	−2.66	3.00	6.00
2	−5.59	−1.49	4.10	346.33	−3.64	3.00	7.00
3	−5.58	−1.61	3.97	312.27	−2.97	2.00	6.00
4	−5.77	−0.97	4.80	472.66	4.62	2.00	5.00
5	−5.79	0.82	6.61	446.67	4.34	3.00	4.00
6	−5.80	0.80	6.60	416.64	4.76	2.00	3.00
7	−5.59	−1.44	4.15	316.30	−2.66	3.00	6.00
8	−6.25	−1.36	4.89	692.79	0.73	7.00	12.00
9	−6.28	−1.44	4.84	530.65	2.47	4.00	7.00
10	−6.28	−1.44	4.84	384.51	3.36	2.00	3.00

3.2 Molecular docking analysis

The assessment of the orientation of the selected compounds from *S. natalensis* bulb in the active site of the targets glutathione S-transferase (PDB ID: 1gtb) and thioredoxin-glutathione reductase (PDB ID: 3h4k) were carefully studied using docking method. The biochemical and biological connections between the studied complexes were exposed as well as the calculated binding affinity for the studied complexes were thoroughly investigated and reported. Adeoye *et al.* (2022) reported that biochemical and biological capability of any compound may and may not reveal its inhibition capacity. The inhibition capacity of any compound against the target is a function of the type of nonbonding interactions that occur between such complexes (Latona *et al.*, 2022b). Therefore, 5-[(3*S*,8*R*,9*S*,10*R*,13*R*,14*S*,17*R*)-14-hydroxy-10,13-dimethyl-3-(3,4,5-trihydroxy-6-methyloxan-2-yl)oxy-1,2,3,6,7,8,9,11,12,15,16,17-dodecahydrocyclopenta[a]phenanthren-17-yl]pyran-2-one (compound **9**) with −34.3 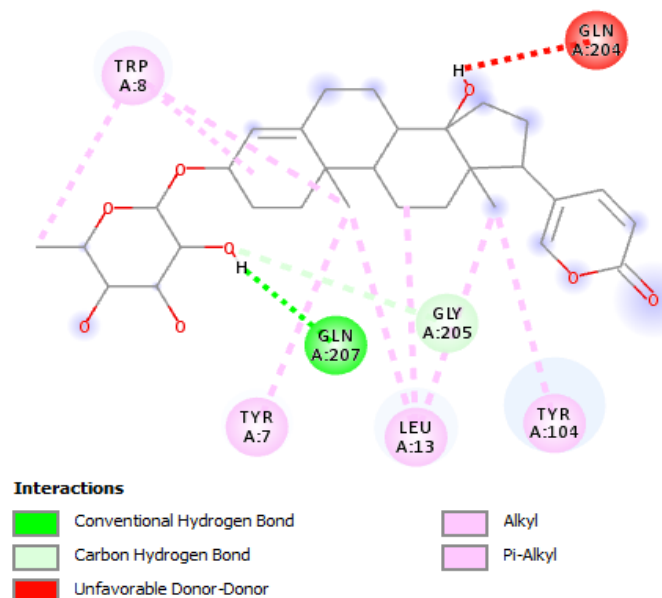kJ mol⁻¹ (PDB ID: 1gtb) and −39.3 kJ mol⁻¹ (PDB ID: 3h4k) possessed greater tendency to inhibit glutathione S-transferase and thioredoxin-glutathione reductase than other studied compounds (Figs. 2 and 3). The calculated binding affinities for compound **1**–**10** against glutathione S-transferase (PDB ID: 1gtb) were −29.7, −29.3, −31.0, −31.4, −31.8, −33.5, −30.5, −34.3, −34.3, and −31.4 kJ mol⁻¹, respectively. This showed that all the compounds, except compounds 1, 2 and 7, could be good

inhibitors for glutathione S-transferase as compared to Praziquantel. Also, docking results of optimized compounds **1**–**10** against thioredoxin-glutathione reductase (PDB ID: 3h4k) were −31.8, −32.2, −34.3, −33.9, −34.3, −33.5, −32.6, −34.7, −39.3, and −36.8 kJ mol⁻¹, respectively, indicating that all the phytochemicals could serve as inhibitors for thioredoxin-glutathione reductase (Table 3). According to Olasupo *et al.* (2021), the lower the binding affinity value of a compound, the better the ability of the compound to inhibit the target; hence, compound **9** has outstanding binding affinity and a greater tendency to inhibit glutathione S-transferase and thioredoxin-glutathione reductase, thereby hindering the activities of schistosomiasis. Also, this work agreed well with the work carried out by El-Seedi *et al.* (2012), which authenticated the biological activity of Asparagaceae as antischistosomiasis. Similar results were reported by Akachukwu *et al.*, (2017) when 27 bioactive compounds of some medicinal plants were screened against *Schistosoma* cell lines (PDB ID: 1M9A and 2X99). The docking results revealed that quercetin-(3`-O 4```)-3``-O-methyl kaempferol and quercetin presented binding energies of −39.41 and −38.99 kJ mol⁻¹ against 1M9A cell lines of *Schistosoma*, respectively. Also, the binding affinities calculated for β-solamarine, solamargine and quercetin-(3`-O 4```)-3``-O-methyl kaempferol against 2X99 cell lines of *Schistosoma* were −38.99, −38.58 and −39.41 kJ mol⁻¹, respectively (Akachukwu *et al.*, 2017). This was similar to binding energy calculated for 5-[(3*S*,8*R*,9*S*,10*R*,13*R*,14*S*,17*R*)-14-hydroxy-10,13-

dimethyl-3-(3,4,5-trihydroxy-6-methyloxan-2-yl)oxy-1,2,3,6,7,8,9,11,12,15,16,17-dodecahydrocyclopenta[a]phenanthren-17-yl]pyran-2-one (9) against thioredoxin-glutathione reductase (PDB ID: 3H4K). This was higher than binding affinities reported by Mtemeli *et al.* (2022) from docking *Cucurbita maxima* against *Schistosoma mansoni* purine nucleoside phosphorylase (*Sm*PNP) and *Schistosoma haematobium* 28-kDa glutathione S-transferase (*Sh*28kDaGST). The results showed that binding affinities of the most promising compounds, momordicoside I aglycone and balsaminoside B were –33.1 and –32.2 kJ mol^{-1} with *Sm*PNP and *Sh*28kDaGST, respectively.

Figure 2. Biochemical interaction between Compound **9** and glutathione S-transferase.
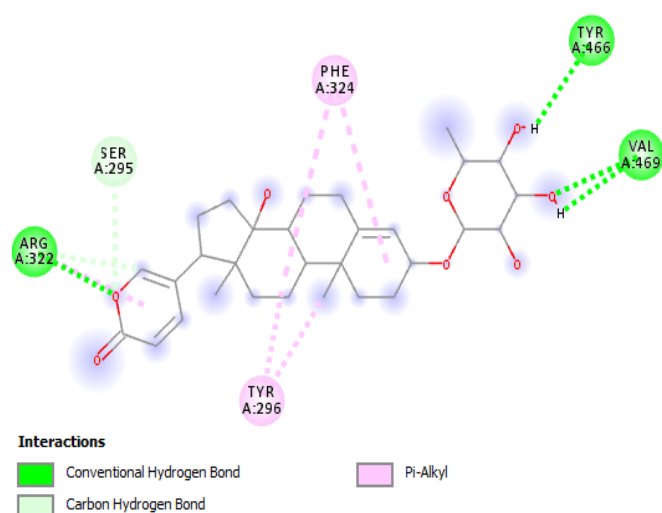
Figure 3. Biochemical interaction between Compound **9** and thioredoxin-glutathione reductase.

Table 3. Calculated binding affinity and residues involved in the interactions.

	Binding affinity (kJ mol^{-1})	
	Glutathione S-transferase	Thioredoxin-glutathione reductase
1	–29.7	–31.8
2	–29.3	–32.2
3	–31.0	–34.3
4	–31.4	–33.9
5	–31.8	–34.3
6	–33.5	–34.7
7	–30.5	–32.6
8	–31.8	–34.7
9	–34.3	–39.3
10	–31.4	–36.8
Praziquantel	–30.1	–33.1

Moreover, the work carried out by El-Seedi *et al.* (2012) on *Asparagus stipularis* Forssk., which was commonly known in Egypt as *agool gabal*, revealed the efficacy of medicinal plant as antischistosomiasis. The extracted asparagalin A was observed to be effective against schistosomiasis. This was confirmed through the efficiency of the studied compound (asparagalin A) against worm egg-laying capacity of *S. mansoni* thereby down-regulating the activity of schistosomiasis (El-Seedi *et al.*, 2012) and this correlated with the inhibiting activity of the studied *S. natalensis* bulbs.

More so, the inhibiting capacity of three medicinal plants (*Artemisia annua*, *Nigella sativa*, and *Allium sativum*) explored by Fadladdin *et al.* (2022) against *S. mansoni* adult worms was experimentally studied. The concentration of 500 m/dm^3, 250 m/dm^3, and 125 m/dm^3

of *A. annua* proved to be more effective against adult worms when compared to similar concentration of *N. sativa*, and *A. sativum* against the adult worms. Greater morphological changes were observed in the activity of *A. annua* on *S. mansoni* adult worms; however, lesser morphological changes were shown in the activities of *N. sativa*, and *A. sativum* on the *S. mansoni* adult worms. This inhibiting activity of *A. annua* on *S. mansoni* agreed with efficiency of *S. natalensis* bulbs as antischistosomiasis due to greater ability to hinder the activity of *S. mansoni* than praziquantel (reference drug) (Fadladdin *et al.*, 2022).

3.3 Pharmacokinetic study

The ADMET properties for compounds **9** and praziquantel (referenced drug) were accomplished using ADMETlab software and series of factors were considered such as physicochemical property, medicinal chemistry, absorption, distribution, metabolism, excretion, toxicity, environmental toxicity, tox21 pathway, toxicophore rules. The calculated molecular weight for compound **9** fell within the acceptable range of 100–600 amu and this was confirmed to help it physicochemical property. Also, number of hydrogen bond acceptors (0–12), number of hydrogen bond donors (0–7), number of rotatable bonds (0–11), number of rings (0–6), number of atoms in the biggest ring (0–18), number of heteroatoms (1–15), formal charge (–4 to 4), topological polar surface area (0–140) for compound **9** were within the acceptable range and its ability to act as potential drug proved to be valid (Supplementary Material 2 and 3).

As shown in Supplementary Material 2 and 3, synthetic accessibility score (SAscore) for compound **9** (5.052) was within the acceptable range for ease of synthesis of drug-like molecules (< 6) and this showed that compound **9** can easily be synthesized. Also, compound **9** obeyed Lipinski rule of five and other factors considered were reported in Supplementary Material 2 and 3. More so, the ADMET properties for compound **9** were in line with the ADMET properties obtained for the referenced drug (praziquantel).

4. Conclusions

The biochemical and biological activities of selected compounds from *S. natalensis* bulb were thoroughly investigated via *in silico* approach. We observed that *S. natalensis* bulb have the potential anti-schistosomiasis

activities which was described via the calculated descriptors. Also, 5-[(3*S*,8*R*,9*S*,10*R*,13*R*,14*S*,17*R*)-14-hydroxy-10,13-dimethyl-3-(3,4,5-trihydroxy-6-methyloxan-2-yl)oxy-1,2,3,6,7,8,9,11,12,15,16,17-dodecahydrocyclopenta[a]phenanthren-17-yl]pyran-2-one (**9**) was reported with highest tendency to inhibit glutathione S-transferase and thioredoxin-glutathione reductase, better than other studied compounds. It was observed that compound **9** have ability to inhibit more than one target as proved in this work. The ADMET properties were investigated and reported in this work.

Authors' contribution

Data availability statement

All data sets were generated or analyzed in the current study.

Funding

Acknowledgments

References

Adeoye, M. D.; Olarinoye, E. F.; Oyebamiji, A. K.; Latona, D. F. Theoretical evaluation of potential anti-alanine dehydrogenase activities of acetamide derivatives. *Biointerface Res. Appl. Chem.* **2022**, *12* (6), 7469–7477. https://doi.org/10.33263/BRIAC126.74697477

Akachukwu, I.; Olubiyi, O. O.; Kosisochukwu, A.; John, M. C.; Justina, N. N. Structure-based study of natural products with anti-schistosoma activity. *Curr. Comput. Aided Drug Des.* **2017**, *13* (2), 91–100. https://doi.org/10.2174/1573409913666170119114859

Allotey, P.; Reidpath, D. D.; Pokhrel, S. Social sciences research in neglected tropical diseases 1: The ongoing neglect in the neglected tropical diseases. *Health Res. Policy Sys.* **2010**, *8*, 32. https://doi.org/10.1186/1478-4505-8-32

Angelucci, F.; Sayed, A. A.; Williams, D. L.; Boumis, G.; Brunori, M.; Dimastrogiovanni, D.; Miele, A. E.; Pauly, F.; Bellelli, A. Inhibition of *Schistosoma mansoni* thioredoxin-glutathione reductase by auranofin. *J. Biol. Chem.* **2009**, *284* (42), 28977–28985. https://doi.org/10.1074/jbc.M109.020701

Colley, D. G.; Bustinduy, A. L.; Secor, W. E.; King, C. H. Human schistosomiasis. *Lancet.* **2014**, *383* (9936), 2253–2264. https://doi.org/10.1016/S0140-6736(13)61949-2

Cunningham, A. B. *An investigation of the herbal medicinal trade in Natal/KwaZulu.* Investigational Report 29; Institute of Natural Resources, 1988.

Engels, D.; Zhou, X.-N. Neglected tropical diseases: An effective global response to local poverty-related disease priorities. *Infect. Dis. Poverty.* **2020**, *9*, 10. https://doi.org/10.1186/s40249-020-0630-9

Eloff, J. N. A Sensitive and quick microplate method to determine the minimal inhibitory concentration of plant extracts for bacteria. *Planta Med.* **1998**, *64* (8) 711–713. https://doi.org/10.1055/s-2006-957563

El-Seedi, H. R.; El-Shabasy, R.; Sakr, H.; Zayed, M.; El-Said, A. M. A.; Helmy, K. M. H.; Gaara, A. H. M.; Turki, Z.; Azeem, M.; Ahmed, A. M.; Boulos, L.; Borg-Karlson, A-K.; Göransson, U. Anti-schistosomiasis triterpene glycoside from the Egyptian medicinal plant *Asparagus stipularis*. *Rev. Bras. Farmacogn.* **2012**, *22* (2), 314–318. https://doi.org/10.1590/S0102-695X2012005000004

Fadladdin, Y. A. J. Evaluation of antischistosomal activities of crude aqueous extracts of *Artemisia annua*, *Nigella sativa*, and *Allium sativum* against *Schistosoma mansoni* in hamsters. *BioMed Res. Inter.* **2022**, *2022*, 5172287. https://doi.org/10.1155/2022/5172287

Hutchings, A. A survey and analysis of traditional medicinal plants as used by the Zulu, Xhosa and Sotho. *Bothalia.* **1989**, *19* (1), a947. https://doi.org/10.4102/abc.v19i1.947

Hutchings, A.; Haxton Scott, A. H.; Lewis, S. G.; Cunningham, A. *Zulu medicinal plants*: An inventory; University of Natal Press, 1996.

Kayuni, S.; Lampiao, F.; Makaula, P.; Juziwelo, L.; Lacourse, E. J.; Reinhard-Rupp, J.; Leutscher, P. D. C.; Stothard, J. R. A systematic review with epidemiological update of male genital schistosomiasis (MGS): A call for integrated case management across the health system in sub-Saharan Africa. *Parasite Epidemiol Control.* **2019**, *4*, e00077. https://doi.org/10.1016/j.parepi.2018.e00077

Klohe, K.; Koudou, B. G.; Fenwick, A.; Fleming, F.; Garba, A.; Gouvras, A.; Harding-Esch, E. M.; Knopp, S.; D'Souza, S.; Utzinger, J.; Vounatsou, P.; Waltz, J.; Zhang, Y.; Rollinson, D. A systematic literature review of schistosomiasis in urban and peri-urban settings. *PLoS Negl. Trop. Dis.* **2021**, *15* (2), e0008995. https://doi.org/10.1371/journal.pntd.0008995

Latona, D. F.; Oyebamiji, A. K.; Mutiu, O. A., Olarinoye, E. F. Evaluation of some benzimidazole derivatives as hepatitis B&C protease inhibitors: Computational study. *Trop. J. Nat. Prod. Res.* **2022a**, *6* (3), 416–421.

Latona, D. F.; Mutiu, O. A.; Adeoye, M. D.; Oyebamiji, A. K.; Akintelu, S. A.; Adedapo, A. S. *In-silico* investigation on chloroquine derivatives: A potential anti-COVID-19 main protease. *Biointerface Res. Appl. Chem.* **2022b**, *12* (6), 8492–8501. https://doi.org/10.33263/BRIAC126.84928501

Lawal, H. A.; Uzairu, A.; Uba, S. QSAR, molecular docking studies, ligand-based design and pharmacokinetic analysis on Maternal Embryonic Leucine Zipper Kinase (MELK) inhibitors as potential anti-triple-negative breast cancer (MDA-MB-231cell line) drug compounds. *Bull. Natl. Res. Centre.* **2021**, *45*, 90. https://doi.org/10.1186/s42269-021-00541-x

Mander, M. *The marketing of indigenous medicinal plants in South Africa: A case study in KwaZulu-Natal*. Investigational Report 164; Institute of Natural Resources, 1997.

McTigue, M. A.; Williams, D. R.; Tainer, J. A. Crystal structures of a schistosomal drug and vaccine target: Glutathione S-transferase from *Schistosoma japonica* and its complex with the leading antischistosomal drug praziquantel. *J. Mol. Biol.* 1995, *246* (1), 21–27. https://doi.org/10.1006/jmbi.1994.0061

Molyneux, D. H. Combating the "other diseases" of MDG 6: Changing the paradigm to achieve equity and poverty reduction? *Trans. R. Soc. Trop. Med. Hyg.* **2008**, *102* (6), 509–519. https://doi.org/10.1016/j.trstmh.2008.02.024

Molyneux, D. H.; Hotez, P. J.; Fenwick, A.; Newman, R. D.; Greenwood, B.; Sachs, J. Neglected tropical diseases and the Global Fund. *Lancet.* **2009**, *373* (9660), 296–297. https://doi.org/10.1016/S0140-6736(09)60089-1

Mtemeli, F. L.; Shoko, R.; Ndlovu, J.; Mugumbate, G. *In silico* study of *Cucurbita maxima* compounds as potential therapeutics against schistosomiasis. *Bioinform. Biol. Insights.* **2022**, *16*, 1–10. https://doi.org/10.1177/11779322221100741

Olasupo, S. B.; Uzairu, A.; Shallangwa, G. A.; Uba, S. Unveiling novel inhibitors of dopamine transporter via in silico drug design, molecular docking, and bioavailability predictions as potential antischizophrenic agents. *Futur. J. Pharm. Sci.* **2021**, *7*, 63. https://doi.org/10.1186/s43094-021-00198-3

Oyeneyin, O. E.; Iwegbulam, C. G.; Ipinloju, N.; Olajide, B. F.; Oyebamiji, A. K. Prediction of the antiproliferative effects of some benzimidazolechalcone derivatives against MCF-7 breast cancer cell lines: QSAR and molecular docking studies. *Org. Commun.* **2022**, *15* (3), 273–277. https://doi.org/10.25135/acg.oc.132.2203.2374

Porto, R.; Mengarda, A. C.; Cajas, R. A.; Salvadori, M. C.; Teixeira, F. S.; Arcanjo, D. D. R.; Siyadatpanah, A.; Pereira, M. L; Wilairatana, P.; Moraes, J. Antiparasitic properties of cardiovascular agents against human intravascular parasite *Schistosoma mansoni. Pharmaceuticals.* **2021**, *14* (7), 686. https://doi.org/10.3390/ph14070686

Reddy, M.; Gill, S. S.; Kalkar, S. R.; Wu, W.; Anderson, P. J.; Rochon, P. A. Oral drug therapy for multiple neglected tropical diseases: A systematic review. *JAMA.* **2007**, *298* (16), 1911–1924. https://doi.org/10.1001/jama.298.16.1911

Saranya, M.; Ayyappan, S.; Nithya, R.; Sangeetha, R. K.; Gokila, A. Molecular structure, NBO and HOMO-LUMO analysis of quercetin on single layer graphene by density functional theory. *Dig. J. Nanomater. Biostructures.* **2018**, *13* (1), 97–105.

Sparg, S. G.; van Staden, J.; Jäger, A. K. Pharmacological and phytochemical screening of two Hyacinthaceae species: *Scilla natalensis* and *Ledebouria ovatifolia. J. Ethnopharmacol.* **2002**, *80* (1), 95–101. https://doi.org/10.1016/S0378-8741(02)00007-7

Ugbe, F. A.; Shallangwa, G. A.; Uzairu, A.; Abdulkadir, I. Theoretical modeling and design of some pyrazolopyrimidine derivatives as *Wolbachia inhibitors*, targeting lymphatic filariasis and onchocerciasis. *In Silico Pharmacol.* **2022**, *10*, 8. https://doi.org/10.1007/s40203-022-00123-3

Wang, X.; Dong, H.; Qin, Q. QSAR models on aminopyrazole substituted resorcylate compounds as Hsp90 inhibitors. *J. Comput. Sci. Eng.* **2020**, *48*, 1146–1156.

World Health Organization (WHO). *Schistosomiasis*. Fact Sheet No 115; WHO, 2020. http://www.who.int/mediacentre/factsheets/fs115/en/. (accessed 2020-Jan-20)

World Health Organization (WHO). *Control of neglected tropical diseases*; WHO, 2022. http://www.who.int/teams/control-of-neglected-tropical-diseases/overview. (accessed 2020-Jan-20)

Supplementary Material 1

Figure S1. Predicted orbital energy for compound 1.
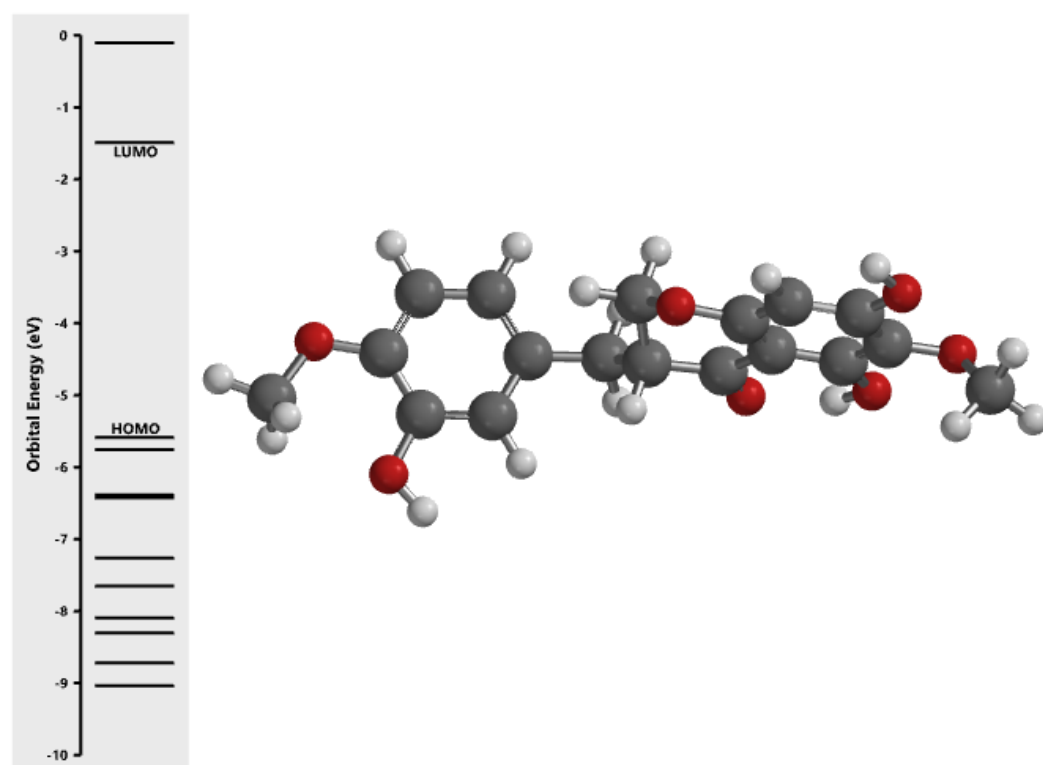
Figure S2. Predicted orbital energy for compound 2.
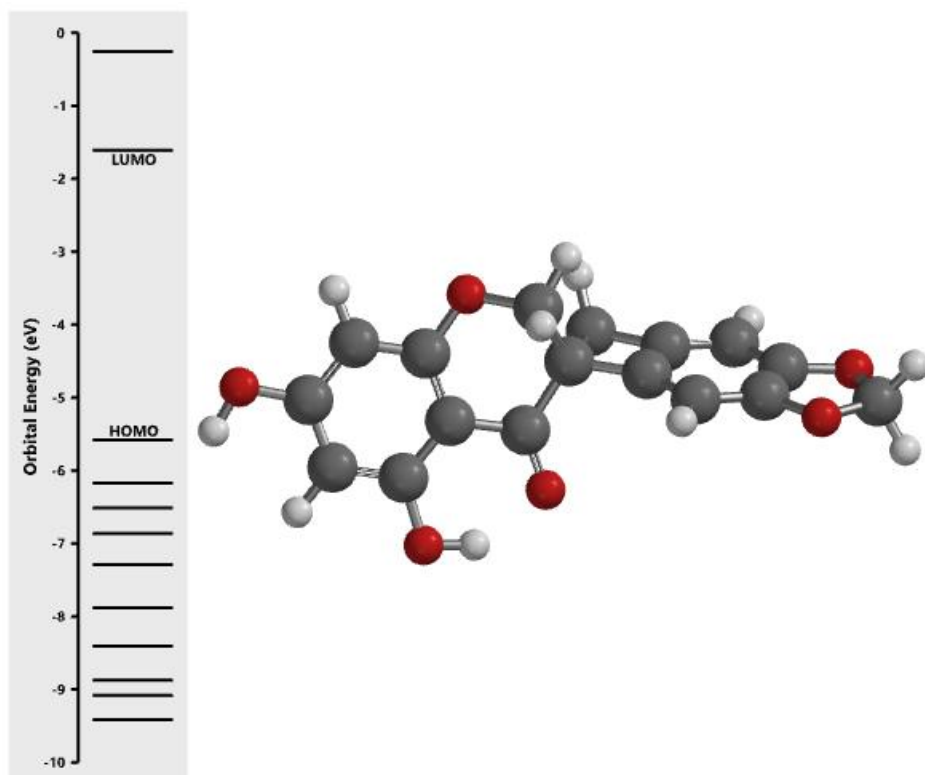
Figure S3. Predicted orbital energy for compound 3.
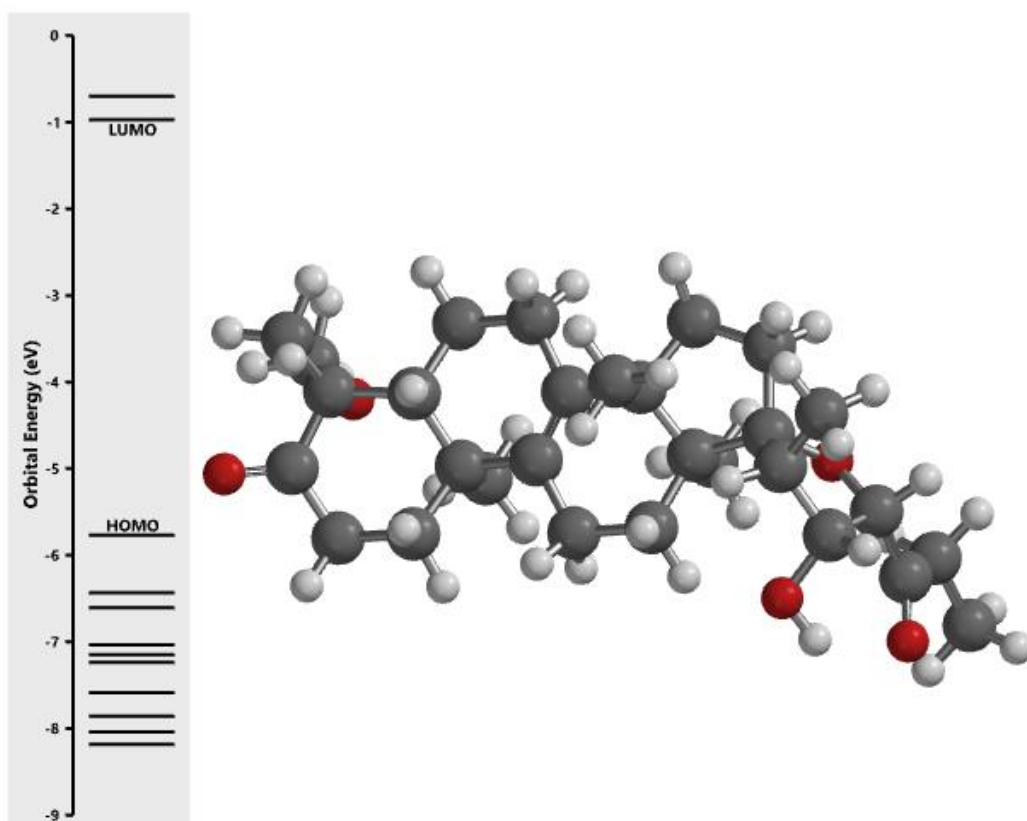
Figure S4. Predicted orbital energy for compound 4.
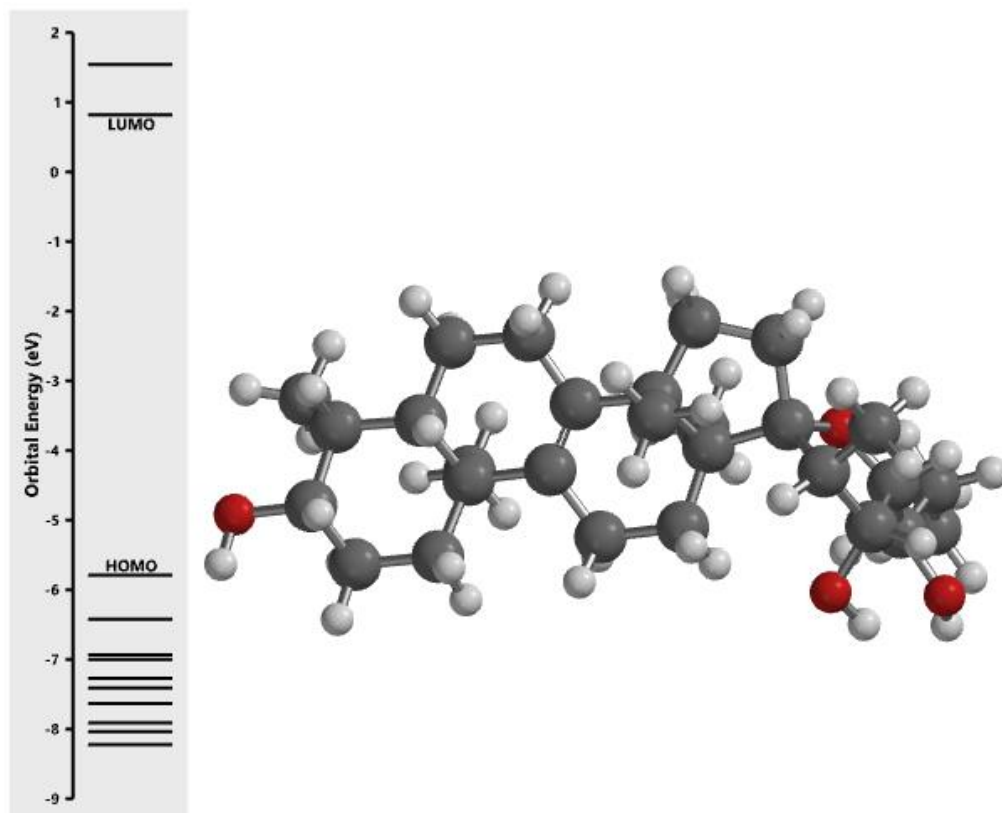
Figure S5. Predicted orbital energy for compound 5.
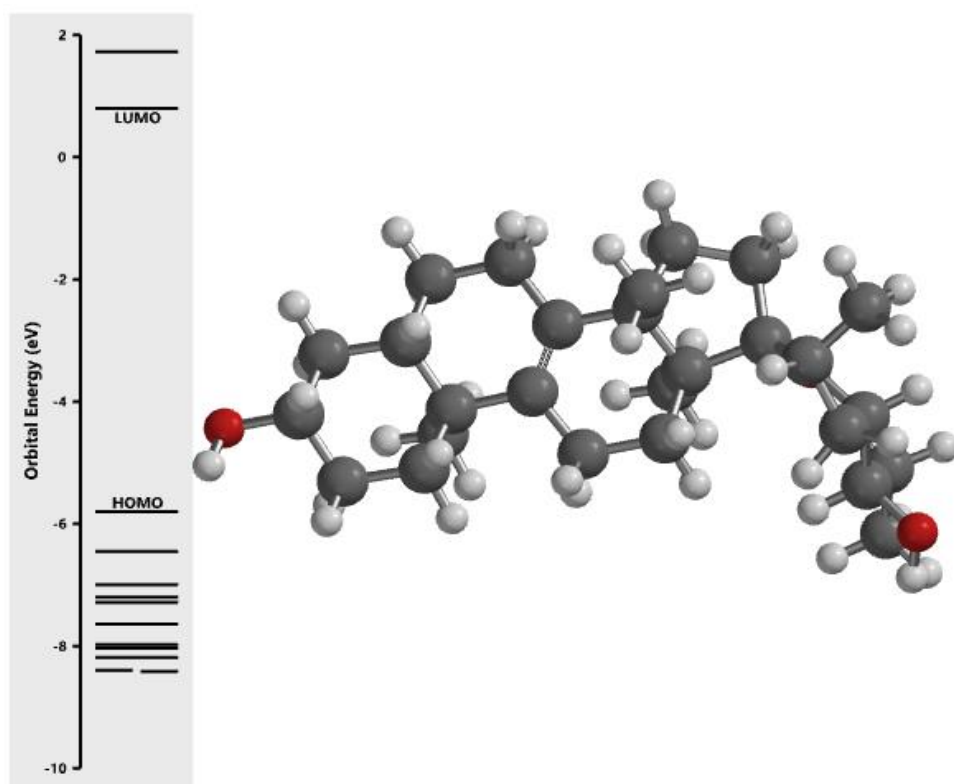
Figure S6. Predicted orbital energy for compound 6,

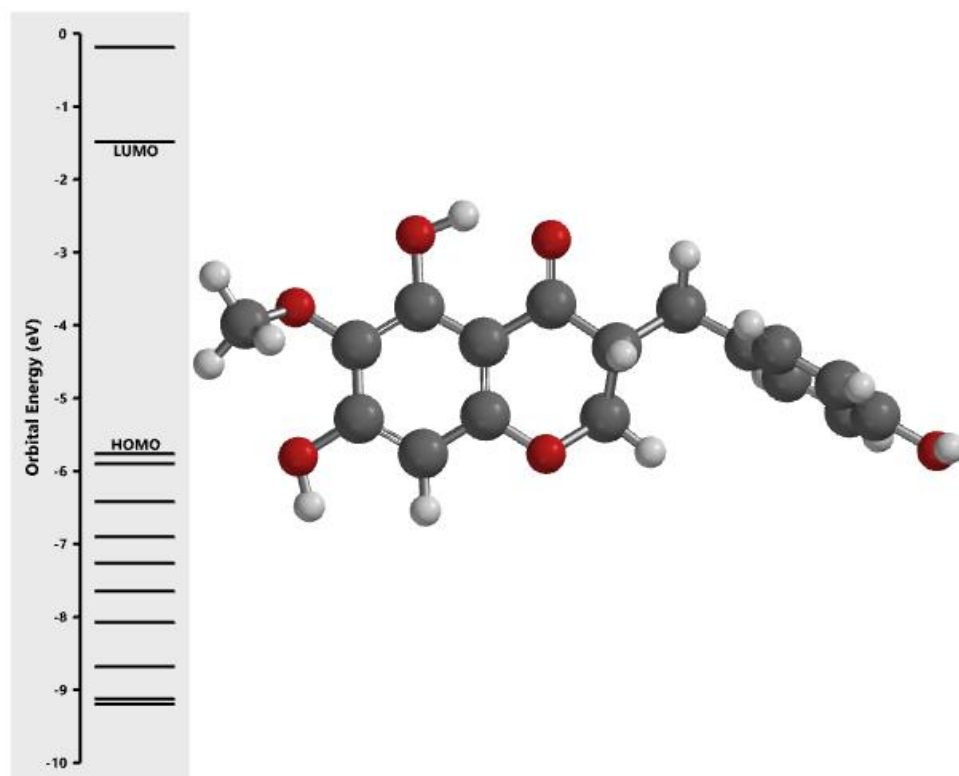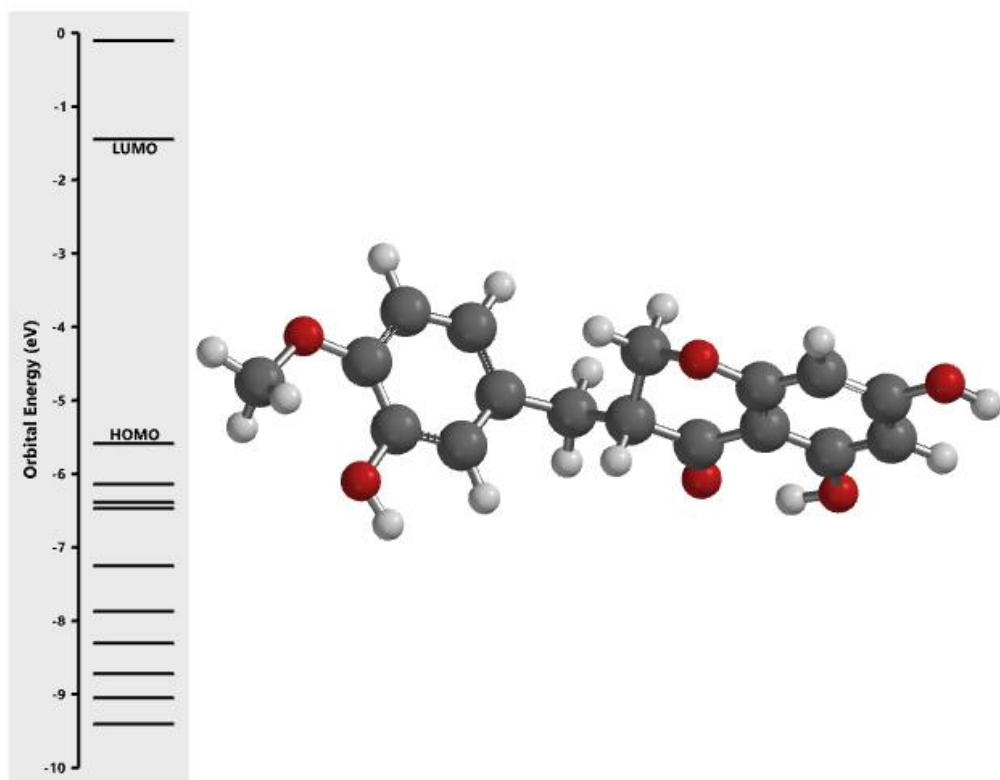**Figure S7.** Predicted orbital energy for compound 7.
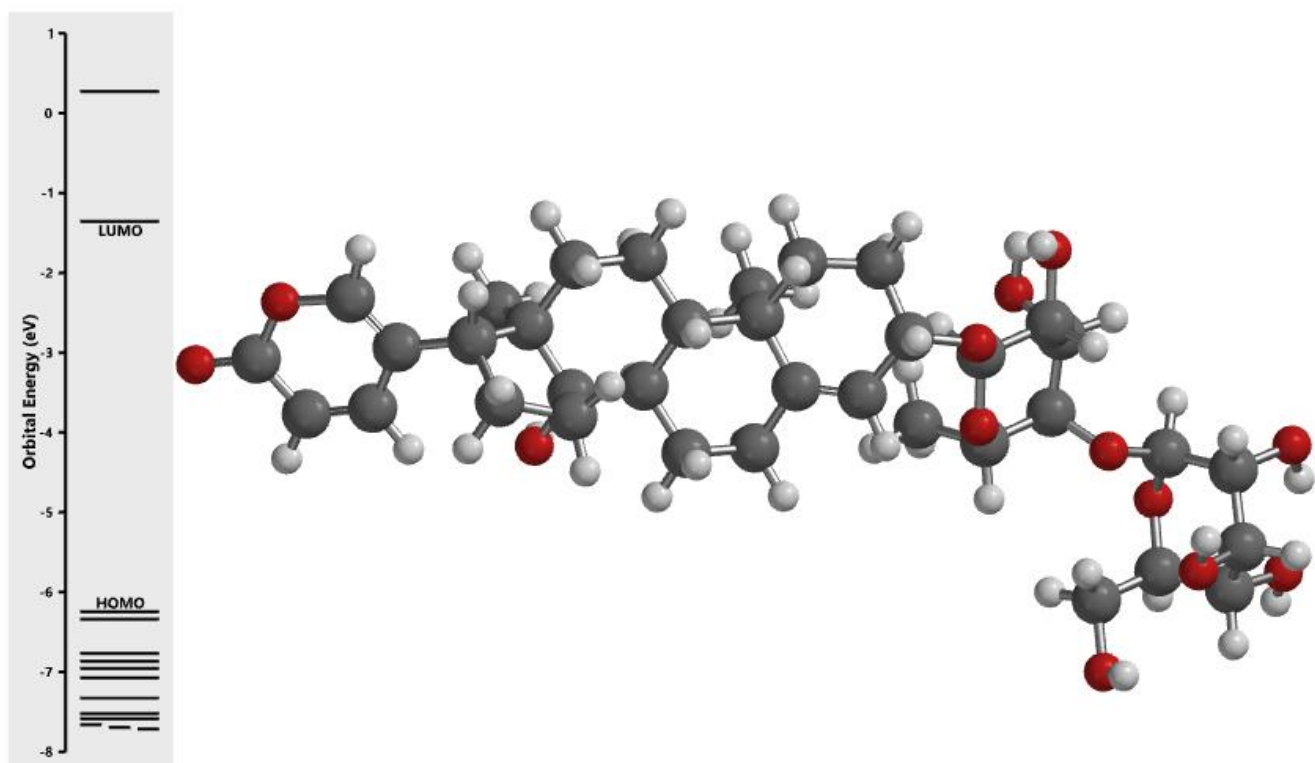
Figure S8. Predicted orbital energy for compound 8.
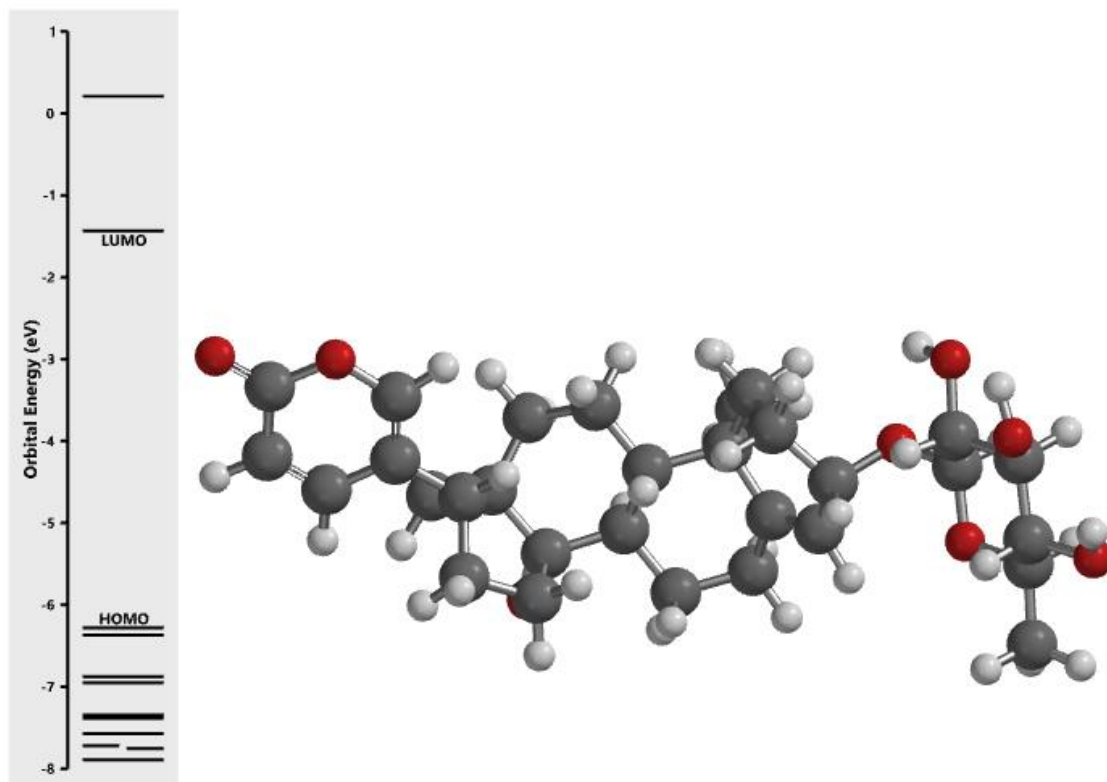
Figure S9. Predicted orbital energy for compound 9.
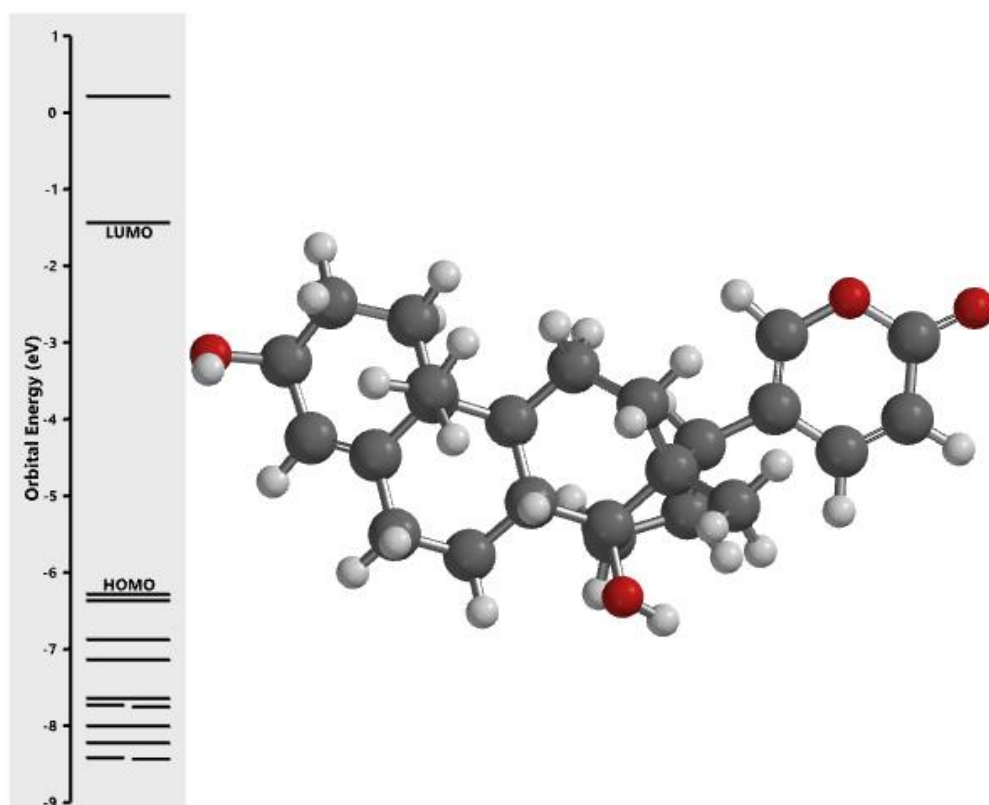
Figure S10. Predicted orbital energy for compound 10.

Supplementary Material 2

Compound 9

Table S1. Physicochemical property.

Property	Value	Comment
Molecular Weight	530.29	Contain hydrogen atoms. Optimal:100~600
Volume	535.873	Van der Waals volume
Density	0.99	Density = MW / volume
nHA	8	Number of hydrogen bond acceptors. Optimal:0~12
nHD	4	Number of hydrogen bond donors. Optimal:0~7
nRot	3	Number of rotatable bonds. Optimal:0~11
nRing	6	Number of rings. Optimal:0~6
MaxRing	17	Number of atoms in the biggest ring. Optimal:0~18
nHet	8	Number of heteroatoms. Optimal:1~15
fChar	0	Formal charge. Optimal: –4 ~4
nRig	33	Number of rigid bonds. Optimal:0~30
Flexibility	0.091	Flexibility = nRot /nRig
Stereo Centers	12	Optimal: ≤ 2
TPSA	129.59	Topological Polar Surface Area. Optimal:0~140
logS	–4.093	Log of the aqueous solubility. Optimal: –4~0.5 log mol L^{-1}
logP	2.698	Log of the octanol/water partition coefficient. Optimal: 0~3
logD	2.071	LogP at physiological pH 7.4. Optimal: 1~3

Table 2. Medicinal Chemistry.

Property	Value	Decision	Comment
QED	0.439	●	A measure of drug-likeness based on the concept of desirability. Attractive: > 0.67; unattractive: 0.49~0.67; too complex: < 0.34.
SAscore	5.052	●	Synthetic accessibility score is designed to estimate ease of synthesis of drug-like molecules. SAscore ≥ 6, difficult to synthesize; SAscore < 6, easy to synthesize.
Fsp3	0.767	●	The number of sp3 hybridized carbons / total carbon count, correlating with melting point and solubility. $Fsp^3 ≥ 0.42$ is considered a suitable value.
MCE-18	146.434	●	MCE-18 stands for medicinal chemistry evolution. MCE-18 ≥ 45 is considered a suitable value.
NPscore	2.731	-	Natural product-likeness score. This score is typically in the range from –5 to 5. The higher the score is, the higher the probability is that the molecule is a NP.
Lipinski Rule	Accepted	●	MW ≤ 500; logP ≤ 5; Hacc ≤ 10; Hdon ≤ 5. If two properties are out of range, a poor absorption or permeability is possible, one is acceptable.
Pfizer Rule	Accepted	●	logP > 3; TPSA < 75. Compounds with a high log P (>3) and low TPSA (<75) are likely to be toxic.
GSK Rule	Rejected	●	MW ≤ 400; logP ≤ 4. Compounds satisfying the GSK rule may have a more favorable ADMET profile
Golden Triangle	Rejected	●	200 ≤ MW ≤ 50; -2 ≤ logD ≤ 5. Compounds satisfying the Golden Triangle rule may have a more favorable ADMET profile.
PAINS	0 alert	-	Pan Assay Interference Compounds, frequent hitters, Alpha-screen artifacts and reactive compound.
ALARM NMR	1 alert	-	Thiol reactive compounds.
BMS	0 alert	-	Undesirable, reactive compounds.
Chelator Rule	0 alert	-	Chelating compounds.

Table S3. Absorption.

Property	Value	Decision	Comment
Caco-2 Permeability	–5.037	●	Optimal: higher than –5.15 Log unit.
MDCK Permeability	2.3x10^{05}	●	Low permeability: $< 2 \times 10^{-6}$ cm s^{-1} Medium permeability: 2–20×10^{-6} cm s^{-1} High passive permeability: $> 20 \times 10^{-6}$ cm s^{-1}
Pgp-inhibitor	0.395	●	Category 1: Inhibitor; Category 0: Noninhibitor. The output value is the probability of being Pgp-inhibitor.
Pgp-substrate	0.998	●	Category 1: substrate; Category 0: Nonsubstrate. The output value is the probability of being Pgp-substrate.
HIA	0.88	●	Human intestinal absorption Category 1: HIA+(HIA < 30%); Category 0: HIA–(HIA < 30%); The output value is the probability of being HIA+
F 20%	0.985	●	20% Bioavailability Category 1: F + (bioavailability < 20%). 20% Category 0: F – (bioavailability ≥ 20%); The output 20% value is the probability of being F+ 20%
F 30%	0.99	●	30% Bioavailability Category 1: F + (bioavailability < 30%). 30% Category 0: F – (bioavailability ≥ 30%); The output 30% value is the probability of being F+ 30%

Table S4. Distribution.

Property	Value	Decision	Comment
PPB	86.87%	●	Plasma protein binding Optimal: < 90%. Drugs with high protein-bound may have a low therapeutic index.
VD	1.468	●	Volume distribution Optimal: 0.04–20 L kg^{-1}
BBB penetration	0.085	●	Blood-brain barrier penetration Category 1: BBB+; Category 0: BBB-; The output value is the probability of being BBB+
FU	6.943%	●	The fraction unbound in plasms Low: < 5%; Middle: 5~20%; High: > 20%

Table S5. Metabolism.

Property	Value	Comment
CYP1A2 inhibitor	0.019	Category 1: Inhibitor; Category 0: Noninhibitor. The output value is the probability of being inhibitor.
CYP1A2 substrate	0.883	Category 1: Substrate; Category 0: Nonsubstrate. The output value is the probability of being substrate.
CYP2C19 inhibitor	0.044	Category 1: Inhibitor; Category 0: Noninhibitor. The output value is the probability of being inhibitor.
CYP2C19 substrate	0.615	Category 1: Substrate; Category 0: Nonsubstrate. The output value is the probability of being substrate.
CYP2C9 inhibitor	0.123	Category 1: Inhibitor; Category 0: Noninhibitor. The output value is the probability of being inhibitor.
CYP2C9 substrate	0.072	Category 1: Substrate; Category 0: Nonsubstrate. The output value is the probability of being substrate.
CYP2D6 inhibitor	0.024	Category 1: Inhibitor; Category 0: Noninhibitor. The output value is the probability of being inhibitor.
CYP2D6 substrate	0.37	Category 1: Substrate; Category 0: Nonsubstrate. The output value is the probability of being substrate.
CYP3A4 inhibitor	0.429	Category 1: Inhibitor; Category 0: Noninhibitor; The output value is the probability of being inhibitor.
CYP3A4 substrate	0.284	Category 1: Substrate; Category 0: Nonsubstrate. The output value is the probability of being substrate.

Table S6. Excretion.

Property	Value	Decision	Comment
CL	3.333	●	Clearance High: > 15 mL min^{-1} kg^{-1}; Moderate: 5–15 mL min^{-1} kg^{-1}. Low: < 5 mL min^{-1} kg^{-1}.
T$_{1/2}$	0.306	-	Category 1: long half-life; Category 0: short half-life. Long half-life: > 3 h; Short half-life: < 3 h. The output value is the probability of having long half-life.

Table S7. Toxicity.

Property	Value	Decision	Comment
hERG blockers	0.436	●	Category 1: active; Category 0: inactive. The output value is the probability of being active.
H-HT	0.236	●	Human hepatotoxicity Category 1: H-HT positive(+); Category 0: H-HT negative(−). The output value is the probability of being toxic.
DILI	0.153	●	Drug induced liver injury. Category 1: drugs with a high risk of DILI; Category 0: drugs with no risk of DILI. The output value is the probability of being toxic.
AMES toxicity	0.066	●	Category 1: AMES positive(+); Category 0: AMES negative(−). The output value is the probability of being toxic.
Rat oral acute toxicity	0.846	●	Category 0: low toxicity; Category 1: high toxicity. The output value is the probability of being highly toxic.
FDAMDD	0.93	●	Maximum Recommended Daily Dose. Category 1: FDAMDD (+); Category 0: FDAMDD (−). The output value is the probability of being positive.
Skin sensitization	0.131	●	Category 1: Sensitizer; Category 0: Nonsensitizer. The output value is the probability of being sensitizer.
Carcinogen city	0.768	●	Category 1: carcinogens; Category 0: noncarcinogens. The output value is the probability of being toxic.
Eye corrosion	0.003	●	Category 1: corrosives; Category 0: noncorrosives. The output value is the probability of being corrosives.
Eye irritation	0.011	●	Category 1: irritants; Category 0: nonirritants. The output value is the probability of being irritants.
Respiratory toxicity	0.957	●	Category 1: respiratory toxicants; Category 0: respiratory nontoxicants. The output value is the probability of being toxic.

Table S8. Environmental toxicity.

Property	Value	Comment
Bioconcentration Factors	1.055	Bioconcentration factors are used for considering secondary poisoning potential and assessing risks to human health via the food chain. The unit is $-\log10[(mg\ L^{-1})/(1000\times MW)]$
IGC 50	3.631	Tetrahymena pyriformis 50% growth inhibition concentration The unit is $-\log10[(mg\ L^{-1})/(1000\times MW)]$
LC FM 50	6.124	96-h fathead minnow 50% lethal concentration The unit is $-\log10[(mg\ L^{-1})/(1000\times MW)]$
LC DM 50	6.207	48-h daphnia magna 50% lethal concentration The unit is $-\log10[(mg\ L^{-1})/(1000\times MW)]$

Table S9. Tox21 pathway.

Property	Value	Decision	Comment
NR-AR	0.886	●	Androgen receptor Category 1: active; Category 0: inactive. The output value is the probability of being active.
NR-AR-LBD	0.975	●	Androgen receptor ligand-binding domain. Category 1: active; Category 0: inactive. The output value is the probability of being active.
NR-AhR	0.003	●	Aryl hydrocarbon receptor Category 1: active; Category 0: inactive. The output value is the probability of being active.
NR-aromatase	0.852	●	Category 1: active; Category 0: inactive. The output value is the probability of being active.
NR-ER	0.932	●	Estrogen receptor Category 1: active; Category 0: inactive. The output value is the probability of being active.
NR-ER-LBD	0.131	●	Estrogen receptor ligand-binding domain Category 1: active; Category 0: inactive. The output value is the probability of being active.
NR-PPAR- gamma	0.916	●	Peroxisome proliferator-activated receptor gamma Category 1: active; Category 0: inactive. The output value is the probability of being active.
SR-ARE	0.725	●	Antioxidant response element Category 1: active; Category 0: inactives; The output value is the probability of being active.
SR-ATAD5	0.701	●	ATPase family AAA domain-containing protein 5 Category 1: active; Category 0: inactive. The output value is the probability of being active.
SR-HSE	0.095	●	Heat shock factor response element Category 1: active; Category 0: inactive. The output value is the probability of being active.
SR-MMP	0.927	●	Mitochondrial membrane potential Category 1: active; Category 0: inactive. The output value is the probability of being active.
SR-p53	0.942	●	Category 1: active; Category 0: inactive. The output value is the probability of being active.

Table S10. Toxicophore rules.

Property	Value	Comment
Acute toxicity rule	0 alerts	20 substructures acute toxicity during oral administration
Genotoxic carcinogenicity rule	0 alerts	117 substructures carcinogenicity or mutagenicity
Nongenotoxic carcinogenicity rule	0 alerts	23 substructures carcinogenicity through nongenotoxic mechanisms
Skin sensitization rule	1 alert	155 substructures skin irritation
Aquatic toxicity rule	3 alerts	99 substructures toxicity to liquid(water)
Nonbiodegradable rule	1 alert	19 substructures non-biodegradable
SureChEMBL rule	0 alerts	164 substructures MedChem unfriendly status

Supplementary Material 3

Praziquantel

Table 1. Physicochemical property.

Property	Value	Comment
Molecular Weight	312.18	Contain hydrogen atoms. Optimal:100~600
Volume	329.346	Van der Waals volume
Density	0.948	Density = MW / volume
nHA	4	Number of hydrogen bond acceptors. Optimal:0~12
nHD	0	Number of hydrogen bond donors. Optimal:0~7
nRot	2	Number of rotatable bonds. Optimal:0~11
nRing	4	Number of rings. Optimal:0~6
MaxRing	14	Number of atoms in the biggest ring. Optimal:0~18
nHet	4	Number of heteroatoms. Optimal:1~15
fChar	0	Formal charge. Optimal: -4 ~4
nRig	24	Number of rigid bonds. Optimal:0~30
Flexibility	0.083	Flexibility = nRot /nRig
Stereo Centers	1	Optimal: ≤ 2
TPSA	40.62	Topological polar surface area. Optimal:0~140
logS	-2.484	Log of the aqueous solubility. Optimal: -4~0.5 log mol/L
logP	2.758	Log of the octanol/water partition coefficient. Optimal: 0~3
logD	2.492	logP at physiological pH 7.4. Optimal: 1~3

Table 2. Medicinal Chemistry.

Property	Value	Decision	Comment
QED	0.799	●	A measure of drug-likeness based on the concept of desirability. Attractive: > 0.67; Unattractive: 0.49~0.67; Too complex: < 0.34.
SAscore	2.709	●	Synthetic accessibility score is designed to estimate ease of synthesis of drug-like molecules. SAscore ≥ 6, difficult to synthesize; SAscore < 6, easy to synthesize.
Fsp3	0.579	●	The number of sp3 hybridized carbons / total carbon count, correlating with melting point and solubility. $Fsp^3 \geq 0.42$ is considered a suitable value.
MCE-18	74.667	●	MCE-18 stands for medicinal chemistry evolution. MCE-18 ≥ 45 is considered a suitable value.
NPscore	-0.813	-	Natural product-likeness score. This score is typically in the range from –5 to 5. The higher the score is, the higher the probability is that the molecule is a NP.
Lipinski Rule	Accepted	●	MW ≤ 500; logP ≤ 5; Hacc ≤ 10; Hdon ≤ 5. If two properties are out of range, a poor absorption or permeability is possible, one is acceptable.
Pfizer Rule	Accepted	●	logP > 3; TPSA < 75. Compounds with a high log P (>3) and low TPSA (<75) are likely to be toxic.
GSK Rule	Accepted	●	MW ≤ 400; logP ≤ 4 Compounds satisfying the GSK rule may have a more favorable ADMET profile.
Golden Triangle	Accepted	●	200 ≤ MW ≤ 50; –2 ≤ logD ≤ 5. Compounds satisfying the Golden Triangle rule may have a more favorable ADMET profile.
PAINS	0 alerts	-	Pan assay interference compounds, frequent hitters, Alpha-screen artifacts and reactive compound.
ALARM NMR	0 alerts	-	Thiol reactive compounds.
BMS	0 alerts	-	Undesirable, reactive compounds.
Chelator Rule	0 alerts	-	Chelating compounds.

Table S3. Absorption.

Property	Value	Decision	Comment
Caco-2 permeability	–4.923	●	Optimal: higher than –5.15 Log unit
MDCK Permeability	2.6x10^{-05}	●	Low permeability: $< 2 \times 10^{-6}$ cm s^{-1} Medium permeability: $2\text{–}20 \times 10^{-6}$ cm s^{-1} High passive permeability: $> 20 \times 10^{-6}$ cm s^{-1}
Pgp-inhibitor	0.226	●	Category 1: Inhibitor; Category 0: Noninhibitor. The output value is the probability of being Pgp-inhibitor.
Pgp-substrate	0.105	●	Category 1: substrate; Category 0: Nonsubstrate. The output value is the probability of being Pgp-substrate.
HIA	0.006	●	Human intestinal absorption Category 1: HIA+(HIA < 30%); Category 0: HIA-(HIA < 30%); The output value is the probability of being HIA+.
F 20%	0.991	●	20% Bioavailability Category 1: F + (bioavailability < 20%); 20% Category 0: F – (bioavailability ≥ 20%); The output 20% value is the probability of being F + 20%
F 30%	0.995	●	30% Bioavailability Category 1: F + (bioavailability < 30%). 30% Category 0: F – (bioavailability ≥ 30%); The output 30% value is the probability of being F + 30%

Table S4. Distribution.

Property	Value	Decision	Comment
PPB	93.68%	●	Plasma protein binding Optimal: < 90%. Drugs with high protein-bound may have a low therapeutic index.
VD	0.662	●	Volume distribution Optimal: 0.04–20 L kg^{-1}.
BBB Penetration	0.997	●	Blood-Brain Barrier Penetration Category 1: BBB+; Category 0: BBB–; The output value is the probability of being BBB+
FU	7.573%	●	The fraction unbound in plasms Low: < 5%; Middle: 5~20%; High: > 20%

Table S5. Metabolism.

Property	Value	Comment
CYP1A2 inhibitor	0.051	Category 1: Inhibitor; Category 0: Noninhibitor. The output value is the probability of being inhibitor.
CYP1A2 substrate	0.447	Category 1: Substrate; Category 0: Nonsubstrate. The output value is the probability of being substrate.
CYP2C19 inhibitor	0.887	Category 1: Inhibitor; Category 0: Non- inhibitor. The output value is the probability of being inhibitor.
CYP2C19 substrate	0.801	Category 1: Substrate; Category 0: Nonsubstrate. The output value is the probability of being substrate.
CYP2C9 inhibitor	0.796	Category 1: Inhibitor; Category 0: Noninhibitor. The output value is the probability of being inhibitor.
CYP2C9 substrate	0.923	Category 1: Substrate; Category 0: Nonsubstrate. The output value is the probability of being substrate.
CYP2D6 inhibitor	0.031	Category 1: Inhibitor; Category 0: Non- inhibitor. The output value is the probability of being inhibitor.
CYP2D6 substrate	0.64	Category 1: Substrate; Category 0: Nonsubstrate. The output value is the probability of being substrate.
CYP3A4 inhibitor	0.771	Category 1: Inhibitor; Category 0: Non- inhibitor. The output value is the probability of being inhibitor.
CYP3A4 substrate	0.678	Category 1: Substrate; Category 0: Nonsubstrate. The output value is the probability of being substrate.

Table S6. Excretion.

Property	Value	Decision	Comment
CL	2.683	●	Clearance High: >15 mL min^{-1} kg^{-1}; Moderate: 5–15 mL min^{-1} kg^{-1}; Low: < 5 mL min^{-1} kg^{-1}
T$_{1/2}$	0.43	-	Category 1: long half-life; Category 0: short half-life. Long half-life: > 3 h; Short half-life: < 3 h. The output value is the probability of having long half-life.

Table S7. Toxicity.

Property	Value	Decision	Comment
hERG Blockers	0.106	●	Category 1: active; Category 0: inactive. The output value is the probability of being active.
H-HT	0.922	●	Human hepatotoxicity Category 1: H-HT positive(+); Category 0: H-HT negative (–). The output value is the probability of being toxic.
DILI	0.166	●	Drug induced liver injury. Category 1: drugs with a high risk of DILI; Category 0: drugs with no risk of DILI. The output value is the probability of being toxic.
AMES Toxicity	0.007	●	Category 1: AMES positive(+); Category 0: AMES negative(-). The output value is the probability of being toxic.
Rat Oral Acute Toxicity	0.515	●	Category 0: low toxicity; Category 1: high toxicity. The output value is the probability of being highly toxic.
FDAMDD	0.929	●	Maximum recommended daily dose Category 1: FDAMDD (+); Category 0: FDAMDD (–). The output value is the probability of being positive.
Skin sensitization	0.713	●	Category 1: sensitizer; Category 0: nonsensitizer. The output value is the probability of being sensitizer.
Carcinogen city	0.187	●	Category 1: carcinogens; Category 0: noncarcinogens. The output value is the probability of being toxic.
Eye corrosion	0.003	●	Category 1: corrosive; Category 0: noncorrosive. The output value is the probability of being corrosives.
Eye irritation	0.013	●	Category 1: irritant; Category 0: nonirritant. The output value is the probability of being irritants.
Respiratory toxicity	0.056	●	Category 1: respiratory toxicants; Category 0: respiratory nontoxicant. The output value is the probability of being toxic.

Table S8. Environmental toxicity.

Property	Value	Comment
Bioconcentration Factors	0.523	Bioconcentration factors are used for considering secondary poisoning potential and assessing risks to human health via the food chain. The unit is $-\log_{10}[(\text{mg L}^{-1})/(1000 \times MW)]$
IGC 50	3.145	Tetrahymena pyriformis 50% growth inhibition concentration The unit is $-\log_{10}[(\text{mg L}^{-1})/(1000 \times MW)]$
LC FM 50	3.915	96-hour fathead minnow 50% lethal concentration The unit is $-\log_{10}[(\text{mg L}^{-1})/(1000 \times MW)]$
LC DM 50	4.834	48-hour daphnia magna 50% lethal concentration The unit is $-\log_{10}[(\text{mg L}^{-1})/(1000 \times MW)]$

Table S9. Tox21 pathway.

Property	Value	Decision	Comment
NR-AR	0.773	● (red)	Androgen receptor Category 1: active; Category 0: inactive. The output value is the probability of being active.
NR-AR-LBD	0.047	● (green)	Androgen receptor ligand-binding domain Category 1: active; Category 0: inactive. The output value is the probability of being active.
NR-AhR	0.237	● (green)	Aryl hydrocarbon receptor Category 1: active; Category 0: inactive. The output value is the probability of being active.
NR-aromatase	0.055	● (green)	Category 1: active; Category 0: inactive. The output value is the probability of being active.
NR-ER	0.348	● (orange)	Estrogen receptor Category 1: active; Category 0: inactive. The output value is the probability of being active.
NR-ER-LBD	0.004	● (green)	Estrogen receptor ligand-binding domain Category 1: active; Category 0: inactive. The output value is the probability of being active.
NR-PPAR-gamma	0.145	● (green)	Peroxisome proliferator-activated receptor gamma Category 1: active; Category 0: inactive. The output value is the probability of being active.
SR-ARE	0.462	● (orange)	Antioxidant response element Category 1: active; Category 0: inactive. The output value is the probability of being active.
SR-ATAD5	0.006	● (green)	ATPase family AAA domain-containing protein 5. Category 1: active; Category 0: inactive. The output value is the probability of being active.
SR-HSE	0.034	● (green)	Heat shock factor response element Category 1: actives; Category 0: inactives; The output value is the probability of being active.
SR-MMP	0.124	● (green)	Mitochondrial membrane potential Category 1: actives; Category 0: inactives; The output value is the probability of being active.
SR-p53	0.028	● (green)	Category 1: actives; Category 0: inactives; The output value is the probability of being active.

Table S10. Toxicophore rules.

Property	Value	Comment
Acute toxicity rule	0 alerts	20 substructures acute toxicity during oral administration
Genotoxic carcinogenicity rule	0 alerts	117 substructures carcinogenicity or mutagenicity
Nongenotoxic carcinogenicity rule	0 alerts	23 substructures carcinogenicity through nongenotoxic mechanisms
Skin sensitization rule	1 alert	155 substructures skin irritation
Aquatic toxicity rule	0 alerts	99 substructures toxicity to liquid (water)
Nonbiodegradable rule	0 alerts	19 substructures nonbiodegradable
SureChEMBL rule	0 alerts	164 substructures MedChem unfriendly status

Oil extraction from seeds of *Carica papaya* L.: Obtaining the lipid profile and thermal evaluation

Mariana Fonseca[1]✉, Marcelo Kobelnik[1+], Gustavo Guadagnucci Fontanari[2]✉, Marisa Spirandeli Crespi[1]✉, Clóvis Augusto Ribeiro[1]✉

1. São Paulo State University, Institute of Chemistry, Araraquara, Brazil.
2. Federal Rural University of Amazonia, Institute of Animal Health and Production, Belém, Brazil.

+Corresponding author: Marcelo Kobelnik, Phone: +55 (17) 98114-1073, Email address: mkobelnik@gmail.com

ABSTRACT: *Carica papaya* L. is frequently found in northern and northeastern Brazil, the Caribbean and Central America. The papaya seed oil was extracted using Soxhlet extraction. Its oil has low acidity, iodine index, saponification and peroxide values adequate and comparable to other commercially available vegetable oils. The lipid profile of this oil was also obtained by gas chromatography; thermal characterization was performed by thermogravimetry (TG) and differential scanning calorimetry (DSC) under various heating rates. The composition of the *in-nature* oil indicates that oleic and palmitic fatty acids are predominant. The DSC analysis under cooling shows that the crystallization phase of this oil is similar to olive oil, and the thermogravimetric results show the thermal decomposition under nitrogen purge gas occurs in only one stage. The activation energy was obtained applying the isoconversional methods proposed by Capela and Ribeiro, Ozawa and Friedman. The obtained kinetics data leads to a dependence on the sample mass and purge gases, which results in several kinetic patterns.
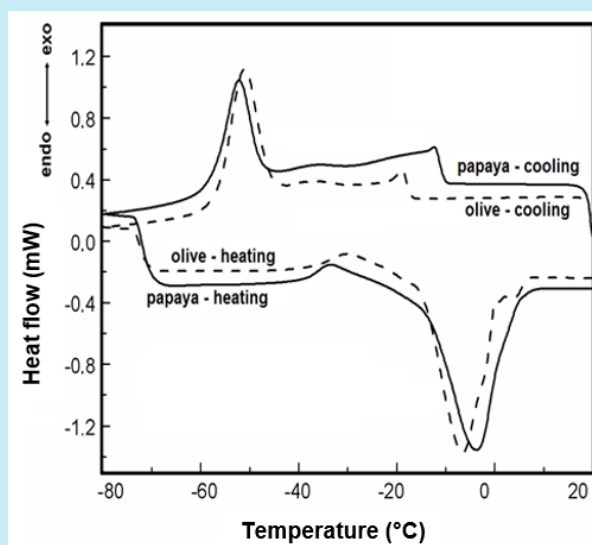
1. Introduction

Brazil is the largest producer and exporter of papaya, with the largest plantation being in Espírito Santo state and the northeastern region of the country (Fontes *et al.*, 2012). The papaya belonging to the Caricaceae family, especially the 'Formosa' papaya group, is widely consumed in Brazil. It is a hybrid of Chinese origin, weighing 0.8 to 2.5 kg of yellow or reddish colors, bulky pulp, and sweet with a content of production of more than 70 tons per year (Alobo, 2003). Its seeds correspond to around 14% of fruit in weight and can be used for extraction of oil for pharmaceutical purposes, with 25% of the industrial income (Anuar *et al.*, 2008; Xu *et al.*, 2008). Papaya is an excellent source of β-carotene, ascorbic acid (Alobo, 2003), potassium, other minerals and fibers. In addition, it contains papain, an important enzyme that is an efficient digestive supplement (Monetta, 1987). Papaya seeds, which constitute about 30–35% of the fruit, are generally discarded, both in domestic consumption and in the food industry (Kardash and Tur'yan, 2005). In order to make better efficient use of the fruit, it is worth investigating and using its seeds as a source of oil (Puangsri *et al.*, 2005).

The main purpose of this paper is the extraction, lipid profile by gas chromatography and thermal evaluation of the oil from seeds of papaya (*C. papaya* L.). The thermal study was carried out through differential scanning calorimetry (DSC) and thermogravimetry (TG). In addition, the physic-chemical properties, i.e., acidity, iodine index, saponification and peroxide index of this oil were evaluated.

2. Experimental

2.1 Extraction of the oil and lecithin

After the first attempts at extraction by Soxhlet using hexane as the extracting solvent, the physical-chemical analysis of the oil extracted from the seeds of papaya showed high acid and iodine indexes (Table 1) and rancidity odor characteristics after the storage period. Therefore, some changes were necessary for this first stage of the work, aiming to obtain oil without the presence of lecithin. This was necessary because lecithin has the property of emulsification and antioxidant effects, but its presence in excess can alter the physical-chemical characteristics of the oil (Judde *et al.*, 2003).

Table 1. Indices of acidity, iodine, saponification and peroxide and for different vegetable oils compared to the papaya oil seeds.

Oil	Acidity	Iodine (Wijs)g/100g	Saponification (mg KOH/g oil)	Peroxide (meq of O_2/kg oil)
cotton	--	99-119	189-198	--
peanut	--	80-106	187-196	--
canola	--	110-126	182-193	--
sesame	0.3	104-120	--	--
corn	--	103-128	187–195	< 10
sunflower	--	120-138	--	--
soybean	2.0	120-143	188–195	--
papaya	0.9167	69.13	189.4	2.97
papaya (only hexane)	15.16	153.6	--	--

First, to minimize undesired effects, seeds were seeded from the fruit by hand and then washed and cooked in hot water, at a temperature around 70 °C for 4 h, exchanging water at 1-hintervals, in order to eliminate soluble residues dissolved in the water.

Soon after cooking, the seeds were dried in an oven (Tecnal model TE 394/1) for 8 h at 70 °C and comminuted in a blender to ensure a larger contact surface between the extracting solvent and the particles. Then, the material was properly packed in Soxhlet, using hexane as an extraction solvent. After the extraction with the hexane, a new step of extraction of the oil was carried out, now to obtain the lecithin (Jangle *et al.*, 2013; Patil *et al.*, 2010). The phosphatidylcholine is the main

constituent of lecithin and it was separated from papaya oil by extraction with ethanol. The precipitate formed during the extraction was filtered and the excess ethanol present in the oil was removed by evaporation in a rotary evaporator. The extraction product, assigned as lecithin, corresponds to approximately 3% of papaya seeds.

Natural papaya seed oil was characterized according to analytical indexes for oils and fats. The acid value, which is the amount of KOH (in mg) required to neutralize the free fatty acids in 1 g of oil, was determined according to ASTM 1980-87 (1998).

The iodine index, which represents the measure of the unsaturation of oils and fats, was determined according to ASTM D5554-95 (2011a). Finally, the saponification

index was also determined, according to the methodology described in ASTM D5558-95 (2011b). All titrations were performed in triplicate, and the result is presented as an average of the obtained values.

2.2 Analysis of fatty acid methyl esters (FAME) and thermal analysis

The used methodology to obtain the lipid profile by gas chromatography analysis, described below, follows a pattern of analysis and the description is like that previously published in other works (Kobelnik et al., 2011; 2012; 2014; 2016; 2021; Marques et al., 2015).

The lipid methylation to produce fatty acid methyl esters was done by the method described by Hartman and Lago (1973), with some modifications: sample (30 mg) was diluted in 1.0 mL of *n*-hexane and saponified under boiling with 1.3 mL of 0.5 mol L^{-1} sodium hydroxide (in methanol); after cooling, 1.7 mL of the esterification reagent (ammonium chloride solution in methanol and sulphuric acid) was added and heated to boiling; to the cold solution, 2.0 mL of saturated NaCl solution were added and the top layer was taken for FAME analysis. Fatty acid analysis was performed in a Shimadzu GC 2010 gas chromatograph equipped with a flame ionization detection, under the following conditions: split injection (1:30 injection volume 1 μL); capillary column SP 2560 (Supelco) (100 m × 0.25 mm × 0.20 μm); injection port and detector temperatures of 250 and 260 °C respectively; initial oven temperature of 140 °C, increasing at 4 °C min^{-1}, to 240 °C, which was maintained for 11 min; and carrier gas of hydrogen at 1.5 mL min^{-1} flow rate. Identification of the fatty acids was achieved by comparing their retention times with pure standards (FAME 37, code 47885, Sigma Chemical Co.). Data were processed by GC Solution Software, from Shimadzu, Kyoto, Japan. The results were expressed as a percentage of the area of each peak over the total fatty acid profile.

DSC analysis of this oil was carried out from DSC1 $Star^e$ from Mettler Toledo. The mass sample used was around 5.5 mg in the aluminum crucible crimped lids and cooled from 25 to –80 °C and subsequently heated from –80 °C up to 25 °C, both at cooling/heating rates of 1, 2.5, 5, and 10 °C min^{-1} under nitrogen purge gas at a flow rate of 50 mL min^{-1}.

Simultaneous TG/DTG and DTA curves were performed on a TA Instruments device, model SDT 2960. The conditions used were platinum crucible, purge gases of nitrogen, and synthetic air, with heating up to 500 °C. The kinetic evaluation was performed using the Friedman Flynn–Wall–Ozawa and Ribeiro–Capela methods, with the DTG curves, which were analyzed in purge gas nitrogen (flow rate from 100 mL min^{-1}), with the heating ratios of 5, 10, 20, and 30 °C min^{-1} (Dias et al., 2015; 2021; Fonseca et al., 2018; Friedman, 1964; Kobelnik et al., 2018a; b).

3. Results and discussion

3.1 Chemical properties and lipid profile of the oil

The solvent selected for the extraction of oil from papaya seeds was hexane. This choice was based on the ease with which this solvent solubilizes the substance of interest and the ease with which it can be removed from the final product, since it has a low boiling point (69 °C). The total fraction of oil extracted with hexane was approximately 24%.

Chemical properties are among the most important characteristics of oils and fats. The values of acidity, iodine index, saponification index, and peroxide values are chemical properties that are important and show the quality of the oil.

Table 1 summarizes the chemical properties of this oil and the comparison of other commercially available vegetable oils. The acidity index value shows a large difference in the values, which is due to the different ways of extracting the papaya seed oil. The value presented with extraction done only in hexane indicates that the acidity is very high. However, when the seed drying process has changed, the acid number decreases considerably. This new value corresponds to the presence of 1.403 to 1.87% of oleic acid in the oil sample. In the literature, we see that the papaya seed oil extracted with hexane presents 0.33% in oleic acid, as showed by Puangsri et al. (2005), and when papaya seed oil is extracted with petroleum ether, as showed by Von Loesecke and Notle (1937), the acid value is 3.05%. The iodine index obtained before and after the methodology adopted in this work is presented in Table 1, which shows the mass of iodine for each 100 g of oil. The work done by Von Loesecke and Notle (1937) showed that the iodine content had a value of 89.8 g of absorbed iodine per 100 g of oil, which is a value much closer to the value obtained after the modifications described by this work. Puangsri et al. (2005) showed that the oil extracted with hexane shows an iodine value equal to 66.0 ± 0.2 g of iodine absorbed per 100 g of oil.

The indicator of the degree of oxidation is called peroxide index, and it shows the amount of sample that oxidizes the potassium iodide. The value obtained was

2.97 meq 1,000 g^{-1} of oil, which is low and indicates a good state of conservation of papaya seed oil.

Finally, the saponification value shows the amount of salt formed from the fatty acids present in the sample. As the saponification index is inversely proportional to the average molecular weight of the fatty acids in the oils (Damodaran *et al.*, 2010) and the lipid profile shows that the results are concordant, it is concluded that the fatty

acids of low molecular weight (palmitic and oleic) are majority in this analyzed oil.

In addition, Table 2 shows a lipid profile comparison of the oil extracted from papaya seeds with other commercial oils. At room temperature, the oil has a yellow color and characteristic odor. Besides, its color is very similar to the color of olive oil. The lipidic profiles obtained of this oil are also shown in Table 2.

Table 2. Fatty acid composition of papaya seed oil, olive, and others edible oils.

Compound/oil	Papaya[+]	Olive[+]	Canola	Corn	Sunflower	Peanut	Soybean
Fatty acid	**Percentage**						
Butiric/C4:0	0.34± 0.02	-	-	-	-	-	-
Caproic/C6:0	-	0.15± 0.03		-	-	-	-
Palmitic/C16:0	14.74± 0.04	10.6± 0.03	3.95	10.48	7.15	12.78	10.82
Estearic/C18:0	4.87± 0.02	3.40± 0.02	1.52	2.17	3.58	3.30	3.83
Araquidic/C20:0	0.37± 0.01	0.41± 0.01	-	-	-	-	-
Behenic/C22:0	0.24± 0.05	0.10± 0.01	-	-	-	-	-
Tricosanoic/C23:0	-	0.25± 0.03	-	-	-	-	-
Lignoceric/C24:0	-	0.05± 0.01	-	-	-	-	-
Palmitoleic/C16:1	-	0.70± 0.03	-	-	-	-	-
Cis-10-heptadecanoic/17:1	-	0.10± 0.01	-	-	-	-	-
Oleic/C18:1 n9	74.2± 0.1	78.0± 0.03	58.19	25.90	79.71	39.46	22.40
Cis-11-eicosanoic/20:1	0.34± 0.01	0.23± 0.01	-	-	-	-	-
Linoleic/C18:2	4.88± 0.01	5.33± 0.01	-	-	-	-	-
Linolenic/C18:3 n3	-	0.65± 0.02	-	-	-	-	-

[+]Mean standard deviation.
Source: Elaborated by the authors using data from Lipp *et al.* (2001).

The composition of fatty acids shows that papaya oil, like most vegetable oils, is composed mainly of unsaturated fatty acids of long chain (79.39%), but, in the case, approximately 74% is monounsaturated (oleic acid). Moreover, the analysis of commercial extra virgin olive oil showed composition very similar with the oil papaya seed. The other fatty acids that were not identified in this study were not quantified, probably because they were below the limit of detection, or were not present in the papaya species used. In addition, the main edible vegetable oils and respective compositions for comparative purposes are the palmitic, stearic, and oleic acids (Kalayasiri *et al.*, 1996; Su *et al.*, 2014).

3.2 Thermal evaluation

Figures 1 and 2 show, respectively, DSC curves of cooling and heating. The cooling at different heating rates shows that events shift as a function of temperature. Besides, the cooling evaluation shows that there are two main events at all heating rates, where the first occurs between −4 and −10 °C and the second has a variable interval due to the heating rates. The baseline change seen in the first event is attributed to an arrangement

between the molecules present in the oil, which occurs during the transition from liquid to the solid stage. Besides, there is an additional baseline change for heating rate of 10 °C min^{-1}, which is also attributed to an orderly arrangement between molecules during cooling. In addition, this event was not present in the other heating rates, which indicate that this event is dependent on the cooling rate. The second exothermic peak is attributed to the crystallization phase, which occurs in a single stage.

The heating shows that there was an exothermic event (to heating rate of 5 and 10°C min^{-1}), which is similar to the event seen in cooling. This event is attributed to a molecular relaxation of the oil molecules due to heating. After this event, it is seen that the oil has an endothermic peak at heating rates of 2.5, 5 and 10 °C min^{-1}, which was attributed to the melting point of the oil, with peaks around −3 °C for these curves. However, for the heating rate of 1 ° C min^{-1}, it did not present a defined peak, but a sequence of events between −17 and 10 °C. Furthermore, the heating of 2.5 and 5 °C C min^{-1} also presents an event between 1 and 10 °C. In other works, it was also seen that during heating and cooling, multiple events occurred, which are successive reactions that are

attributed to the different fatty acid compositions that do not allow us to observe a typical melting point (Kobelnik *et al.*, 2011; 2012; 2014; 2016; 2021; Marques *et al.*, 2015). So, at a heating rate of 10 °C, which is higher than the others, it is possible to see that only one endothermic reaction occurs because there were overlapping reactions attributed due to the components of the fatty acids in the oil.
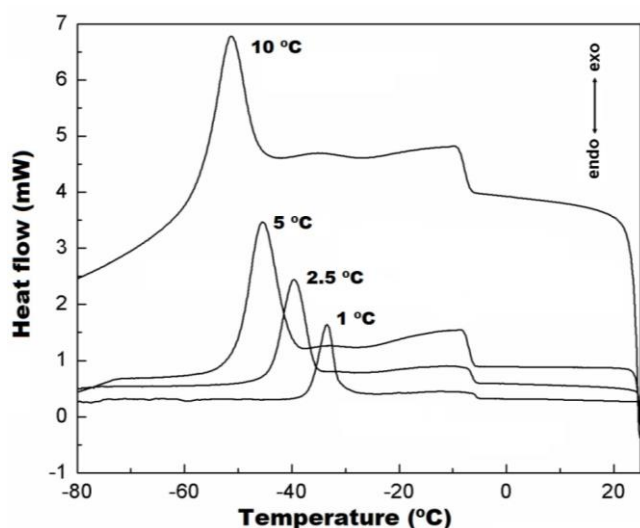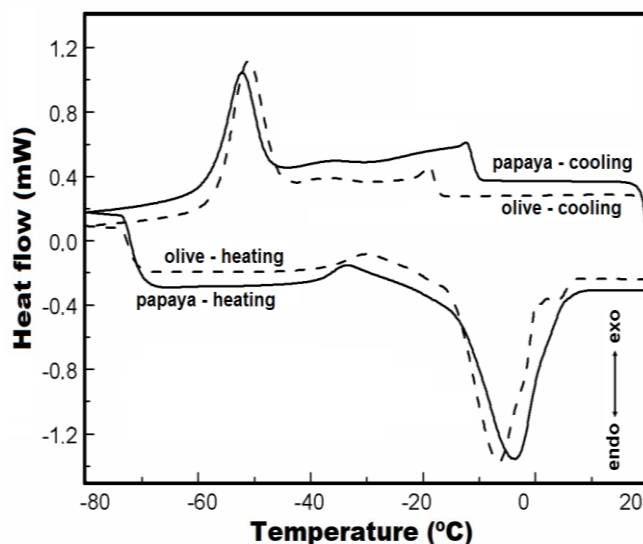

Figure 1. DSC curves of papaya oil in nitrogen purge gas (50 mL min⁻¹), under several cooling rates of 1, 2.5, 5 and 10 °C min⁻¹ from 25 to −80 °C, sample mass around 5 mg in aluminum crucible crimped lids, without drilling.
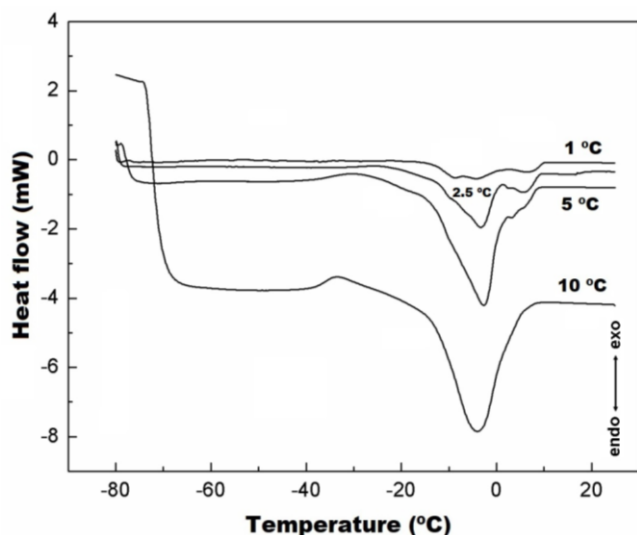
Figure 2. DSC curves of papaya oil in nitrogen purge gas (50 mL min⁻¹), heating rate of 1, 2.5, 5 and 10 °C min⁻¹ from −80 to 25 °C, sample mass around 5 mg in aluminum crucible crimped lids, without drilling.

In addition, a comparison with olive oil was performed. Figure 3 shows that the thermal behavior for

heating and cooling of olive oil is very similar to that of papaya seed oil, which is attributed to a small difference in the composition of both oils. The first thermal event occurs between −6 and −9 °C to papaya oil and −12 and −15 °C to olive oil. The second event is an exothermic peak around −50 °C for both oils, which is attributed to the crystallization phase. Furthermore, it is also possible to see that the differences between both oils during the heating are very small: i) the difference at the first event was 5 °C; and ii) the difference between peaks at the second event (melting point) was 3 °C. Besides, olive oil showed an event between 0 and 7 °C, which was attributed to the overlapping transitions (solid–liquid) due to the melting of fatty acids with a higher melting point.


Figure 3. DSC curves of papaya and olive oil in nitrogen purge gas (50 mL min⁻¹), cooling rate of 10 °C min⁻¹ from 25 to −80 °C, sample mass around 5 mg in aluminum crucible, without drilling.

The thermal behavior of this oil evaluated by thermogravimetry, in nitrogen and synthetic air purge gases are shown in Figs. 4 and 5, respectively.
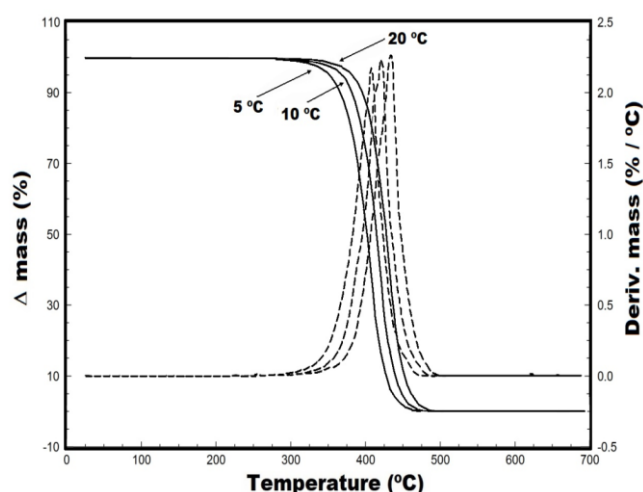
85
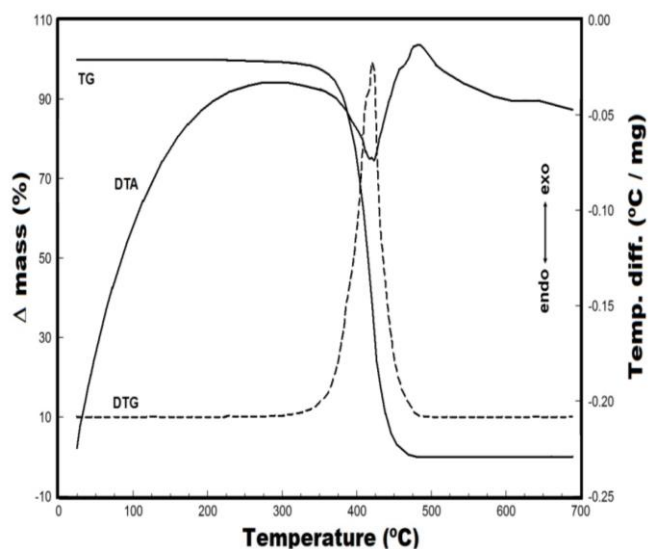
Figure 4. TG/DTG and DTA curves of papaya seed oil: sample mass around 20 mg, heating rate of 10 °C min⁻¹ in nitrogen purge gas (100 mL min⁻¹), in platinum crucible.
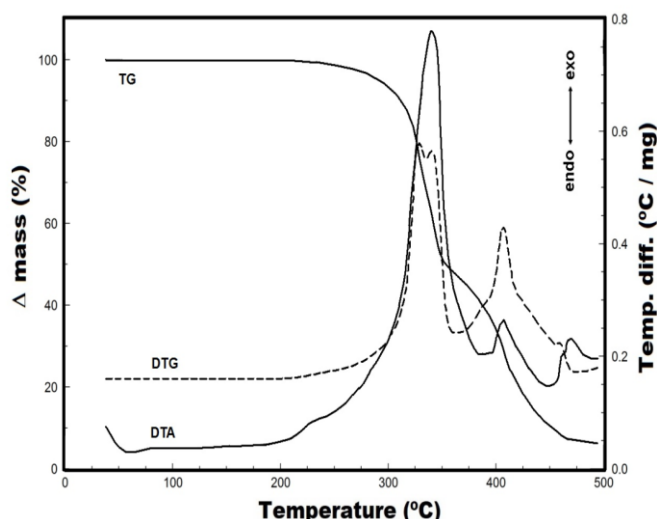
Figure 5. TG/DTG and DTA curves of papaya seed oil: sample mass around 20 mg, heating rate of 10 °C min⁻¹ in synthetic air purge gas (100 mL min⁻¹), in platinum crucible.

This oil showed that there was not a variation of mass until the temperature of 315 °C in nitrogen (Fig. 4). The thermal decomposition stage occurs in a single step up to 487 °C (mass loss of 99.35%). At the end of the thermal decomposition in nitrogen purge gas, the presence of carbonaceous residues was not observed because pyrolysis takes place, and, therefore, this reaction generates lighter products, which are easily volatilized. In addition, in Fig. 6 shows TG/DTG curves of the oil in several heating rates, which were used for the kinetic study in the nitrogen purge gas. It can be seen in DTG

curves that the thermal decomposition behavior of the oil is homogeneous.

Figure 6. TG/DTG curves of papaya seed oil: sample mass around 20 mg, heating rate of 5, 10 and 20 °C min⁻¹ in nitrogen purge gas (100 mL min⁻¹), in platinum crucible.

The analysis in synthetic air (Fig. 5) shows that the DTG curve had a mass variation between 221 and 285 °C, which is attributed to the smoke point, and correspond to the 3.76% of mass variation. This behavior is very common in many oils, as has been cited in the literature (Fontanari *et al.*, 2018; Freire *et al.*, 2013; Jorge *et al.*, 2005; Kobelnik *et al.*, 2021). Thermal decomposition occurs up to 468 °C with two main intervals between 285–363 °C and 363–472 °C, which shows that there are overlapping reactions during decomposition and had weight loss of 47.75% and 40.78%, respectively. At the end of the thermal decomposition, the presence of carbonaceous residues that corresponds to 7.15% of the initial mass was observed. If oxygen is available during the reaction, the molecules will start to be oxidized due to the low activation energy required for oxidation; therefore, molecular scission occurs and generates different products during this degradation, causing the appearance of residues at the end of the reaction.

The DTA (Fig. 5) shows different events on this curve. From the beginning of the curve to the temperature of 195 °C, there was no reaction attributed to the sample. The peak of the exothermic reaction occurs at 341 °C, which is attributed to oil oxidation. After this peak, in the progress of the thermal decomposition, it is possible to see two stages of mass loss at 350–423 and 423–491 °C. In addition, the analysis in nitrogen purge gas shows an endothermic event due to oil pyrolysis.
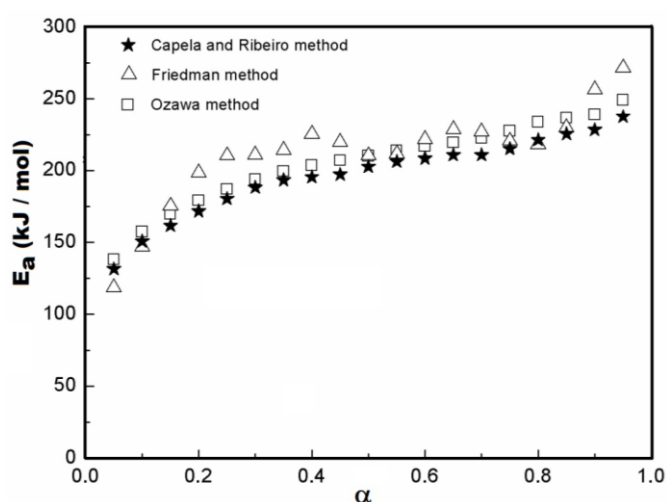
Regarding the kinetic study, the average values of the activation energy (E_a) were obtained by Capela–Ribeiro, Flynn–Wall–Ozawa and Friedman methods as aforementioned, and the respective results are shown in Table 3.
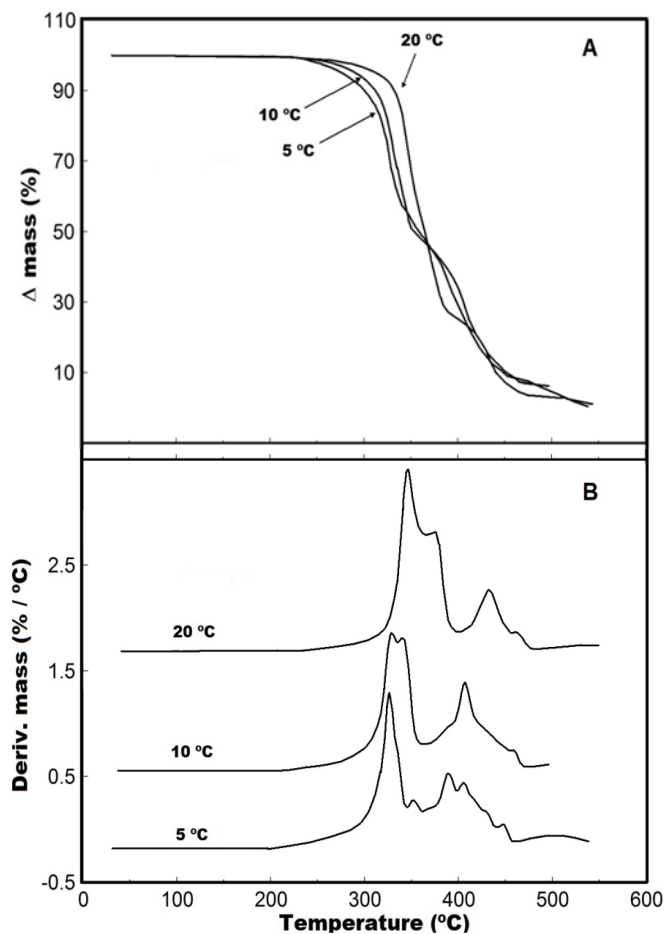
Table 3. E_a (kJ mol^{-1}) and correlation coefficient (r) for decomposition stage.

Purge gas and sample mass	Nitrogen
Temperature ranges (DTG curves)	(5 °C min^{-1}) 300 – 471 °C
	(10 °C min^{-1}) 321 – 480 °C
	(20 °C min^{-1}) 345 – 495 °C
Ozawa method *E_a(kJ mol^{-1}) and (r)	205.4 ± 0.1 (0.99984)
Friedman method *E_a(kJ mol^{-1}) and (r)	211.3 ± 0.2 (0.99448)
Capela–Ribeiro method *E_a(kJ mol^{-1}) and (r) and r	196.6 ± 0.1 (0.9999)

Figure 7 depicts the relationship between the dependence of the activation energy (E_a) with the conversion degree (α), which is defined as $\alpha = (m_0 - m_i)/(m_0 - m_f)$, where m is the initial mass with the subscripts 0; i and f, respectively are, initial and final thermal decomposition stages. The results show the comparison of activation energy vs conversion degree (α) of three kinetic methods under nitrogen purge gas. However, the papaya oil had different thermal decomposition behaviors at different heating rates in synthetic air, as shown in Fig. 8. Therefore, the activation energy data under synthetic air are not shown. This happened because TG/DTG curves are not suitable to obtain an adequate displacement to the kinetic calculation.

Figure 8. TG (A) and DTG (B) curves of papaya seed oil under several heating rates in synthetic air purge gas, with sample mass around 20 mg, heating rate of 5, 10 and 20 °C min^{-1}, in platinum crucible.

The analysis under nitrogen purge gas (Fig. 7) showed a similar behavior between the Ozawa and Ribeiro methods, while there was a shift in some points of the kinetic behavior with the analysis by the Friedman method in relation to the other two methods. Furthermore, the correlation coefficient (r), which is a measure of the proximity of the association of the points in curves, allows the correlation obtained from the kinetic curves to be verified. As the correlation coefficient values are close to 1, there are a strong correlation between the obtained data. In addition, the behavior of this oil in the three methods allowed us to see that there was the same tendency to increase the activation energy in the degree of conversion (α). This effect is attributed to the increase in interactions between the fatty acid molecules present in the oil. Thus, even during decomposition, an increase in activation energy means that molecular collisions are not sufficient to decrease activation energy, that is, the thermal decomposition of the oil only advances with increasing

Figure 7. Activation energy vs conversion degree under nitrogen purge gas.

temperature, as observed in TG curves. However, nitrogen also causes influence, given that there is no reaction with fatty acid molecules because it is inert. In previous works, with different oils of vegetable origin, it was observed that there is a tendency to have an increase in the activation energy, whether in nitrogen purge gas (Kobelnik *et al.*, 2011; 2012; 2014; 2016).

4. Conclusions

This work presents the results of the physical-chemical analysis and lipid profile by gas chromatography and thermal properties of papaya seed oil.

The obtained information about lipid profile reveal that this oil has a predominance of unsaturated fatty acids, being oleic acid majority with 74.17% in your composition, while the percentage of saturated was 20.56. This oil showed that has similar characteristics to olive oil, which may be an alternative source for commercialization. Furthermore, the lipid profile showed that there are different types of fatty acids present in the oil. Thus, the results obtained by DSC showed that the mixture of fatty acids present in the oil present different thermal behavior in the different heating–cooling ratios. During the DSC analysis, it was observed that there was the crystallization of the oil during cooling, which can be attributed to fatty acids with a larger molecular structure and with a greater presence (oleic/C18:1 n9) since the molecular arrangement is slower than the smaller molecules. Furthermore, DSC curves allowed to observe that there was a significant difference between the cooling rate of 1 and 5 °C min^{-1}, which was sufficient for alteration between the relative size and sharpness of the peak of the DSC curves.

From TG, it was possible to establish the thermal behavior and kinetics parameters of thermal decomposition of this oil. The kinetic study of this oil using the three calculation methods allowed a better evaluation of the kinetic curves. The data obtained by Friedmann did not show good adherence to the methods of Ozawa and Ribeiro, but this is attributed to differences that occur in the calculation mode proposed by each method, which was not discussed in this work because it was not within its scope.

Authors' contribution

Conceptualization: Fonseca, M.; Kobelnik, M.
Data curation: Fonseca, M.; Kobelnik, M.
Formal analysis: Ribeiro, C. A.; Crespi, M. S.
Funding acquisition: Not applicable.
Investigation: Fonseca, M.; Kobelnik, M.; Fontanari, G. G.
Methodology: Fonseca, M.; Kobelnik, M.; Fontanari, G. G.
Project administration: Ribeiro, C. A.; Crespi, M. S.
Resources: Ribeiro, C. A.; Crespi, M. S.
Software: Not applicable.
Supervision: Ribeiro, C. A.; Crespi, M. S.
Validation: Fonseca, M.; Kobelnik, M.; Fontanari, G. G.
Visualization: Kobelnik, M.; Ribeiro, C. A.; Fonseca, M.
Writing – original draft: Kobelnik, M.; Ribeiro, C. A.; Fonseca, M.
Writing – review & editing: Kobelnik, M.; Ribeiro, C. A.; Fonseca, M.; Fontanari, G. G.

Data availability statement

The data will be available upon request

References

Anuar, N. S.; Zahari, S. S.; Taib, I. A.; Rahman, M. T. Effect of green and ripe *Carica papaya* epicarp extracts on wound healing and during pregnancy. *Food Chem. Toxic.* **2008**, *46* (7), 2384–2389. https://doi.org/10.1016/j.fct.2008.03.025

Alobo, A. P. Proximate composition and selected functional properties of defatted papaya (*Carica papaya* L.) kernel flour. *Plant Foods Hum. Nutr*. **2003**, *58* (3), 1–7. https://doi.org/10.1023/B:QUAL.0000040319.61845.c2

American Society for Testing and Materials (ASTM). D1980–87. Standard Test Method for Acid Value of Fatty Acids and Polymerizes Fatty Acids. ASTM, 1998.

American Society for Testing and Materials (ASTM). D5554–95. Standard Test Method for Determination of the Iodine Value of Fats and Oils. ASTM, 2011a.

American Society for Testing and Materials (ASTM). D5558–95 Standard Test Method for Determination of the Saponification Value of Fats and Oils. ASTM, 2011b.

Damodaran, S.; Parkin, K. L.; Fennema, O. R. Química de Alimentos de Fennema; Artmed, 2010.

Dias, D. S.; Crespi, M. S.; Ribeiro, C. A.; Kobelnik, M. Evaluation by thermogravimetry of the interaction of the poly(ethylene terephthalate) with oil-based paint. *Eclét. Quím.* **2015**, *40* (1), 77–85. https://doi.org/10.26850/1678-4618eqj.v40.1.2015.p77-85

Dias, D. S.; Crespi, M. S.; Ribeiro, C. A.; Kobelnik, M. Evaluation of the thermal decomposition of blends prepared with poly(3-hydroxybutyrate) (PHB) and recyclable ethylene poly-terephthalate (RPET). *J. Therm. Anal. Calorim.* **2021**, *143*, 3447–3457. https://doi.org/10.1007/s10973-020-09885-4

Fonseca, M; Ferreira, L. M. B.; Soares, R. A. M.; Kobelnik, M.; Fontanari, G. G.; Crespi, M. S.; Ribeiro, C. A. Extraction of soursop oil (*Annona muricata* L.) by ultrasonic technique. *J. Therm. Anal. Calorim.* **2018**, *134* (3), 1893–1901. https://doi.org/10.1007/s10973-018-7753-2

Fontanari, G. G.; Kobelnik, M.; Marques, M. R.; Arêas, J. A. G.; Franzin, B. T.; Pastre, I. A.; Fertonani, F. L. Thermal and kinetic studies of white lupin (*Lupinus albus*) oil. *J. Therm. Anal. Calorim.* **2018**, *131* (1), 775–782. https://doi.org/10.1007/s10973-017-6468-0

Fontes, R. V.; Viana, A. P.; Pereira, M. G.; Oliveira, J. G.; Vieira, H. D. Manejo da cultura do híbrido de mamoeiro (*Carica papaya* L.) do grupo 'Formosa' UENF/CALIMAN: 01 para melhoria na qualidade do fruto com menor aplicação de adubação NPK. *Rev. Bras. Frutic.* **2012**, *34* (1), 143–151. https://doi.org/10.1590/S0100-29452012000100020

Freire, P. C. M.; Mancini-Filho, J.; Ferreira, T. A. P. C. Principais alterações físico-químicas em óleos e gorduras submetidos ao processo de fritura por imersão: regulamentação e efeitos na saúde. *Rev. Nutr.* **2013**, *26* (3), 353–358. https://doi.org/10.1590/S1415-52732013000300010

Friedman, H. L. Kinetics of thermal degradation of char-forming plastics from thermogravimetry. Application to a phenolic plastic. *J. Polym. Sci. Part C.* **1964**, *6* (1), 183–195. https://doi.org/10.1002/polc.5070060121

Hartman, L.; Lago, R. C. Rapid preparation of fatty acid methyl esters from lipids. *Lab. Pract.* **1973**, *22* (6), 475–476.

Jangle, R. D.; Magar, V. P.; Thorat, B. N. Phosphatidylcholine and its purification from raw de-oiled soya lecithin. *Sep. Sci. Technol.* **2013**, *102*, 187–195. https://doi.org/10.1016/j.seppur.2012.10.002

Jorge, N.; Soares, B. B. P.; Lunardi, V. M.; Malacrida, C. R. Physico-chemical alterations of sunflower, corn and soybean oils in deep fat frying. *Quim. Nova.* **2005**, *28* (6), 947–951. https://doi.org/10.1590/S0100-40422005000600003

Judde, A.; Villeneuve, P.; Rossignol-Castera, A.; Le Guillou, A. Antioxidant effect of soy lecithins on vegetable oil stability and their synergism with tocopherols. *J. Am. Oil Chem. Soc.* **2003**, *80* (12), 1209–1215. https://doi.org/10.1007/s11746-003-0844-4

Kalayasiri, P.; Jeyashoke, N.; Krisnagkurak, K. Survey of seed oils for use as diesel fuel. *J. Am. Oil Chem. Soc.* **1996**, *73* (4), 471–474. https://doi.org/10.1007/BF02523921

Kardash, E.; Tur'yan, Y. I. Acid value determination in vegetable oils by indirect titration in aqueous-alcohol media. *Croat. Chem. Acta.* **2005**, *78* (1), 99–103. https://hrcak.srce.hr/2797

Kobelnik, M.; Cassimiro, D. L.; Dias, D. S.; Ribeiro, C. A.; Crespi, M. S. Thermal behavior of jerivá oil (*Syagrus romanzoffiana*). *J. Therm. Anal. Calorim.* **2011**, *106* (3), 711–715. https://doi.org/10.1007/s10973-011-1308-0

Kobelnik, M.; Cassimiro, D. L.; Dias, D. S.; Ribeiro, C. A.; Crespi, M. S. Thermal behavior of araca oil (*Psidium cattleianum* Sabine). *J. Therm. Anal. Calorim.* **2012**, *108* (3), 1281–1286. https://doi.org/10.1007/s10973-011-1700-9

Kobelnik, M.; Fontanari, G. G.; Soares, R. A. M.; Figueiredo, A. G.; Ribeiro, C. A. Study of the thermal behavior of bicuíba oil (*Virola bicuyba*). *J. Therm. Anal. Calorim.* **2014**, *115* (3), 2107–2113. https://doi.org/10.1007/s10973-013-3315-9

Kobelnik, M.; Fontanari, G. G.; Marques, M. R.; Ribeiro, C. A.; Crespi, M. S. Thermal behaviour and chromatographic characterization of oil extracted from the nut of the butia (*Butia capitata*). *J. Therm. Anal. Calorim.* **2016**, *123* (3), 2517–2522. https://doi.org/10.1007/s10973-016-5239-7

Kobelnik, M.; Fontanari, G. G.; Ribeiro, C. A.; Crespi, M. S. Evaluation of thermal behavior and chromatographic characterization of oil extracted from seed of *Pittosporum undulatum*. *J. Therm. Anal. Calorim.* **2018a**, *131* (1), 371–378. https://doi.org/10.1007/s10973-017-6763-9

Kobelnik, M.; Quarcioni, V. A.; Almeida, A. E.; Ribeiro, C. A.; Crespi, M. S. Study of the thermal behavior in solid state of Mn(II)-Diclofenac Complex. *Eclét. Quím.* **2018b**, *43* (1), 59–66. https://doi.org/10.26850/1678-4618eqj.v43.1.59-66. https://doi.org/10.26850/1678-4618eqj.v43.1.2018.p59-66

Kobelnik, M.; Fontanari, G. G.; Soares, R. A. M.; Sampaio, G.; Ribeiro, C. A.; Crespi, M. S. Extraction of fatty acids contained in fruit from *Ficus benjamina*: lipid profile and thermal studies. *J. Therm. Anal. Calorim.* **2021**, *146* (4), 1687–1693. https://doi.org/10.1007/s10973-020-10187-y

Lipp, M.; Simoneau, C.; Ulberth, F.; Anklam, E.; Crews, C.; Brereton, P.; Greyt, W.; Schwack, W.; Wiedmaier, C. Composition of genuine cocoa butter and cocoa butter equivalents. *J. Food Comp. Anal.* **2001**, *14* (1), 399–408. https://doi.org/10.1006/jfca.2000.0984

Marques, M. R.; Fontanari, G. G.; Kobelnik, M.; Freitas, R. A. M. S.; Arêas, J. A. G. Effect of cooking on the thermal behaviour of the cowpea bean oil (*Vigna unguiculata* L. Walp). *J. Therm. Anal. Calorim.* **2015**, *120* (1), 289–296. https://doi.org/10.1007/s10973-014-4125-4

Monetta, L. Uso da papaína nos curativos feitos pela enfermagem. *Rev. Bras. Enferm.* **1987**, *40* (1) 66–73. https://doi.org/10.1590/S0034-71671987000100012

Patil, V. V.; Galge, R. V.; Thorat, B. N. Extraction and purification of phosphatidylcholine from soyabean lecithin. *Sep. Sci. Technol.* **2010**, *75* (2), 138–144. https://doi.org/10.1016/j.seppur.2010.08.006

Puangsri, T.; Abdulkarim, S. M.; Ghazali, H. M. Properties of *Carica papaya* L. (papaya) seed oil following extractions using solvent and aqueous enzymatic methods. *J. Food Lip.* **2005**, *12* (1), 62–76. https://doi.org/10.1111/j.1745-4522.2005.00006.x

Su, M. H.; Shih, M. C.; Lin, K-H. Chemical composition of seed oils in native Taiwanese *Camellia* species. *Food Chem.* **2014**, *156*, 369–373. https://doi.org/10.1016/j.foodchem.2014.02.016

Von Loesecke, H. W.; Notle, A. J. Characteristics and composition of papaya seed oil. *J. Am. Chem. Soc.* **1937**, *59* (12), 2565–2567. https://doi.org/10.1021/ja01291a024

Xu, W.; Bai, W.; Guo, F.; Luo, Y.; Yuan, Y.; Huang, K. A papaya-specific gene, papain, used as an endogenous reference gene in qualitative and real-time quantitative PCR detection of transgenic papayas. *Eur. Food Res. Technol.* **2008**, *228* (2), 301–309. https://doi.org/10.1007/s00217-008-0935-6